CATALYTIC ALKYLATION AND TRANSALKYLATION REACTIONS OVER LARGE PORE ZEOLITES BETA, Y AND ZSM-12

A THESIS
SUBMITTED TO THE
UNIVERSITY OF PUNE
FOR THE DEGREE OF
DOCTOR OF PHILOSOPHY
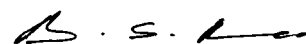(IN CHEMISTRY)

BY
RAJIB BANDYOPADHYAY

CATALYSIS DIVISION
NATIONAL CHEMICAL LABORATORY
PUNE 411 008, INDIA

SEPTEMBER 1996

Certificate

*Certified that the work incorporated in the thesis entitled **"Catalytic Alkylation and Transalkylation Reactions over Large Pore Zeolites Beta, Y and ZSM-12,"** submitted by **Rajib Bandyopadhyay**, was carried out by the candidate under my supervision. Such material as has been obtained from other sources has been duly acknowledged.*

(DR. B.S. RAO)

Supervisor

ACKNOWLEDGMENTS

Rajib Bandyopadhyay

TABLE OF CONTENTS

1. GENERAL INTRODUCTION

2. SYNTHESIS, MODIFICATION AND CHARACTERIZATION OF LARGE PORE ZEOLITES

3. ALKYLATION REACTIONS OVER ZEOLITE BETA

4. TRANSALKYLATION REACTIONS OF ALKYL AROMATICS OVER LARGE PORE ZEOLITES

5. TRANSALKYLATION REACTIONS OF N-CONTAINING AROMATICS OVER LARGE PORE ZEOLITES

6. CONCLUSION

CHAPTER 1

GENERAL INTRODUCTION

1.1 Introduction

Zeolites are hydrated, crystalline, microporous aluminosilicates which are constructed from TO_4 tetrahedra (T = tetrahedral atom, e.g., Si, Al); each apical oxygen is shared with an adjacent tetrahedra. The crystallographic unit cell of the zeolites may be represented by the general formula:[1]

$$M_{x/n} \; [(AlO_2)_x \; (SiO_2)_y] \; zH_2O$$
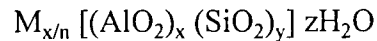
The net negative charge of the framework is same as the number of aluminium atoms and is balanced by exchangeable charge compensating cations M of valence n, typically Na^+, NH_4^+ or H^+. z is the number of water molecules, and x + y represents total number of tetrahedra in the unit cell of zeolite. In general, the ratio y/x > 1, and controls the acidity, and to a lesser extent, the morphology of zeolites.

1.2 Classification and Nomenclature

Several attempts have been made to classify families of zeolites on the basis of their morphological characteristics,[1-4] crystal structure,[1,2,5] chemical composition,[1,2,6] effective pore diameter[1,2,7] and natural occurrence.[1,2] On the basis of their morphology, zeolites are classified as fibrous, lameller, and those having framework structures. Structural classification of zeolites has been proposed depending on differences in secondary building units. With the addition of new synthetic and natural zeolites, they are grouped into ten classes: Analcime, Natrolite, Chabazite, Philipsite, Heulandite, Mordenite, Faujasite, Laumonite, Pentasil and Clantharate. Based on their chemical compositions, zeolites are classified as low silica zeolites, medium silica zeolites, high silica zeolites and silicalites (Table 1.1). Zeolites are also classified based on their pore sizes, namely small, medium, large and extra-large pore zeolites (Table 1.2).

Table 1.1

Classification of zeolites based on chemical composition

Group	SiO_2/Al_2O_3	Example
Low silica	2 to 3	Sodalite, A, X
Intermediate silica	4 to 10	L, Mordenite, Omega
High silica	10 to several thousands	ZSM-5, EU-1
Silicalite	∞ (No alumina)	Silicalite-1, Silicalite-2

Table 1.2

Classification of zeolites based on pore size

Pore size	No. of Tetrahedra in pore opening	Max. free diameter (Å)	Example
Small	6 and 8	4.3	Erionite
Medium	10	6.3	ZSM-5
Large	12	7.5	Y, Beta, ZSM-12
Extra large	18	~ 12	VPI-5, JDF-20

The nomenclature of zeolites was haphazard until the IUPAC commission published certain guidelines for their nomenclature.[8] Barrer and his co-workers identified products of their synthesis as A, B, C, and so on. Scientist of Union Carbide also used alphabetical nomenclature. Mobil Oil Corporation used Greek alphabets such as beta, omega. The IUPAC nomenclature system is based on their framework density and number of T-atoms per 1000 Å, irrespective of their composition, distribution of T-atoms, cell dimensions or symmetry parameters. This does not contain numbers and characters other than capital Roman letters. For example, MFI stands for ZSM-5, MEL for ZSM-11, MTW for ZSM-12, and AEL stands for $AlPO_4$-11 structures.

1.3 Synthesis of Zeolites

The era of synthetic zeolites began with the pioneering work by Barrer on their synthesis and adsoroption.[2] The formation of zeolites is a nucleation-controlled process occurring from inhomogeneous hydrogels[7] in the temperature range of 348 to 523 K. Zeolites are synthesized hydrothermally by the combination of cations (both organic and inorganic), a source of silicon, a source of aluminium and water. Silicon sources normally used include: sodium silicate, silica sol, silica gel, fumed silica and tetraethylorthosilicate. Aluminium sources include: sodium aluminate, aluminium sulphate and aluminium nitrate.

The major factors which influence the structure of zeolites are hydrothermal synthesis temperature and time. The silica to alumina ratio determines the elemental framework composition of the crystalline product. Various other factors such as OH^- concentration, water concentration, cations (both organic and inorganic) and anions other than OH^- influence the synthesis. In addition, there are history-dependent factors such as aging period, stirring, and order of mixing which may influence the synthesis behavior.

The first step in the synthesis of zeolites involves the dissolution or depolymerization of aluminium and silicon to form aluminate and silicate anions. These species are then brought together to form gel by condensation or polymerization. The different steps occurring during the crystallization process of zeolites have been discussed by Sand.[9] The stabilization of the zeolite crystals is brought about by the guest species that occupy the channels and cavities of the aluminosilicate framework, and this species is referred to as a template.[10] The tetramethylammonium cation (TMA) was introduced as the first organic cation in zeolite synthesis by Barrer and co-workers.[11,12] The large number of organic molecules used (Table 1.3) and their effect on zeolite synthesis and morphology have been discussed in several publications.[13-17]

The exact role played by the template is rather complex and not yet fully understood, although it is believed that zeolite structures grow around the template thus stabilizing certain pore systems. In addition to this structure directing effect, templates may have roles such as a gel modifier, increasing the solubilities of different species in the gel, acting as a buffer to maintain the pH of the gel, and acting as a void filler to organize the water molecules.[18]

1.4 Properties of Zeolites

1.4.1 Ion Exchange

Ion exchange is a function of the aluminium present in the zeolite framework. The negative charge created by each tetrahedral aluminium is balanced by cations to stabilize the zeolite framework. These charge compensating cations, usually alkali or alkaline earth metal cations, are loosely held to the framework aluminium, and they are easily exchangeable with different monovalent and multivalent cations.[19,20] The rate and degree of cation exchange in zeolites depend upon several factors which include: size and charge

Table 1.3

Organic template - zeolite structure relationships[17]

Organic template	Structure
Tetraethylammonium (TEA)	Beta
	ZSM-8
	ZSM-12
	ZSM-20
	ZSM-25
	Mordenite
Methyltriethyammonium (MTEA)	ZSM-12
Tetrapropylammonium (TPA)	ZSM-5
n-Propylamine	ZSM-5
Tetrbutylammonium (TBA)	ZSM-11
Choline	ZSM-38
	ZSM-34
	ZSM-43
	CZH-5
TMA + TEA	ZSM-39
TMA + n-propylamine	ZSM-39
	ZSM-48
Pyrrolidine	ZSM-35
	ZSM-21
	ZSM-23
1,2-Diaminoethane	ZSM-5
	ZSM-21
	ZSM-35
1,2-Diaminopropane	ZSM-5
	ZSM-35
1,4-Diaminobutane	ZSM-5
	ZSM-35
1,5-Diaminopentane	ZSM-5
1,6-Diaminohexane	ZSM-5
1,7-Diaminoheptane	ZSM-11
1,8-Diaminooctane	ZSM-11
	ZSM-48
1,9-Diaminononane	ZSM-11
1,10-Diaminodecane	ZSM-11
DDO	ZSM-10
MDQ	ZK-20
MQ	LZ-132
TQA	ZSM-18
Dihexamethylenetriamine	ZSM-30
Neopentylamine	Mordenite

of the cation, concentration of the exchanging solution, temperature of the ion exchange treatment, location of the cation in the zeolite, and structure of the zeolite.

1.4.2 Acidity

The existence of aluminium in a tetrahedrally coordinated silicon structure in zeolite requires the existence of compensating cations which are located in the porous system of the structure. These cations are accessible for ion exchange, and thus, acidity can be achieved in zeolites by ion exchange with NH_4^+, followed by the thermal decomposition of NH_4^+ in air. Brönsted acid sites thus formed can also be further involved in dehydroxylation reactions, to form Lewis acid sites, under thermal treatments at temperatures usually above 773K as described below[1]

Brönsted acid site   Lewis acid site
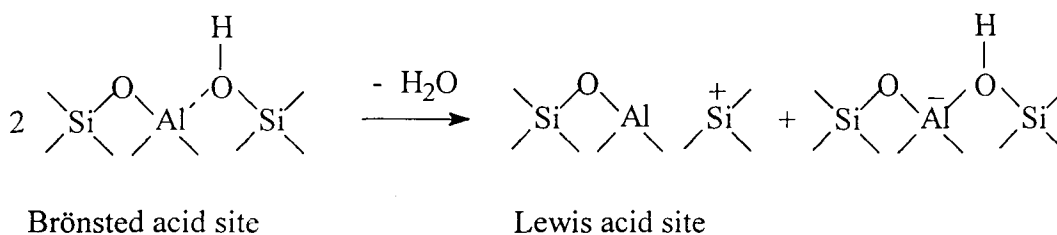
Several methods have been developed[21-23] to determine the number and strength of both types of acid sites, among which the most important are: titration method, adsorption and desorption of bases, IR spectroscopy of adsorbed bases and OH groups, and NMR spectroscopy of adsorbed bases and OH groups.

1.4.3 Adsorption and Diffusion

Zeolites posses uniform pores and internal channels with large void volume. Zeolites have also high surface area which are accessible to molecules of comparable size to diffuse through the pores. Due to the high surface area and void volume coupled with electrostatic field, zeolites act as selective adsorbents. Sorption studies of nitrogen, oxygen, water, n-hexane and other hydrocarbons give several types of information[18]

which include: void volume of the zeolite, pore size of the zeolite, degree of crystallinity, hydrophilicity/hydrophobicity and acidity. Sorption of various gases and vapors on natural and synthetic zeolites has been extensively studied by Barrer and co-workers.[24-29] Various thermodynamic parameters such as entropy, and heat and free energy of sorption have also been studied by them. Sorption studies of zeolites also provide information about interactions between sorbate and sorbents.[30]

Migration or diffusion of sorbed molecules through the pores and cages within the crystals plays an important role in the process of catalysis and selective adsorption/separation by zeolites. The different aspects of diffusion in zeolite catalysis have been reviewed by several authors.[31-33] There are three types of diffusion relevant to the zeolite system, namely molecular diffusion, Knudsen diffusion and configurational diffusion.

In molecular or bulk diffusion, the mean free path of a molecule is much smaller than the pore diameter of the zeolite, and molecular collisions are more frequent than collisions with the walls of the catalyst pore. Here, the rate of molecular diffusion is independent of the pore radius. Knudsen diffusion occurs when the pore diameter of the solid is less than the mean free path of the molecule. In this case, molecules usually strike the pore wall before colliding with a second molecule. Configurational diffusion occurs when the sizes of the molecules and the pores of the zeolites are comparable. A striking feature of this diffusion regime is that, very small changes in the molecule to pore size relationship induce very large changes in the diffusion coefficient, and this is the phenomena that induces shape selectivity.

1.4.4 Shape Selectivity

The term 'shape-selective catalysis' was coined by Weisz and Frillette[34] more than three decades ago. A striking feature of zeolites and related materials is that their pore sizes are of molecular dimensions (Fig. 1.1). The comparable sizes of zeolite pores and
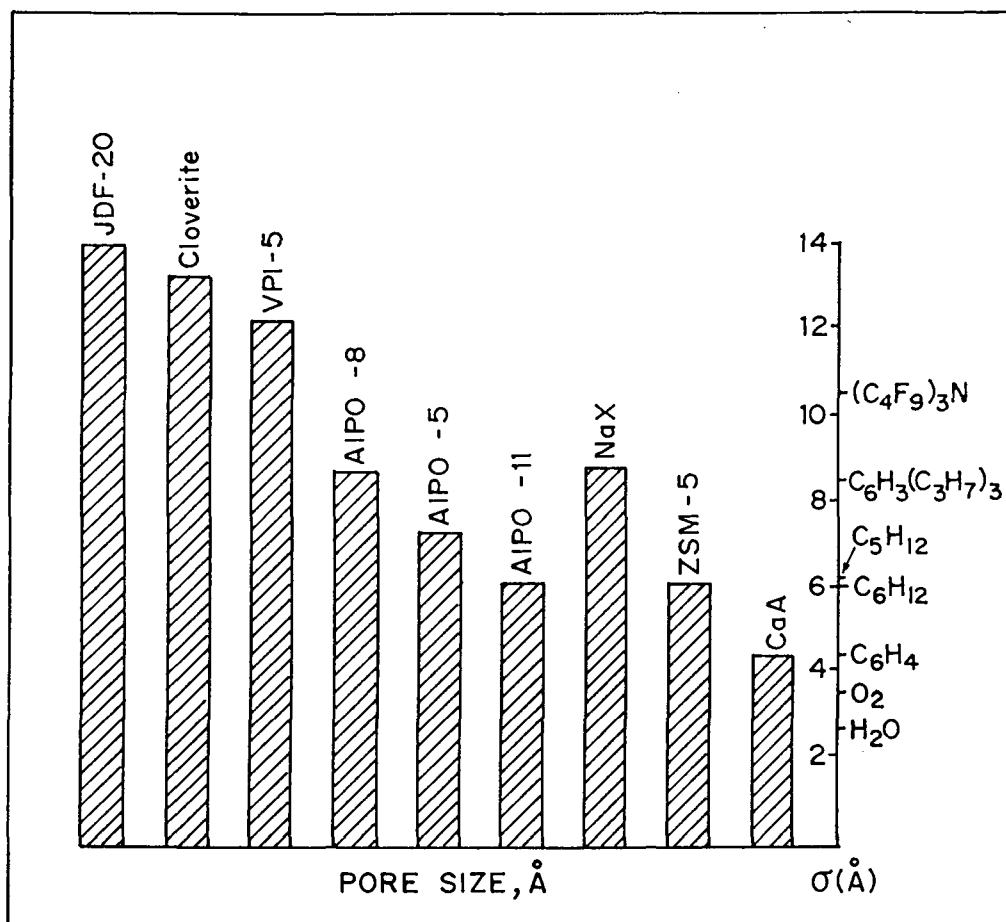
Fig. 1.1   Correlation between pore size of molecular sieves and the diameter (σ) of various molecules (Adapted from Ref. 122c)

different organic molecules play a major role in the shape selectivity in zeolite catalysis. The principles and applications of shape selective catalysis have been comprehensively reviewed and critically discussed by several authors.[35-42] Shape selectivity consists of a combination of shape, size and configuration of reactants, transition states and products with dimension, geometry and tortuosity of the channels and cages of the zeolite. Csicsery[37] has categorized these shape selective effects as follows:

1.4.4.1 Reactant Selectivity

Reactant selectivity takes place when only part of the reactant molecules are small enough to diffuse through the catalyst pores. For example, due to their large size and bulky shape, highly branched C_{13} isoparaffins are prevented from entering and reacting inside the pore system of ZSM-5, whereas linear paraffins, due to the absence of steric constraints, easily enter the pores and undergo reaction (Fig. 1.2a).[39]

1.4.4.2 Product Selectivity

Product selectivity occurs when zeolite pores show 'molecular sieving effect,' where some of the products formed within the pores are too bulky to diffuse out as observed products. This effect is demonstrated in Fig. 1.2b.[39] Inside the small pore zeolite Linde A, isomerization of a n-C_6 paraffin to a branched isomer can occur within the ~11.4-Å α cage, but egress of the *iso* product through the 4.1-Å 8-ring window is prevented due to its larger dimensions. Faster diffusion of *para* xylene compared to its *ortho* and *meta* analogs from the pore of ZSM-5 is another example of product selectivity.

1.4.4.3 Restricted Transition-State Selectivity

Restricted transition-state selectivity occurs when certain reactions are prevented because some transition state in the reaction pathway requires more space than is available inside the catalyst pore. An example of this type of selectivity is the reaction of 1-methyl-2-ethylbenzene over mordenite at 477-588K.[43] Formation of the unsymmetrical

Fig. 1.2 Shape selectivity in zeolites; (a) Reactant Selectivity, (b) Product Selectivity, and (c) Transition-State Selectivity

11
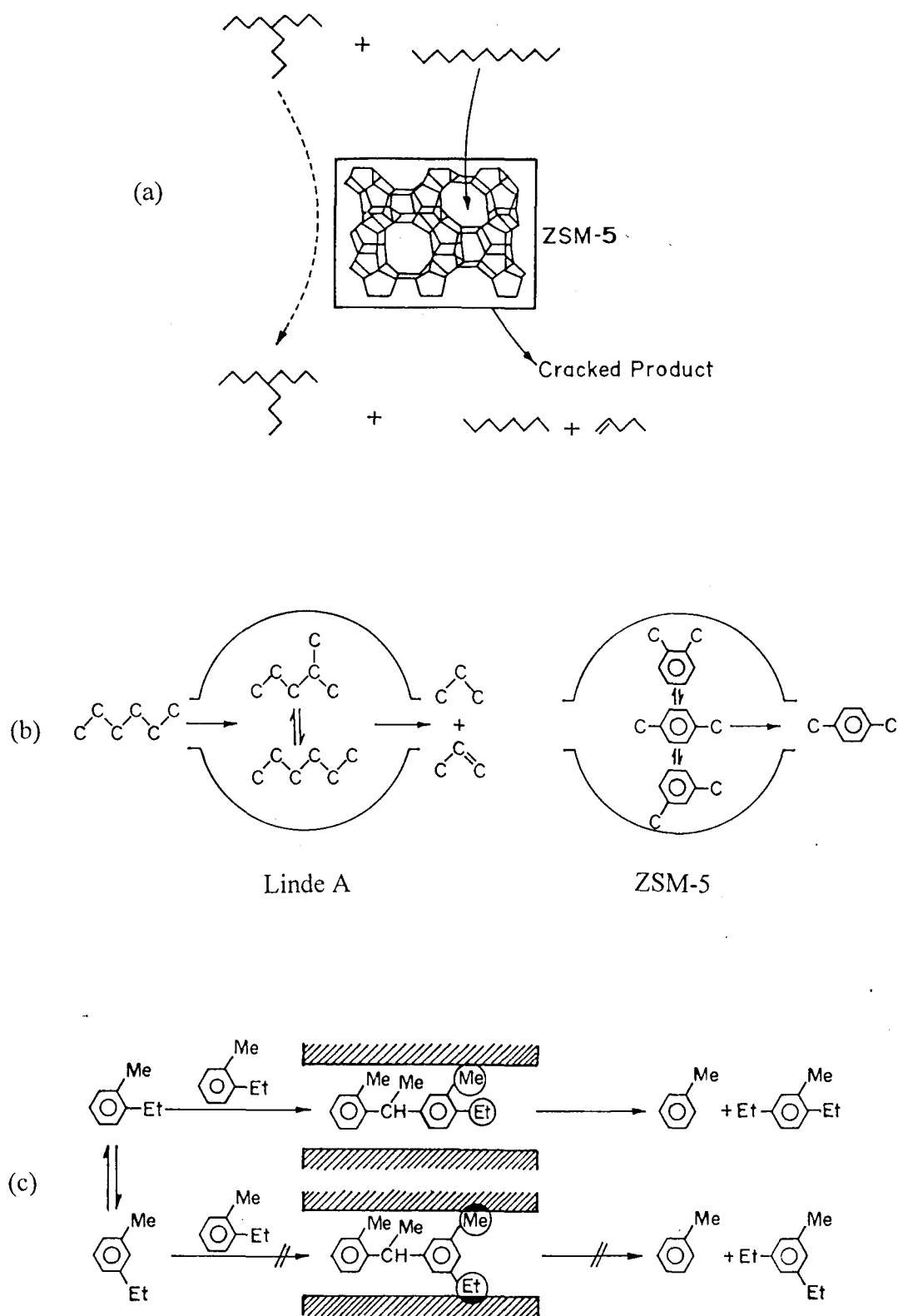
1,3,5-isomer is significantly hindered because of spatial limitations on the formation of the diarylmethane intermediate (Fig. 1.2c).

Other less common terminology for molecular shape selectivity includes: concentration effect,[44] molecular traffic control,[45] molecular circulation[46] and energy gradient selectivity.[47]

1.5 Physico-Chemical Characterization of Zeolites

1.5.1 X-Ray Diffraction

Among the different analytical tools available for characterization of zeolites, X-ray diffraction is one of the most important and versatile technique.[3,18,48] Several important structural features of zeolites are obtained from XRD data; these include: phase purity, uniqueness of structure, and degree of crystallinity of the samples. When isomorphous substitution in zeolite occurs, the extent of incorporation of the isomorphous element can be correlated with unit cell expansion or contraction.[49-52] Elucidation of the structure of single crystals[53,54] and determination of new structures using Rietveld analyses and *ab initio* calculations are also possible with XRD.[53-55]

1.5.2 Infrared Spectroscopy

IR-spectroscopy is a supplementary technique to X-ray diffraction since it is sensitive to zeolite framework vibrations. In the IR spectrum of zeolites in the range of 300-1300 cm^{-1}, the lattice vibrations can be divided into structure-insensitive and structure-sensitive vibrations. Flanigen *et al.*[56] assigned the following bands positions:

Structure insensitive vibrations
asymmetric stretch	950 - 1250 cm^{-1}
symmetric stretch	650 - 720 cm^{-1}
T-O bending	420 - 500 cm^{-1}

Structure sensitive vibrations

asymmetric stretch	1050 - 1150 cm^{-1}
symmetric stretch	750 - 820 cm^{-1}
double ring vibrations	500 - 650 cm^{-1}
pore opening vibrations	300 - 420 cm^{-1}

Infrared data on the fundamental structures of many minerals and synthetic zeolites have been published by several authors.[56-59] Information about zeolite acidity can also be obtained from the IR spectroscopy of OH groups[60] and absorbed bases such as ammonia, pyridine and benzene.[61] IR spectroscopy is also used to confirm isomorphous substitution. Incorporation of B, Fe or Ga in place of Al shifts certain OH vibrations to lower or higher wave numbers.[62]

1.5.3 Thermal Analysis

Thermal stability of zeolites is one of the important features that makes zeolites applicable as selective sorbents and potential catalysts. Thermal behavior of zeolites as well as information regarding their syntheses and associated reaction mechanisms can be obtained by thermal techniques.[63,64] The thermal stability of zeolites are often examined from the shape of the high-temperature differential thermal analysis (DTA) exotherm. Various physico-chemical changes such as the dehydration of adsorbed water, the decomposition of occluded template material, and dehydroxylation leading to the formation of Lewis acid sites during thermal treatment can be analyzed from the thermo-analytical curves.[65,66] Kinetics of the dehydration of zeolites as well as oxidative decomposition of occluded organics have also been extensively studied using this technique.[23,67]

1.5.4 Temperature Programmed Desorption of Ammonia

TPD of ammonia is a useful method for characterizing the acidity of zeolites in terms of acid strength and the number of acid sites.[68,69] Jacobs *et al.*[70] have characterized

acid sites as weak, medium and strong sites according to the temperature of the release of ammonia from these sites over a large temperature range during acidity measurements on USY and ZSM-5 zeolites. According to Lok *et al.*,[71] in general, the first NH_3-TPD peak (< 473 K) represents mainly physisorbed NH_3 molecules. The second peak (473 K - 673 K) is associated with NH_3 molecules adsorbed on hydroxyl groups, and the third peak (> 673 K) is associated with dehydroxylation, strong Brönsted acid sites and/or Lewis acid sites.

1.6 Applications of Zeolites

There are several unique properties which make zeolites superior over other heterogeneous and homogeneous catalysts; these include: well-defined crystalline microporous structure, high thermal stability, high internal surface area, ion exchange properties, ease of regeneration and their environmentally friendly nature. Due to these properties, zeolites and other molecular sieves are finding widespread applications in diverse areas such as catalysis, ion exchange, separation and drying processes.

As catalysts, zeolites exhibit appreciable activity with shape selective features not available in compositionally equivalent amorphous catalysts. In addition, these materials can act as supports for numerous catalytically active metals and metal oxides.

The industrial use of zeolites as catalysts started in the early 1960s with the replacement of cracking catalysts based on amorphous aluminosilicates.[72-75] As catalysts, zeolites have found greatest use in the hydrocarbon processing field in petroleum and petrochemical industries. Some major zeolite-based commercial processes involving petroleum, petrochemicals and oil refining industries are listed in Table 1.4. In more traditional oil refining, zeolite catalysis is involved in the processing of almost every fraction of the crude oil barrel.[97]

Table 1.4

Major commercial processes based on shape selective zeolites

Name of the process	Purpose	Reference
Selectoforming	Octane boosting	76
M-forming	Octane boosting	77-80
Catalytic cracking	Octane boosting	81,82
MDDW	Distillate dewaxing	83,84
Jet fuel dewaxing	Heavy distillate dewaxing	85
MLDW	Lube dewaxing	86,87
MOGD	Light olefins to gasoline	88
M2 - forming	Paraffins, olefins,naphthalene to aromatics and light gases	89
MVPI, MHTI	Xylene isomerization	90-92
MTDP	Toluene disprportionation	92
Mobil/Badger EB process	Ethylbenzene synthesis	93
ALBENE	Ethylbenzene synthesis	94
MTG	Methanol to gasoline	95
MTO	Methanol to light olefins	96

Compared to the successful use of zeolites in hydrocarbon processing, their use in the synthesis of organic intermediates and fine chemicals started at a later stage, but the progress of research in this field is significant in recent years. The potential of zeolites in this field has been demonstrated for a variety of organic reactions such as alkylation,[98-102] transalkylation,[103-105] isomerization,[106-108] rearrangement,[109-111] oxidation,[112-115] reduction[116] and condensation.[117-119]

1.7 Large and Extra-Large Pore Zeolites

In the last two decades, medium pore zeolites have been extensively used as shape-selective catalysts in many industrial applications in the petroleum and petrochemical industries.[36] In contrast, the area of large pore zeolites was restricted to the catalytic cracking of cracking of oils. Ideas about acid catalysis have been gathered from many years of research on medium pore zeolites.[120] Recently, these ideas have been applied to the transformation of large organic substrates using large pore zeolites as catalysts.[121,122] Existing large pore zeolites such as faujasite, beta, mordenite, ZSM-12, and L have been increasingly used for the catalysis of fine chemicals. The discovery of extra-large pore molecular sieves such as VPI-5,[123] AlPO$_4$-8,[124] cloverite,[125] MCM-41[126,127] and JDF-20[128] has also promoted the use of zeolites in combination with large organic subsrates.

Large and extra-large pore molecular sieves are useful for the conversion of large hydrocarbon molecules at the heavy end of petroleum fractions, as well as for the selective transformation of other bulkier organic molecules. Moreover, they possess large theoretical void volumes which make them microporous adsorbents with high adsorption capacities. Large pore molecular sieves can also act as hosts, immobilizing bulky guest molecules such as salen[129] and phthalocyanines[130-132] which may be used to isolate active transition-metal species. In recent years, large pore zeolites like beta, mordenite and

16

ZSM-12 have been used for shape selective catalysis with cumene,[133,134] naphthalene[135-139] and biphenyls.[140,141]

1.8 Alkylation and Transalkylation Reactions of Aromatic Hydrocarbons

The reaction of benzene and amyl chloride to produce amyl benzene was the first typical alkylation reaction reported by Charles Friedel and James Crafts, and the reaction was named after them as the Friedel-Crafts reaction.[142] Today Friedel-Crafts reaction is applied in several industrial processes[143] to manufacture high-octane gasoline, synthetic rubber, fibers, plastics, and detergents. In addition, the reaction presents classical features in the field of modern organic chemistry as it includes electrophilic aromatic substitution and rearrangement.

Although the alkylating agent involved in the Friedel-Crafts reaction was an alkyl halide, many other alkylating agents such as olefins, alcohols, and ethers are widely used.[93,97,144,145] The aromatic ring to which the alkylating group gets attached may be benzene, substituted benzene or polynuclear aromatics such as naphthalene or anthracene.

Since alkyl groups activate the aromatic ring towards further attack, there is a positive tendency for polysubstitution during the alkylation reaction. It was shown that alkyl groups can be transferred from one aromatic ring to another by the catalytic effect of aluminium chloride and hydrogen chloride.[143] Transfer of an alkyl groups between two similar or dissimilar aromatic molecules in the presence of an acid catalyst is known as transalkylation reaction. This reaction is industrially important since some of the low valued products like polyalkylbenzenes can be converted to their monosubstituted homologs having higher demands, e.g., transalkylation of diisopropylbenzene with benzene to form cumene.

Friedel-Crafts alkylation and transalkylation are acid-catalyzed reactions and can be catalyzed by both Brönsted and Lewis acids.[146] Anhydrous aluminium chloride and solid

phosphoric acid are extensively used in alkylation. Apart from these two catalysts, several other catalysts have been used in the alkylation of aromatics.[143,146,147] These include: (i) Lewis acids such as $FeCl_3$, BF_3, $TiCl_4$, $SnCl_4$ and $ZnCl_4$, (ii) Brönsted acids such as HF, H_2SO_4 and polyphosphoric acid, (iii) solid super acids such as perfluorinated sulphonic acid, and (iv) inorganic acidic oxides such as phosphorous pentoxide on aluminium. Most of these catalysts are used in liquid phase and the use of such catalysts entails problems of corrosivity, toxicity, work-up and effluent pollution. For this reason, replacement of homogeneous catalysts by heterogeneous catalysts is desirable. Solid acid catalysts such as zeolites are free from corrosion and environmental problems, and they deserve their reputation as effective catalysts for various alkylation and transalkylation reactions. Moreover, owing to their tunable acidity and shape-selectivity, zeolites are highly favored for these reactions.

1.9 Scope of The Work

Rather than focusing solely on the subtleties of the zeolites used as catalysts in this thesis, our main objective was to investigate various alkylation and transalkylation reactions over these materials. First, the formation of cymenes has been studied by alkylation reactions over Beta and cation-exchanged Beta zeolites. The catalytic performance of these Beta zeolites has been compared in the alkylation of toluene with isopropanol, and cumene with methanol. Transalkylation is another route to form alkyl aromatics, and this class of reactions has been explored for the formation of cymenes and cumene over large pore zeolites Beta, Y and ZSM-12.

The reaction studies on the alkyl aromatic molecules mentioned above provided a basis from which to extend alkylation and transalkylation to some new substrates, specifically N-containing aromatics. Except for one patent by Klug *et al.*,[148] formation of N-methylaniline by a transalkylation mechanism has not been thoroughly investigated.

Aniline and N,N-dimethylaniline have been transalkylated to form N-methylaniline over large pore zeolites with different structures and acidity. Reaction temperature and basicity of zeolite influence the product patterns in this reaction. To investigate these effects, the same reaction has also been studied over alkali cation-exchanged Beta zeolites (Cs^+ and K^+ forms).

The zeolites used in this study have also been synthesized and thoroughly characterized. Zeolite Beta and ZSM-12 have been synthesized, and zeolite Beta has been modified by ion-exchange with cations, namely La^{3+}, Mg^{2+}, Cs^+ and K^+. Commercially obtained NH_4-Y was converted to H-Y, and has also been exchanged to its rare-earth form. All the above samples have been characterized by using various physico-chemical techniques set forth in further detail in the next chapter.

1.10 References

1. D.W. Breck, in *Zeolite Molecular Sieves*, John Wiley and Sons, New York, (1974).

2. R.M. Barrer, in *Hydrothermal Chemistry of Zeolites*, Academic Press, New York, (1982).

3. W.M. Meier and D.H. Olson, in *Atlas of Zeolite Structure Types*, 2nd. Edn., Butterworths, London, (1987).

4. W.L. Bragg, in *The Atomic Structure of Minerals*, Cornell University Press, Ithaca, New York, (1937).

5. W.M. Meier, in *Molecular Sieves*, Soc. Chem. Ind., London, (1968) 10.

6. E.M. Flanigen, *Proc. 5th Int. Zeol. Conf.*, L.V.C. Rees (Ed.), Heyden and Sons, London, (1980) 760.

7. L.B. Sand, *Econ. Geol.*, (1967) 191.

8. R.M. Barrer, *Pure Appl. Chem.*, 51 (1979) 1091.

9. L.B. Sand, *Pure Appl. Chem.*, 52 (1980) 2105.

10. E.M. Flanigen, *ACS Symp. Ser.*, 121 (1973) 119.

11. R.M. Barrer and P.J. Denny, *J. Chem. Soc.*, (1961) 971.

12. R.M. Barrer and P.J. Denny and E.M. Flanigen, *US Pat.*, 3,306,922 (1967).

13. E. Moretti, S. Contessa and P. Padovan, *Chim. Ind.*, 76 (1985) 21.

14. E.W. Valyocsik and L.D. Rollmann, *Zeolites*, 5 (1985) 123.

15. F.J. van der Gaag, J.C. Jansen and H. van Bekkum, *Appl. Catal.*, 17 (1985) 261.

16. J.L. Casci, *Stud. Surf. Sci. Catal.*, 28 (1986) 215.

17. B.M. Lok, T.R. Cannan and C.A. Messina, *Zeolites*, 3 (1983) 282.

18. R. Szostak, in *Molecular Sieves, Principles of Synthesis and Modification*, Van Nostrand Reinhold, New York, (1989).

19.   H.S. Sherry, in *Molecular Sieve Zeolites, Adv. Chem. Ser.*, 101 (1971) 350.

20.   L.V.C. Rees and A. Rao, *Trans. Faraday Soc.*, 62 (1970) 2103.

21.   J.H.C. van Hooff and J.W. Roelofsen, *Stud. Surf. Sci. Catal.*, 58 (1991) 242.

22.   H.G. Karge, *Stud. Surf. Sci. Catal.*, 65 (1991)133.

23.   P.A. Jacobs, in *Carboniogenic Activity of Zeolites*, Elsevier, Amsterdam, (1977) 33.

24.   R.M. Barrer, *Proc. Royal Soc.*, A167 (1938) 392.

25.   R.M. Barrer and D.W. Riley, *Trans Faraday Soc.*, 46 (1950) 853.

26.   R.M. Barrer and A.B. Robins, *Trans Faraday Soc.*, 49 (1953) 1049.

27.   R.M. Barrer and W.I. Stuart, *Proc. Royal Soc.*, A249 (1959) 464, 484.

28.   R.M. Barrer and R.M. Gibbons, *Trans Faraday Soc.*, 59 (1963) 2569, 2875.

29.   R.M. Barrer, *Pure Appl. Chem.*, 52 (1980) 2143.

30.   R.J. Neddenriep, *J. Colloid Interface Sci.*, 28 (1968) 293.

31.   P.B. Weisz, *Chemtech*, 3 (1973) 498.

32.   M.F.M. Post, *Stud. Surf. Sci. Catal.*, 58 (1991) 391.

33.   J. Karger and D.M. Ruthven, in *Diffusion in Zeolites and Other Microporous Solids*, John Wiley and Sons, New York, (1992).

34.   P.B. Weisz and V.J. Frilette, *J. Phys. Chem.*, 64 (1960) 382.

35.   S.M. Csicsery, in *Zeolite Chemistry and Catalysis*, ACS Monograph 171, J.A. Rabo (Ed.), American Chemical Society, Washington DC, (1976) 680.

36.   N.Y. Chen, W.E. Garwood and F.G. Dwyer, in *Shape Selective Catalysis in Industrial Applications*, Marcel Dekker, New York, (1989).

37.   S.M. Csicsery, *Zeolites*, 4 (1984) 202.

38.   S.M. Csicsery, *Pure Appl. Chem.*, 58 (1986) 841.

39.   P.B. Venuto, *Microporous Mater.*, 2 (1994) 297.

40.   E.G. Derouane, in *Zeolites: Science and Technology*, F. Ramôa Ribeiro *et al.*, (Eds.), NATO ASI Series E 80, Martinus Nijhoff Pub., The Hague, (1984) 347.

41.   P.B. Weisz, *Pure Appl. Chem.*, 52 (1980) 2019.

42.   F. Ramôa Ribeiro, F. Alvarez, C. Henriques, F. Lemos, J.M. Lopes and M.F. Rebeiro, *J. Mol. Catal.*, 96 (1995) 245.

43.   S.M. Csicsery, *J. Catal.*, 23 (1971) 124.

44.   J.A. Rabo, R. Bezman and M.L. Postma, *Acta Phys. Chem.*, 24 (1987) 39.

45.   E.G. Derouane and Z. Gabelica, *J. Catal.*, 65 (1980) 486.

46.   C. Mirodatos and D. Barthomeuf, *J. Catal.*, 57 (1979) 136.

47.   C. Mirodatos and D. Barthomeuf, *J. Catal.*, 93 (1985) 246.

48.   R. van Ballmoos, in *Collection of Simulated XRD Powder Patterns for Zeolites*, Butterworths, London, (1984).

49.   G. Perego, G. Bellussi, C. Corno, M. Taramaso, F. Buonomo and A, Esposite, in *New Developments in Zeolite Science and Technology*, Y. Murakami *et al.*, (Eds.), Elsevier, Amsterdam, (1986) 129.

50.   P. Ratnasamy, A.N. Kotasthane, V.P. Shiralkar, A. Thagaraj and S. Ganapathy, in *Zeolite Synthesis*, ACS Symp. Ser., 398 (1989) 405.

51.   R. Szostak and T.L. Thomas, *J. Catal.*, 100 (1986) 555.

52.   D.K. Simmons, R. Szostak and P.K. Agarwal, *J. Catal.*, 106 (1987) 287.

53.   J.J. Pluth, J.V. Smith and J.M. Bennett, *Acta Crystallog.*, C42 (1986) 283.

54.   J.F. Charnell, *J. Cryst. Growth*, 8 (1971) 291.

55.   H.M. Rietveld, *J. Appl. Crystallog.*, 2 (1969) 65.

56.   E.M. Flanigen, H. Khatami and H.A. Szymanski, *Adv. Chem. Ser.*, 101 (1971) 201.

57. A.C. Wright, J.P. Rupert and W.T. Granquist, *Am. Miner.*, 53 (1968) 1293.

58. S.P. Zhdnov, A.V. Keseler, V.I. Lygin and T.I Titova, *Russ. J. Phys. Chem.*, 38 (1964) 1299.

59. E.M. Flanigen and R.W. Grose, *Adv. Chem. Ser.*, 101 (1971) 76.

60. W.J. Ward, in *ACS Monograph 171*, J.A. Rabo (Ed.), (1976).

61. P.A. Jacobs, J.A. Martens, J. Weitkamp and H.K. Beyer, in *Selectivity in Heterogeneous Catalysis*, Far. Disc. Chem. Soc., 72 (1981) 351.

62. C.T.W. Chu and C.D. Chang, *J. Phys. Chem.*, 89 (1985) 1569.

63. E.G. Derouane, S. Detremmerie, Z. Gabelica and N. Blom, *Appl. Catal.*, 1 (1981) 20.

64. R.M. Barrer and D.A. Langley, *J. Chem. Soc.*, (1958) 3804, 3811, 3817.

65. I.G. Gal, O. Tankovie, S. Malcis, R. Raoovanor and M. Tadorivic, *Trans Faraday Soc.*, 67 (1971) 999.

66. H. Bremer, W. Morke, P. Schodel and F. Vogt, *Adv. Chem. Ser.*, 121 (1973) 249.

67. L.S. de Saldarriga, C. Saldarriga and M.E. Davis, *J. Am. Chem. Soc.*, 109 (1987) 2686.

68. J.R. Anderson, F.K. Mole, R.A. Rajadhyaksha and J.V. Sanders, *J. Catal.*, 58 (1979) 114.

69. J.G. Post and J.H.C. van Hooff, *Zeolites*, 4 (1984) 9.

70. P.A. Jacobs, J.B. Utterhoeven, M. Steyns, G. Froment and J. Weitkamp, *Proc. 5th Int. Zeol. Conf.*, L.V.C. Rees (Ed.), Heyden and Sons, London, (1980) 607.

71. B.M. Lok, B.K, Marcus and C.L. Angel, *Zeolites*, 6 (1986) 185.

72. P.B. Weisz, V.J. Frilette, R.W. Maatman and E.B. Mower, *J. Catal.*, 1 (1962) 307.

73. C.J. Plank, E.J. Rosinski and M.P. Howthorne, *Ind. Eng. Chem. Proc. Des. Dev.*, 3 (1964) 165.

74. P.B. Venuto and E.T. Habib, Jr., in *Chemical Industries*, Marcel Dekker, New York, 1 (1979).

75. W. Hölderich and E. Gallei, *Chem. Eng. Tech.*, 56 (1984) 908.

76. N.Y. Chen, N. Maziuk, A.B. Schwartz and P.B. Weisz, *Oil Gas J.*, 66 (1968) 154.

77. N.Y. Chen, *US Pat.*, 3,729,409 (1973).

78. H. Heinamann, *Catal. Rev. Sci. Eng.*, 15 (1977) 53.

79. J.C. Bonaccsi and J.R. Patterson, *US Pat.*, 4,292,167 (1981).

80. N.Y. Chen, W.E. Garwood and R.H. Heck, *Ind. Eng. Chem. Proc. Des. Dev.*, 26 (1987) 706.

81. C.D. Anderson, F.G. Dwyer, G. Koch and P. Niiranen, *Proc. 9th Iberoamerican Symp. Catal.*, Lisbon, Port., July, (1984).

82. S.J. Yanik, E.J. Demmel, A.P. Humphries and R.J. Campagna, *Oil Gas J.*, 83 (1985) 108.

83. N.Y. Chen, R.L. Gorring, H.R. Ireland and T.R. Stein, *Oil Gas J.*, 75 (1977) 165.

84. R.J. Perry, Jr., C. Redini, A.S. Raff and L. Fava, Hydrocarbon Process, 58 (1979) 119.

85. N.Y. Chen and W.E. Garwood, *Ind. Eng. Chem. Proc. Des. Dev.*, 25 (1986) 641.

86. R.G. Graven and J.R. Green, *Proc. Congr. Australia Inst. Petrol.*, Sydney, Sept. 15-17, (1980).

87. K.W. Smith, W.C. Starr and N.Y. Chen, *Oil Gas J.*, 78 (1980) 75.

88. S.A. Tabak, *Proc. AIChE Nat. Mtg.*, Philadelphia, (1984).

89. N.Y. Chen and T.Y. Yan, *Ind. Eng. Chem. Proc. Des. Dev.*, 25 (1986) 151.

90. W.O. haag and D.H. Olson, *US Pat.*, 3,856,871 (1974).

91. S.A. Tabak and R.A. Morrison, *US Pat.*, 4,188,282 (1980).

92. D.H. Olson and W.O. Haag, *ACS Symp. Ser.*, 248 (1984) 275.

93. F.G. Dwyer in *Catalysis of Organic Reactions*, W.R. Moser (Ed.), Marcel Dekker, New York, (1981) 39.

94. Developed at NCL, Pune, *NCL Annual Report*, 1989-90.

95. A.Y. Kam, M. Schreiner and S. Yurchak, in *Handbook of Synfuels Technology*, R.A. Meyers (Ed.), McGraw-Hill, New York, (1984) 2.

96. C.D. Chang, J.N. Miale and R.F. Socha, *J. Catal.*, 90 (1984) 84.

97. I.E. Maxwell and W.J.H. Stork, *Stud. Surf. Sci. Catal.*, 58 (1991) 571.

98. P.B. Venuto, L.A. Hamilton, P.S. Landis and J.J. Wise, *J. Catal.*, 5 (1966) 81.

99. W.W. Kaeding, M.M.Wu, L.B. Young and G.T. Burress, *US Pat.*, 4,197,413 (1980).

100. P.Y. Chen, M.C. Chen, H.Y Chu, N.S. Chang and T.K. Chuang, *Stud. Surf. Sci. Catal.*, 28 (1986) 739.

101. K.S.N. Reddy, B.S. Rao and V.P. Shiralkar, *Appl. Catal.*, 95 (1993) 53.

102. A.R. Pradhan, A.N. Kotasthane and B.S. Rao, *Appl. Catal.*, 72 (1991) 311.

103. A.R. Pradhan and B.S. Rao, *Appl. Catal.*, 106 (1993) 143.

104. R. Bandyopadhyay, P.S. Singh and R.A. Shaikh, *Appl. Catal.*, 135 (1996) 249.

105. L. Forni, G. Cremona, F. Missineo, G. Bellusi, C. Perego and G. Pazzuconi, *Appl. Catal.*, 121 (1995) 261.

106. P. Cartraud, A. Cointot, M. Dufour, N.S. Gnep, M. Guisnet, G. Joly and J. Tejada, *Appl. Catal.*, 21 (1986) 85.

107. R.J. Pellet, P.K. Coughlin, E.S. Shamshoum and J.A. Rabo, *ACS Symp. Ser.*, 368 (1988) Ch. 33.

108. F.J. Weigert, *US Pat.*, 4,593,124 (1986).

109. A. Molner, I. Bucsi and M. Bartok, *Acta Phys. Chem.*, 31 (1985) 571.

110. C. Neri and F. Buonomo, *Eur. Pat. Appl.*, 110,117 (1983).

111. P.S. Singh, R. Bandyopadhyay and B.S. Rao, *Appl. Catal.*, 136 (1996) 249.

112. R.A. Sheldon, *J. Mol. Catal.*, 7 (1980) 107.

113. P.R.H.P. Rao, A.V. Ramaswamy and P. Ratnasamy, *J. Catal.*, 141 (1993) 604.

114. J.S. Reddy, S. Sivasanker and P. Ratnasamy, *J. Mol. Catal.*, 71 (1992) 373.

115. A. Thangaraj, S. Sivasanker and P. Ratnasamy, *Zeolites*, 12 (1992) 135.

116. M. Iwamoto, H. Yahiro, K. Tanda, N. Mizumo, *J. Phys. Chem.*, 95 (1991) 3727.

117. M.A. Tobias, *US Pat.*, 3,728,408 (1973).

118. C.J. Plank, E.J. Rosinski and G.T. Kerr *US Pat.* 4,011,278 (1977).

119. Y. Servotte, J. Jacobs and P.A. Jacobs, *Acta. Phys. Chem.*, 31 (1985) 609.

120. E.M. Flanigen, *Stud. Surf. Sci. Catal.*, 58 (1991) 13.

121. J. Weitkamp, *Stud. Surf. Sci. Catal.*, 65 (1991) 21.

122. (a) M.E. Davis, *Ind. Eng. Chem. Res.*, 30 (1991) 1675; (b) M.E. Davis, *Chem. Ind.*, 17 Feb. (1992) 137; (c) M.E. Davis, *Acc. Chem. Res.*, 26 (1993) 111.

123. M.E. Davis, C. Saldarriga, C. Montes, J. Graces and C. Crowder, *Nature*, 331 (1988) 698.

124. R.M. Dessau, J.L. Schlenker and J.B. Higgins, *Zeolites*, 10 (1990) 522.

125. M. Eastermann, L.B. McCusker, C. Baerlocher, A. Merrouche and H. Kessler, *Nature*, 352 (1991) 320.

126. C.T. Kresge, M.E. Leonowicz, W.J. Roth and J.C. Vartuli, *US Pat.*, 5,102,643 (1992).

127. C.T. Kresge, M.E. Leonowicz, W.J. Roth J.C. Vartuli and J.S. Beck, *Nature*, 359 (1992) 710.

128. Q. Huo, R. Xu, S. Li, Z. Ma, J.M. Thomas, R.H. Jones and A.M. Chippindale, *J. Chem. Soc. Chem. Commun.*, (1992) 875.

129. K.J. Balkus, Jr., A.A. Welch and B.E. Gnade, *Zeolites*, 10 (1990) 722.

130. G. Meyer, D. Wöhrle, M. Mohl and G. Schulz-Ekloff, *Zeolites*, 4 (1984) 30.

131. R.F. Parton and L. Utterhoeven and P.A. Jacobs, *Stud. Surf. Sci. Catal.*, 59 (1991) 395.

132. R. Raja and P. Ratnasamy, *Appl. Catal.*, 143 (1996) 145.

133. W.W. Kaeding, *J. Catal.*, 120 (1989) 409.

134. K.H. Chung, T. Komatsu, S. Namba, T. Yashima, *Microporous Mater.*, 3 (1995) 377.

135. J. Weitkamp and M. Neubar, *Stud. Surf. Sci. Catal.*, 60 (1991) 241.

136. A. Katayama, M. Toba, G. Takeuchi, F. Mizukami, S. Niwa and S. Mitamura, *J. Chem. Soc. Chem. Commun.*, (1991) 39.

137. C. Song and S. Kirby, *Microporous Mater.*, 2 (1994) 467.

138. S.J. Chu and Y.W. Chen, *Appl. Catal.*, 123 (1995) 51.

139. P. Moreau, A. Finiels, P. Geneste and J. Solofo, *J. Catal.*, 136 (1992) 487.

140. G.S. Lee, J.J. Maj, S.C. Rocke, J.M. Garces, *Catal. Lett.*, 2 (1989) 243.

141. J.R. Butruille and T.J. Pinnavia, *Catal. Lett.*, 2 (1989) 187.

142. F.C. Friedel and J.M. Crafts, *Bull. Soc. Chim. Fr.*, 27 (1877) 530.

143. R.M. Roberts and A.A. Khalaf, in *Friedel-Crafts Alkylation Chemistry, A Century of Discovery*, Marcel Dekker, New York, (1982).

144. L.B. Young, *US Pat.*, 3,962,364 (1976).

145. W.W. Kaeding, L.B. Young and C.C. Chu, *J. Catal.*, 89 (1984) 267.

146. F.A. Drahowzal, in *Friedel-Crafts and Related Reactions*, G.A. Olah (Ed.), Wiley, New York, 2 (1964) 446.

147. S.H. Patinkin and B.S. Friedman, in *Friedel-Crafts and Related Reactions*, G.A. Olah (Ed.), Wiley, New York, 2 (1964) 1.

148. G. Klug, H.J. Buysch and L. Pappe, *Ger. Offen. DE*, (1989) 3803662.

CHAPTER 2

SYNTHESIS, MODIFICATION AND CHARACTERIZATION OF LARGE PORE ZEOLITES

2.1 Introduction

Zeolite Beta was first synthesized by Wadlinger, Kerr and Rosinski.[1] The silica to alumina ratio of the as synthesized sample was between 10 and 200 and tetraethylammonium hydroxide (TEAOH) was used as the organic templating agent. Pérez-Pariente et al.[2] found that zeolite Beta nuclei were formed via a liquid phase synthesis mechanism and aluminium is an essential element of the precursor species. It possesses a three dimensional, 12-membered ring (MR) pore system. Other researchers have since found[3,4] that zeolite Beta is a disordered intergrowth of two isomorphs which are permeated by a tridimensional network of 12-MR ring channels. Both isomorphs result from the same centrosymmetrical, tertiary building units arranged in layers. Fig. 2.1 (a) and (b) depict representation of the framework structures of these zeolite Beta polymorphs. The density of stacking faults in the zeolite Beta structure is high relative to other zeolites because successive layers must interconnect in either a left- or right-handed fashion. The dimension of the pores are 7.5 × 5.7 Å along the linear channels and 6.5 × 5.6 Å along the tortuous channels.[5]

Zeolite ZSM-12 was first synthesized by Rosinski and Rubin[6] using a mixture of diethylsulphate and triethylamine as organic templates. Since then, various other organic additives such as (i) quaternary tetraalkylammonium[7,8] and mixed alkyl/aryl ammonium[9,10] compounds, (ii) dimethylpyrrolidium bromide and (iii) diquaternary ammonium cations[11,12] have been used for the synthesis of ZSM-12. Shou-He and Hexuan[13] reported that ZSM-12 can be synthesized with silica to alumina ratios of 45 to ∞ (i.e., silicalite) using methyltriethylammonium bromide (MTEABr) as an organic template. Later, Ernst et al.[14] extended this work and studied the influence of gel composition and crystallization kinetics. Ernst and coworkers found that, sodium cations seemed to intervene in the nucleation and crystal growth process whereas MTEA
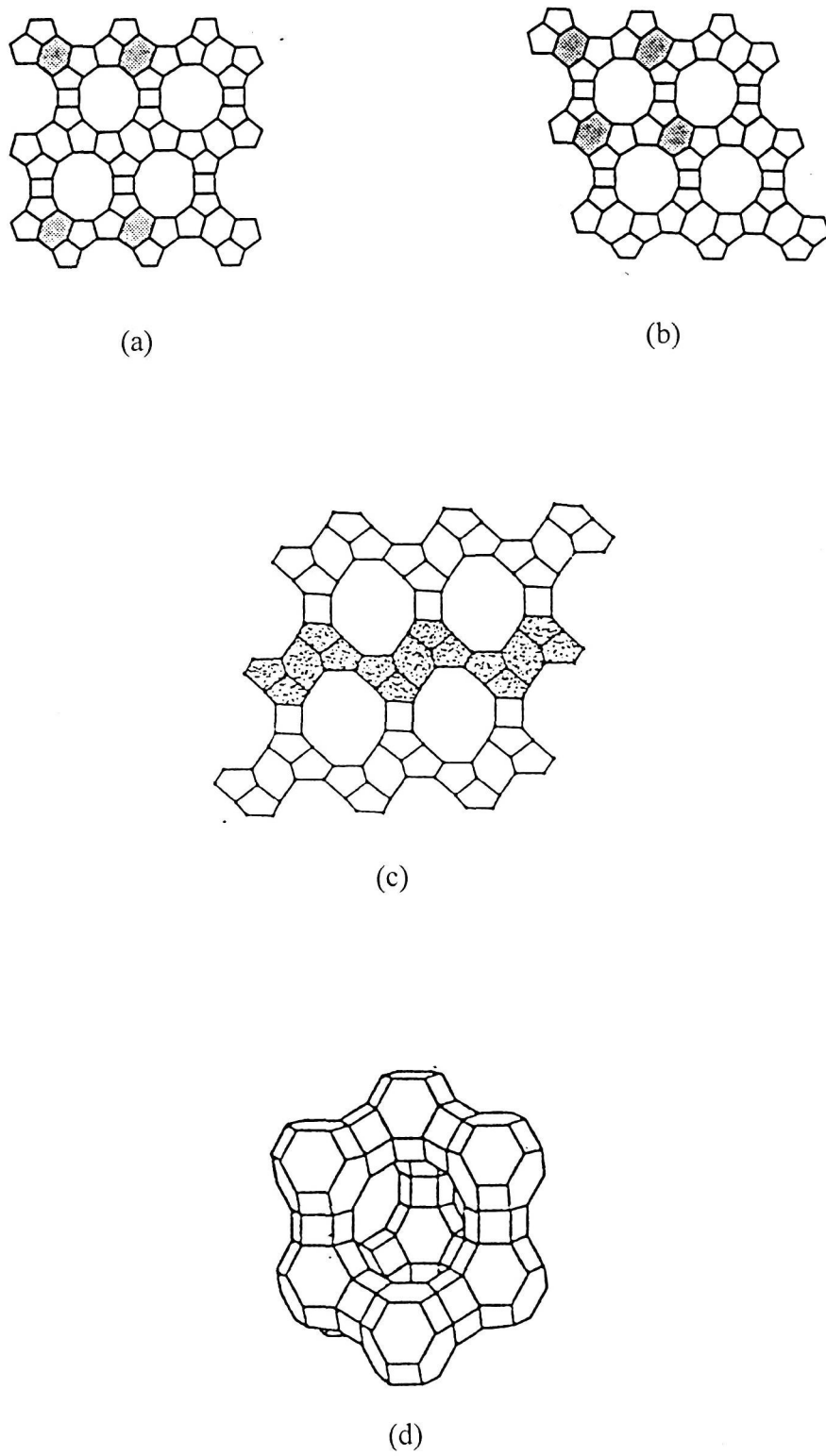
Fig. 2.1 Framework structures of zeolites (a) Beta: Polymorf A, (b) Beta: Polymorf B, (c) ZSM-12, and (d) Y

probably acted only as a pore filling agent. Similar to ZSM-5 synthesis, they found that, diluting the synthesis mixture increased the crystal size, and increasing the SiO_2/Al_2O_3 ratio in the gel enhanced the rate of crystallization. The pore structure of ZSM-12 consists of linear, non-interpenetrating, unidimensional channels having a 12-MR openings. The aperture of the ring is 5.7×6.1 Å. Fig. 2.1 (c) presents a representation of ZSM-12's pore system. The presence of twinning and inergrowth in the framework of ZSM-12 has resulted in constraints in the long range percolation of its channel system.

Zeolite Y consists of linked truncated octahedra called sodalite units, which have a cage of diameter 6.5 Å (β cage) and accessible through six membered rings of oxygen atoms.[15] These units are connected along two six membered rings, giving rise to hexagonal prism. The polyhedra formed in this way encloses a supercage (α cage) with an internal diameter of 12.5 Å and accessible through four 12-membered rings of oxygen atoms with a free aperture of 7.4 Å. The framework structure of zeolite Y is depicted in Fig. 2.1 (d).

In this chapter, the syntheses of zeolite Beta and ZSM-12 are described. Beta has also been modified by ion exchange with cations such as La^{3+}, Mg^{2+}, Cs^+ and K^+. All the samples are characterized by various physico-chemical techniques. Commercially obtained NH_4-Y zeolite has been converted to its protonic form and also modified by ion exchange with rare earth cations.

2.2 Synthesis and Modification

2.2.1 Synthesis of Zeolite Beta

Zeolite Beta was synthesized hydrothermally from a $(TEA)_2O$- Na_2O-SiO_2-Al_2O_3-H_2O system. The reaction gel was prepared by mixing appropriate amount of silica sol (31.3 wt.% SiO_2), sodium aluminate (39 wt.% Al_2O_3, 27 wt.% Na_2O), sodium hydroxide

(99 wt.%, AR Grade), tetraethylammonium hydroxide (TEAOH, 40 wt.% solution in water, Aldrich) and distilled water. A typical synthesis procedure of a sample with silica to alumina ratio 30 is as follows: 1.42 g sodium aluminate, 1.28 g sodium hydroxide, 30 g TEAOH and 18.18 g distilled water were mixed together and stirred vigorously to obtain a homogeneous mixture. The mixture was then added slowly to 31.21 g silica sol in a polyethylene beaker and the mixture was stirred vigorously for 1 h. The pH of the final gel was 13.8 and the calculated molar composition of the gel was

$$4.5 \ Na_2O : 7.5 \ (TEA)_2O : 30 \ SiO_2 : Al_2O_3 : 593 \ H_2O$$
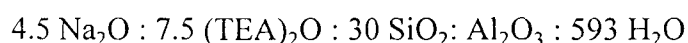
The final gel was transferred to a teflon lined stainless steel autoclave (capacity 200 ml, see Fig. 2.2) and hydrothermally treated at 423 K and autogeneous pressure for 7 days. After that the autoclave was quenched to room temperature in cold water. The solid material obtained was filtered, washed with distilled water and dried at 393 K. The crystalline sample thus obtained was calcined at 773 K for 24 h to decompose the organic template. The protonic form of the zeolite was obtained by repeated exchange with ammonium acetate solution (10 wt.%), followed by calcination at 773 K for 24 h in a flow of dry air. The yield based on total alumina input was more than 90%.

2.2.2 Preparation of Cation-Exchanged Zeolite Beta

La-H-Beta and Mg-H-Beta were prepared by treating 5 g of H-Beta synthesized by the method described above with 100 ml of a 2 wt.% solution of lanthanum chloride and magnesium acetate respectively at 353 K for 8 h. The exchange was repeated thrice. After the exchange, the samples were thoroughly washed with deionized water until the filtrate was free from acetate and chloride ions. The samples were then dried at 393 K and calcined at 773 K for 12 h.

Cs-H-Beta and K-H-Beta were prepared by ion-exchange with 0.5M solution of cesium and potassium chloride respectively. 5 g of H-Beta was treated with 100 ml 0.5M of chloride solution of the corresponding metal-chloride salt at 353 K for 8 h. The

31
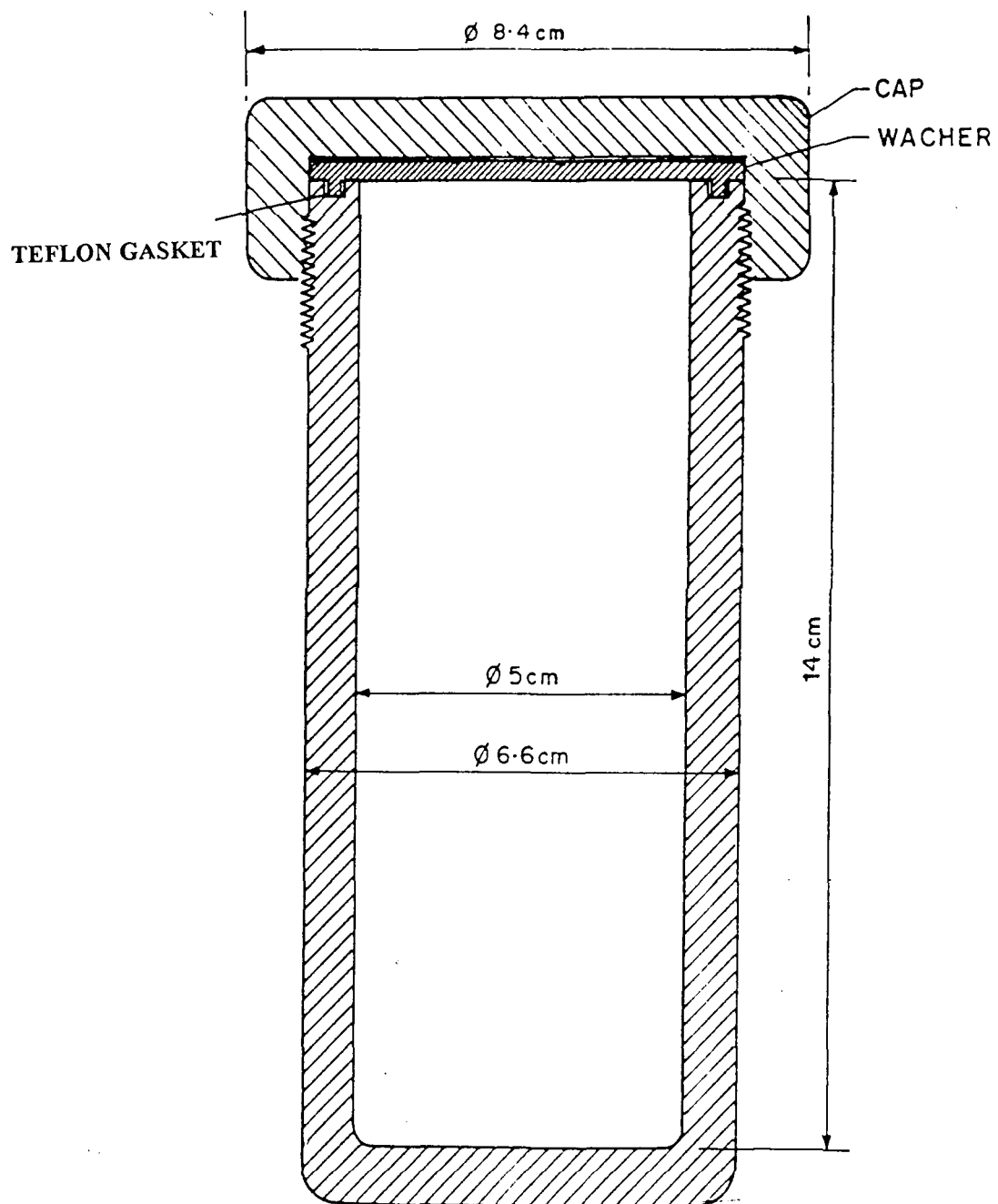
Fig. 2.2 Stainless-steel autoclave with teflon gasket for hydrothermal synthesis

material was then washed with distilled water until the filtrate was free from chloride ions followed by drying and calcining in the same manner described above.

2.2.3 Synthesis of Zeolite ZSM-12

Zeolite ZSM-12 was synthesized following the procedure described by Ernst *et al.*[14] from a system consisting of $(MTEA)_2O$- Na_2O-SiO_2-Al_2O_3-H_2O. The reaction gel was prepared by mixing appropriate amount of sodium silicate (28.6 wt.% SiO_2, 8.8 wt.% Na_2O, 62.7 wt% H_2O), aluminium nitrate [$Al(NO_3)_3.9H_2O$, BDH, 99 wt.%), methyltriethylammonium bromide (MTEABr, Aldrich, 99 wt.%), conc. H_2SO_4 (Ranbaxy, 98 wt.%) and distilled water. In a typical procedure, 13.48 g of sodium silicate solution was mixed with 13 g distilled water in a polyethylene beaker. While stirring this mixture, a solution of 5 g MTEABr in 17 g distilled water was added, followed by a solution containing 0.32 g $Al(NO_3)_3.9H_2O$ in 5 g distilled water. Finally a solution of 1.11 g of H_2SO_4 in 15 g distilled water was added to the above mixture and the gel was stirred for 1 h. The pH of the final gel was 10.7. The molar composition of the gel was

$$\frac{SiO_2}{Al_2O_3} = 150, \quad \frac{OH^-}{SiO_2} = 0.2, \quad \frac{Na_2O}{(MTEA)_2O} = 1.5, \quad \frac{H_2O}{OH^-} = 250$$

The gel was transferred to a teflon lined stainless steel autoclave and treated at 423 K for 10 days. Afterwards the autoclave was quenched with cold water and the solid crystalline material was filtered, washed with distilled water and dried at 393 K. The organic matter inside the zeolite was decomposed by calcining the sample at 773 K for 24 h. The protonic form of the zeolite was obtained by repeated exchange with 10 wt.% ammonium acetate solution at 353 K for 8 h followed by washing with distilled water, drying at 393 K and calcining at 773 K for 24 h in a flow of dry air. The yield based on total alumina input was more than 95%.

2.2.4 Preparation and Modification of Zeolite H-Y

Ammonium form of zeolite Y (NH$_4$-Y) was obtained commercially from Union Carbide, USA. The protonic form of the zeolite was prepared by calcining the catalyst at 773 K for 24 h in a flow of dry air. To convert this material to rare earth, cation exchanged Y zeolite, the H-Y was exchanged with 15 wt.% solution of didymium nitrate at 353 K for 8 h. Didymium nitrate is a mixed rare-earth salt containing approximately 18 wt.% Pr, 48 wt.% Nd and the rest being La and a few percent of other rare-earth elements. After the ion-exchange, the sample was filtered, washed with distilled water and dried at 393 K. Finally, the sample was calcined at 773 K for 24 h in presence of air.

2.3 Physico-Chemical Characterization

The applications of several of the physico-chemical characterization techniques to zeolite chemistry have been described in Chapter 1 (i.e., XRD, IR, TG-DTA and TPD). The sorption properties of zeolites have also been included in Chapter 1 as well as by various authors in the literature.[16-20] Principles of SEM technique and examples of application of SEM characterization of zeolites are also available in the literature[21-25] and will not be described in detail here. A careful development of BET methods to measure the surface area of porous media have been presented by Gregg and Sing[26,27] and further details about this method are beyond the scope of this chapter. In the application of porosimetry measurements to determine zeolite surface area, pore volume and pore size distribution, several authors provide extensive background information.[28-30] The XRF measurements made in connection with this thesis focused primarily on cross checking the Si/Al ratio determined by chemical methods. Again, detailed information on the principles of the XRF technique and its application for the determination of Si/Al ratio are available in the literature[31,32] and are beyond the scope of this chapter.

X-Ray Diffraction

The samples synthesized and used during the course of present work were analyzed by X-ray diffraction (XRD) for qualitative and quantitative phase identification. The XRD pattern of the samples were recorded using an automated diffractometer (Model D-MAX-III VC, Rigaku, Japan) with a Ni filtered CuKα radiation (λ = 1.5404 Å). Data were collected in the 2θ range of 5° to 50° at a scan rate of 2°/min with silicon as an internal standard.

Scanning Electron Microscopy (SEM)

The morphology of the samples were investigated using a scanning electron microscope (JEOL JSM 5200). The sample was suspended in ethanol and a thin film was evaporated on a brass sample holder. The sample was then coated with a thin film of gold to prevent surface charging and to protect the zeolite material from thermal damage by the electron beam. For all samples a uniform thickness of about 0.1 mm was maintained.

Thermal Analysis

The thermal analysis of the samples were carried out on a Thermogravimetric-differential thermal analysis (TG-DTA) instrument (Model TG/DTA-32, Seiko Instruments Inc., Japan). The analysis conditions are given below:

Rate of heating:	283 K/min
Temperature:	298 K to 1273 K
Purge gas:	Air
Wt. of the sample:	5 to 10 mg
Reference material:	α alumina

The temperature at any point on the thermogram is displayed by the computer to the accuracy of 0.1°C. The sample was placed in a platinum pan and was put on the sample pan of the thermobalance. The weight of the sample was automatically recorded with an

accuracy of ±1 μg. The reference material was placed in the second pan and the amount of the material was adjusted by compensating the weight of the sample. The TG sensitivity of the instrument was ±25 μg while those of DTG and DTA were ±1 μg and ±1 μV respectively.

Infrared Spectroscopy

IR spectra of the samples were recorded in the scan range of 400-1300 cm^{-1} using a Perkin Elmer spectrometer (Model 1620). Samples were mixed with KBr and pressed to make a thin film which was used for recording the spectra.

Surface Area Measurement

Omnisorp 100 CX (Coulter Corporation, USA) unit was used for the measurement of surface area of the samples. The sample was activated at 673 K for 2 h in high vacuum (10^{-6} mm). The anhydrous weight of the sample was measured and the sample was cooled to 94 K using liquid nitrogen and allowed to adsorb nitrogen gas. Finally surface area of the sample was calculated by the BET method.[26]

Sorption Measurement

The sorption measurements of water and liquid hydrocarbons were carried out in an all-glass McBain gravimetric adsorption unit. A diagram of the sorption unit is shown in Fig. 2.3. A silica spring (sensitivity 68 cm/g) was used for the measurement of changes in weight. The sample (50-60 mg) was pressed into a pellet and weighed taking it in an aluminium bucket and the bucket was fixed to the spring. The unit was then evacuated by means of two stage rotary pump and mercury diffusion pump to 10^{-6} Torr. The sample was then dehydrated at 673 K in the vacuum until a constant weight was obtained. The sample was then cooled by immersing in a thermoflask containing cold water and exposed to the adsorbate at the desired vapor pressure. The change in the weight of the

To low vacuum

To high vacuum

Gas supply (NH₃)

A - Silica spring
B - Aluminium bucket
C - Furnace or Thermostat
D - Thermocouple
E - Reference point
F - Liquid bulb
G - Thermoflask
H - Baratron pressure gauge
I - Gas reservoir
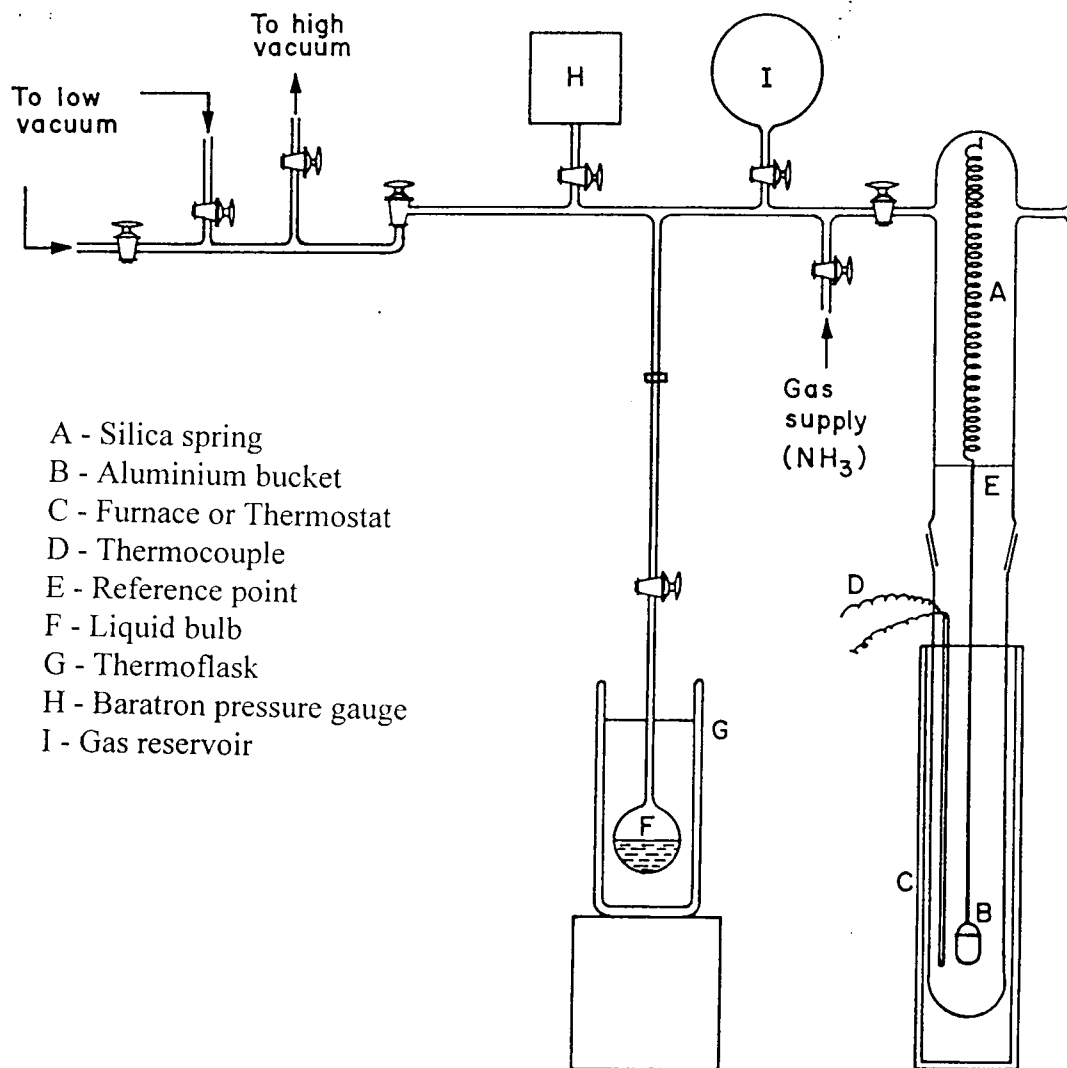
Fig. 2.3   All glass gravimetric adsorption unit

37

sample due to sorption was measured on an optical scale (accuracy ± 0.01 mm) as a function of time.

Chemical Analysis

A known amount of sample (~ 0.5 g) was taken in a platinum crucible and burned in air until a constant weight was obtained. The residue was then dissolved in 10 ml HF (40%) and evaporated to dryness. The procedure was repeated twice. From the loss in weight, amount of silica in the sample was estimated. The residue was then dissolved in 1:1 dilute HCl and the solution was diluted to a known volume by adding distilled water. Chemical analysis of the solution was performed using atomic absorption spectrometer (Model Z-8000, Hitachi, Japan).

For the analysis of rare earth elements in the zeolites, a known amount of sample was ignited with a fusion mixture and extracted with 1N HCl solution. The procedure was repeated to ensure the complete extraction of rare earth elements. The pH of the solution was adjusted to 4-5, oxalic acid solution (1N) was added to extracted solution and rare earth ions were precipitated as rare earth oxalates. The precipitate was filtered, washed thoroughly with distilled water to remove chloride ion, and the precipitate was calcined to convert the oxalates into rare earth oxides. The amount of rare earth atoms were then estimated gravimetrically from the oxide residue.

X-ray Fluorescence Spectroscopy (XRF)

Silica to alumina ratios of the samples were verified by XRF using a wavelength dispersive X-ray spectrometer (Rigaku, 3070) with rhodium target energized at 45 KV and 40 MA. The borate fusion technique was applied for sample preparation. For the calibration of silica and alumina, a pentaerythrital (PET) crystal was used. For the analysis Kα lines were selected and pulses were collected for 40 s using flow-proportional detector. A background correction was applied.

Acidity Measurement

Temperature programmed desorption (TPD) of NH_3 was carried out to evaluate the acidic properties of the zeolites. A SORBSTAR unit (Model 200, Institute of Isotopes, Hungary) was used for the measurements. 0.3 g zeolite sample was crushed, pelleted and sieved to 10-20 mesh size and placed in a quartz holder. In a flow of argon, the sample was slowly heated up to 773 K and was maintained at this temperature for 2 hrs. The sample was then cooled down to room temperature. Pure ammonia gas was allowed to pass over the sample for 2 hrs. Nitrogen was then passed over the sample at room temperature for 2 hrs. to desorb the physically adsorbed ammonia. The ammonia chemisorbed at room temperature was desorbed stepwise in a flow of nitrogen (40 ml/min) at temperatures from 303 K to 823 K at the rate of 10 K/min and the concentration of desorption was recorded by a thermal conductivity detector.

2.4 Results and Discussion

The unit cell compositions of the large pore zeolites used in the present study are listed in Table 2.1. Some major crystallographic and physico-chemical properties of large pore zeolites namely H-Beta, H-Y and H-ZSM-12 are shown in Table 2.2. Lower sorption capacity of water and hydrocarbons in H-ZSM-12 indicates its lower void volume compared to H-Beta and H-Y due to its unidimensional channel system. The decrease in surface area from H-Beta to H-ZSM-12 is in accordance with the increase in crystallite size.

The X-ray diffractograms of as synthesized Beta and ZSM-12 zeolites are shown in Fig. 2.4 and Fig. 2.5 respectively. The XRD of commercially obtained zeolite NH_4-Y is also shown in Fig. 2.6. The D-values and relative intensities match well with the literature values.[1,2,6,14,15] High intensity of peaks, narrow peak shape and absence of any baseline

Table 2.1

Unit cell compositions of large pore zeolites

Sample	Unit cell composition (anhydrous)	No. of U.C./g × 10^{-20}
H-Beta	$H_{3.4}Na_{0.1}Al_{3.5}Si_{60.5}O_{128}$	1.5675
La-H-Beta	$H_{0.5}Na_{0.1}La_{0.9}Al_{3.3}Si_{60.7}O_{128}$	1.5192
Mg-H-Beta	$H_{2.1}Na_{0.1}Mg_{0.6}Al_{3.4}Si_{60.6}O_{128}$	1.5621
Cs-H-Beta	$H_{0.9}Na_{0.1}Cs_{2.3}Al_{3.3}Si_{60.7}O_{128}$	1.4528
K-H-Beta	$H_{0.8}Na_{0.1}K_{2.5}Al_{3.4}Si_{60.6}O_{128}$	1.5296
H-Y	$H_{57.5}Na_{0.5}Al_{58}Si_{134}O_{384}$	0.5223
H-ZSM-12	$H_{0.2}Na_{0.1}Al_{0.3}Si_{27.7}O_{56}$	3.5804

Table 2.2

Crystallographic and physico-chemical properties of large pore zeolites

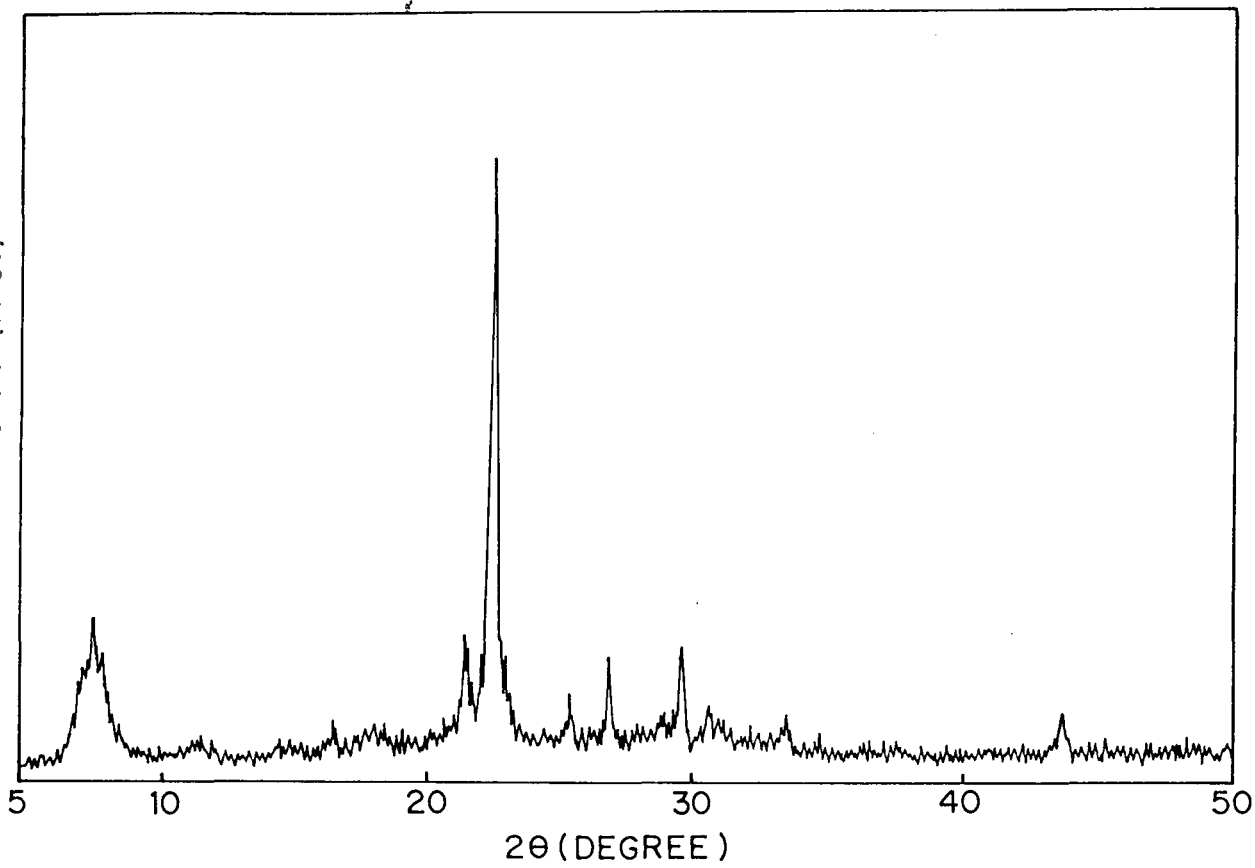| Catalyst	H-Beta	H-Y	H-ZSM-12
Channel Structure	Three dimensional with interlinking channels	Three dimensional with interlinking channels	Unidimensional with interlinking channels
Pore opening (12 MR, Å)	5.7 × 7.5 (linear) 5.6 × 6.5 (tortuous)	7.4	5.7 × 6.1
Unit cell crystal symmetry	Distorted	Cubic	Monoclinic
Crystal size (μm)	0.5-0.7	2.0	4-6
SiO_2/Al_2O_3	30	4.1	150
Surface area (m^2/g)	745	712	456
Sorption capacity (Wt.%)			
Water	21.3	23.2	7.6
Benzene	21.9	20.3	13.2
n-Hexane	19.0	18.5	10.1
Cyclohexane	19.8	19.2	11.4

Fig. 2.4   XRD pattern of zeolite Beta (as-synthesized)

42
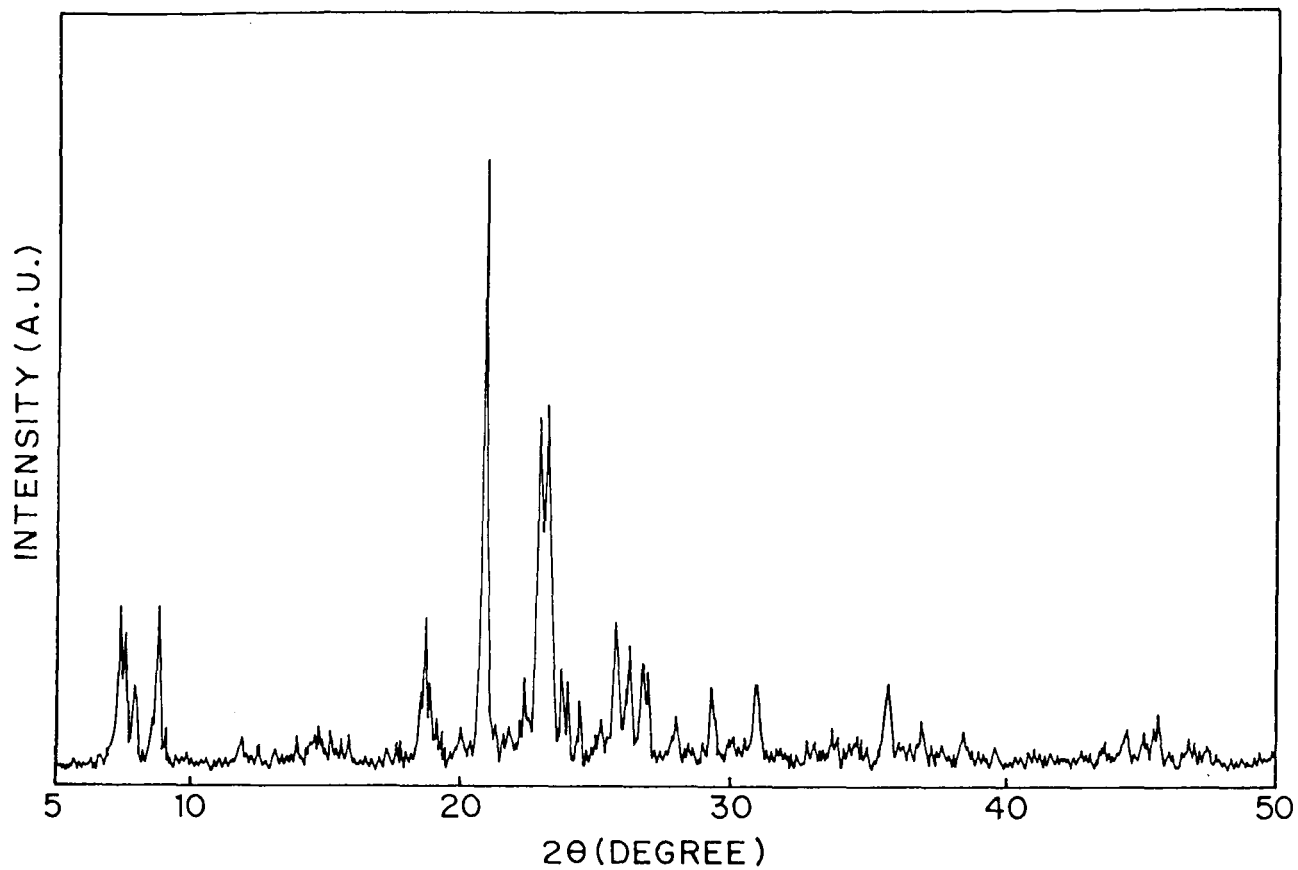
Fig. 2.5 XRD pattern of zeolite ZSM-12 (as-synthesized)

drift in the XRD patterns indicate that the samples are highly crystalline (98%). XRD patterns do not show the presence of other impurity phases.

Scanning electron micrographs of zeolite Beta and ZSM-12 are shown in Fig. 2.7, and these micrographs indicate the absence of any amorphous material or other crystalline phase impurities. The crystals of Beta zeolite are cuboid in shape with average size of 0.5 to 0.7 μm. The crystals of ZSM-12 are elongated in shape. The length and diameter of the crystals are 4 to 6 μm and 1 μm respectively which are similar to the literature values.[14]

The TGA-DTA-DTG patterns of as synthesized Beta are shown in Fig 2.8. The DTA pattern shows four stages which correspond to the temperature zones of approximately 298 K-561 K, 561 K-663 K, 663 K-773 K, and 773 K-973 K. The first step is slightly endothermic and assigned to the desorption of water. The other three zones are exothermic and are associated with the oxidation of organic materials. The first two exothermic steps are ascribed to the decomposition of TEAOH occluded in the zeolite and pyrolysis of TEA$^+$ cations respectively. The exothermic step at 773 K-973 K is ascribed to the oxidative decomposition of residual coke formed by the decomposed template materials occluded in the zeolite channels. These steps in DTA pattern are complementary to the steps in TGA and DTG patterns. Similar observations were also noticed by Pérez-Pariente et al.[2] The TGA-DTG-DTA patterns of as synthesized ZSM-12 are presented in Fig. 2.9. The DTA pattern shows two distinct steps, the first endothermic and the second exothermic. The endothermic step corresponds to the water desorption from the zeolite whereas the exothermic step results from the decomposition of organic template. There is also a shoulder in the DTA pattern at approximately 773 K which contributes to the exothermic step. However, analysis of the combination of TGA and DTG curves revealed that, there are four distinct steps of weight loss which correspond to the temperature zones of approximately 298 K-523 K, 523 K-678 K, 678 K- 773 K, and

Fig. 2.6   XRD pattern of zeolite NH_4-Y

(a)

(b)
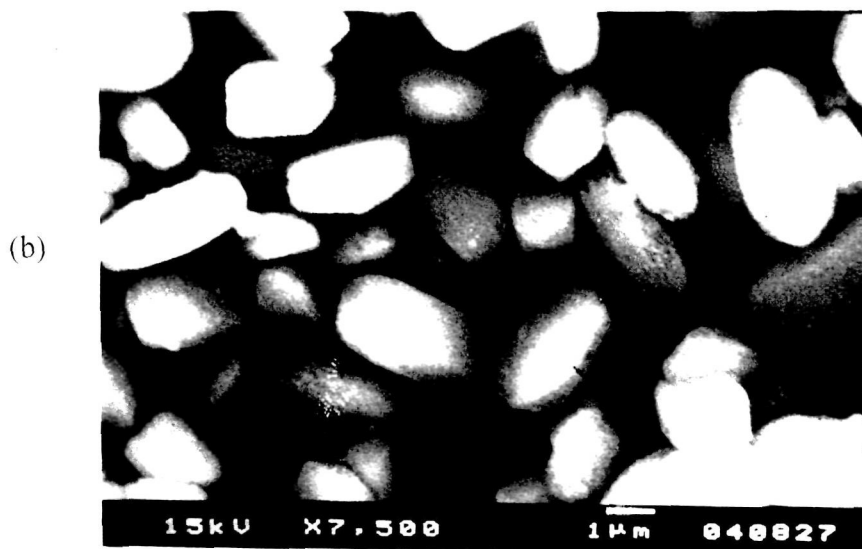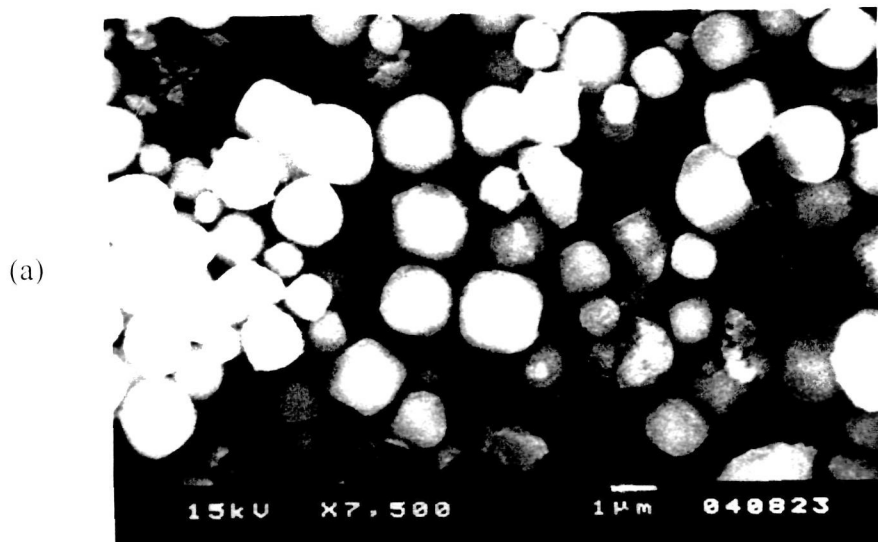
Fig. 2.7   SEM photographs of (a) zeolite Beta, (b) zeolite ZSM-12
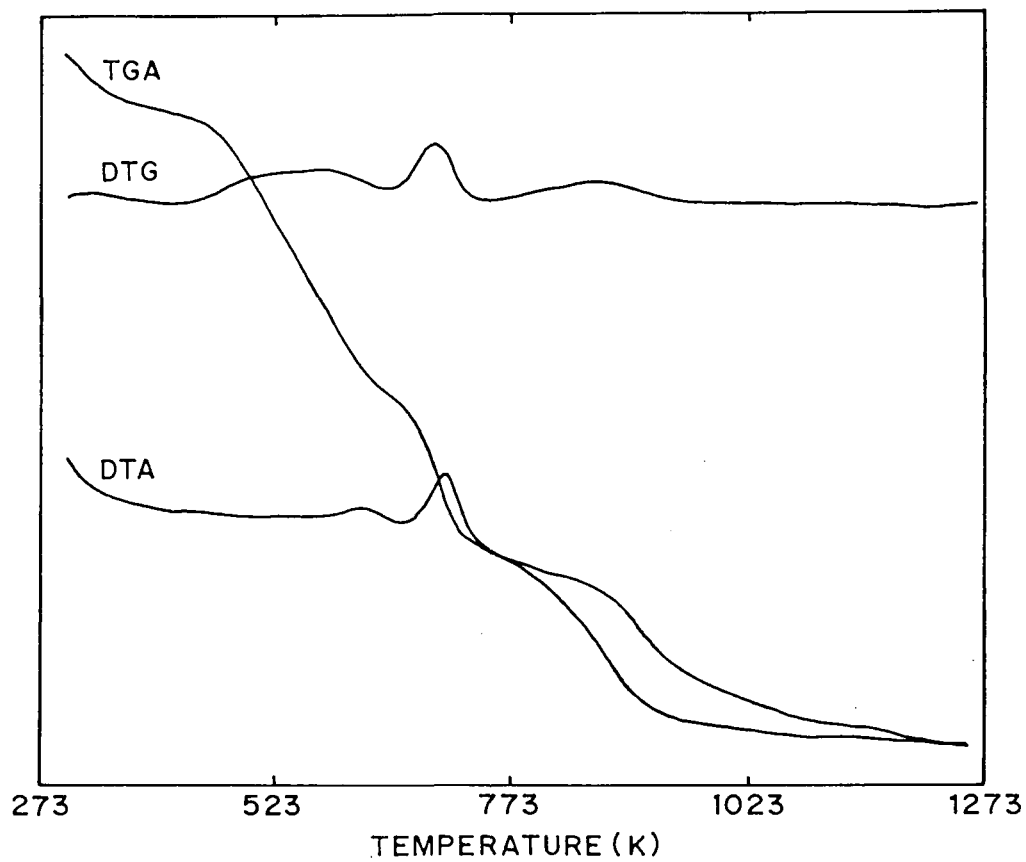
Fig. 2.8   Thermograms of zeolite Beta (as-synthesized)

47

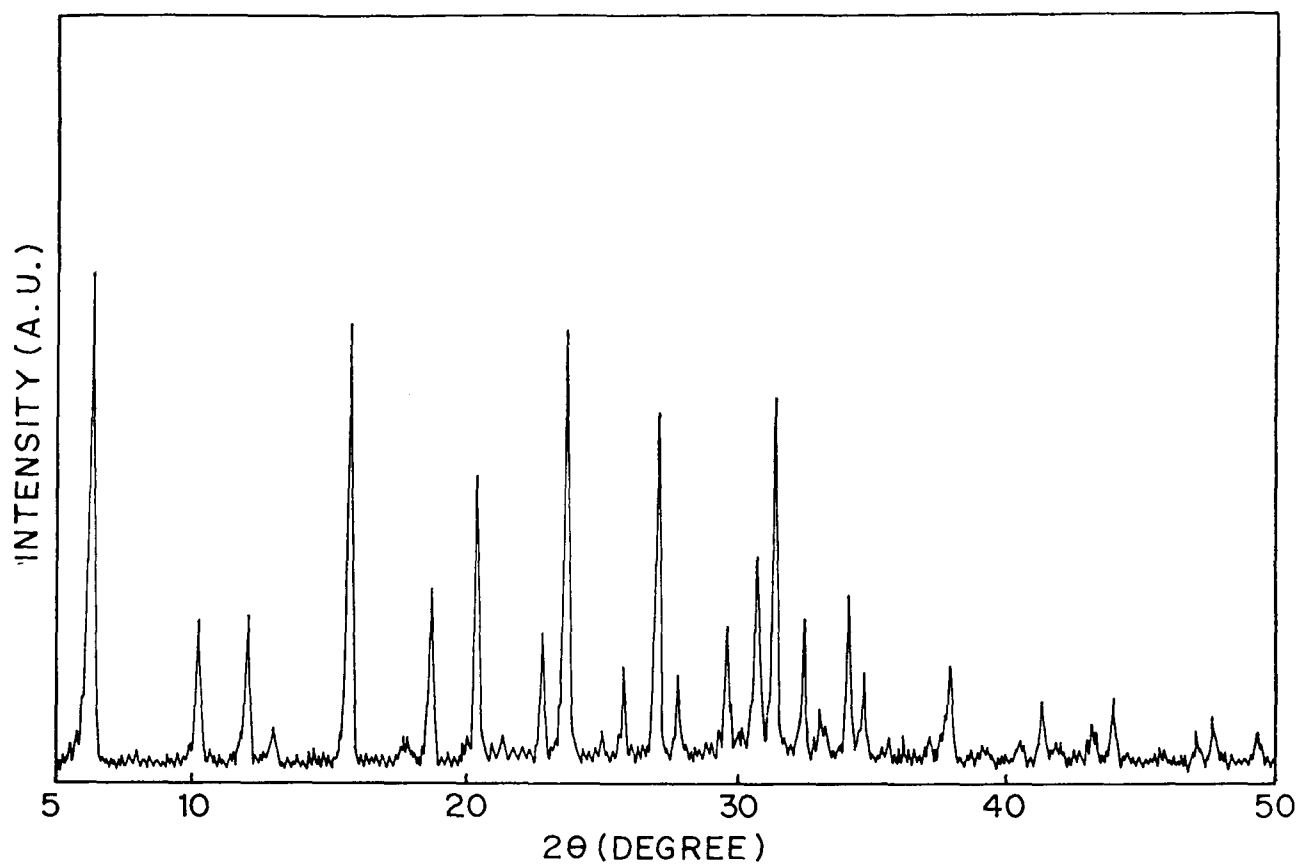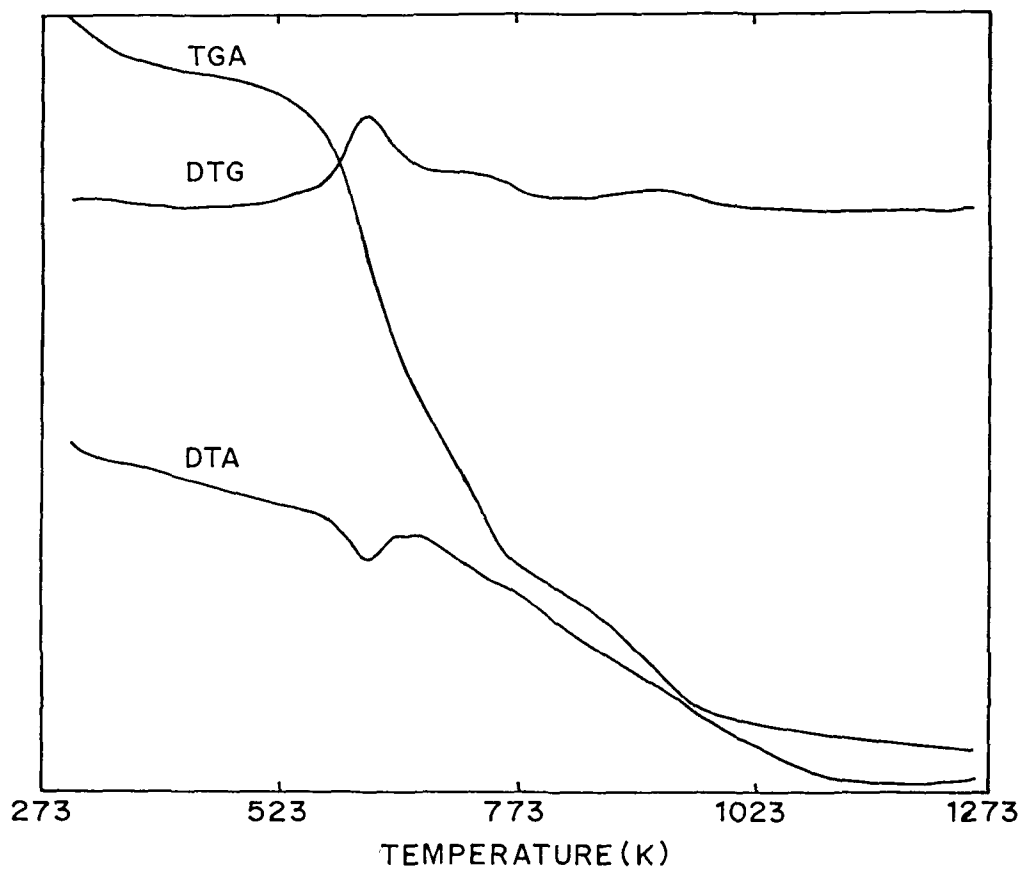**Fig. 2.9**   Thermograms of zeolite ZSM-12 (as-synthesized)

773 K-953 K. The energetic of fourth TG/DTG region is not clearly represented in the DTA trace.

The IR spectra of H-Beta recorded in the framework region (450 cm^{-1}-1300 cm^{-1}) is shown in Fig. 2.10. The major absorption bands found are 1225 cm^{-1}, 1096 cm^{-1}, 800 cm^{-1}, 728 cm^{-1}, 615 cm^{-1}, 572 cm^{-1}, 520 cm^{-1} and 465 cm^{-1}. Among these bands, the bands at around 575 cm^{-1} and 525 cm^{-1} (572 cm^{-1} and 520 cm^{-1} respectively in the present study) are characteristic structural bands of zeolite Beta.[2] The bands around 1096 cm^{-1}, 800 cm^{-1} and 465 cm^{-1} correspond to asymmetric stretching, symmetric stretching and T-O bending vibrations of internal tetrahedra respectively.[33] The band at 1225 cm^{-1} indicates the presence of 5-membered ring in the zeolite framework.[34] Fig. 2.11 depicts the framework IR spectra of H-ZSM-12 zeolite. The major absorption bands found are 1225 cm^{-1}, 1074 cm^{-1}, 788 cm^{-1}, 725 cm^{-1}, 635 cm^{-1}, 583 cm^{-1}, 547 cm^{-1} and 480 cm^{-1}. Bands around 1074 cm^{-1}, 788 cm^{-1}, and 480 cm^{-1} correspond to asymmetric stretching, symmetric stretching and T-O bending vibrations of internal tetrahedra respectively[33] and a band around 583 cm^{-1} indicates the presence of double five membered ring in the framework.[34]

The NH$_3$-TPD spectra of Beta, Y and ZSM-12 are shown in Fig. 2.12. In general, TPD profile of acidic zeolites show three peaks. According to Lok *et al.*,[35] for low Si to Al ratio (Si/Al < 10) zeolites, the first NH$_3$-TPD peak is associated largely with weakly chemisorbed NH$_3$ molecules. However, for high Si to Al ratio (Si/Al > 10) zeolites the first NH$_3$-TPD peak represents mainly physically adsorbed NH$_3$ molecules. The second NH$_3$-TPD peak is associated with NH$_3$ molecules adsorbed on hydroxyl groups. The third peak is associated with dehydroxylation, strong Brönsted acid sites and/or Lewis acid sites. As expected, the TPD profile of large pore zeolites reveals that HY possesses the highest total acidity and H-ZSM-12 shows lowest total acidity. The results are in accordance with their silica to alumina ratios. The NH$_3$-TPD spectra of H-Beta and cation exchanged H-Beta are shown in Fig. 2.13. The second and third peaks are absent in the
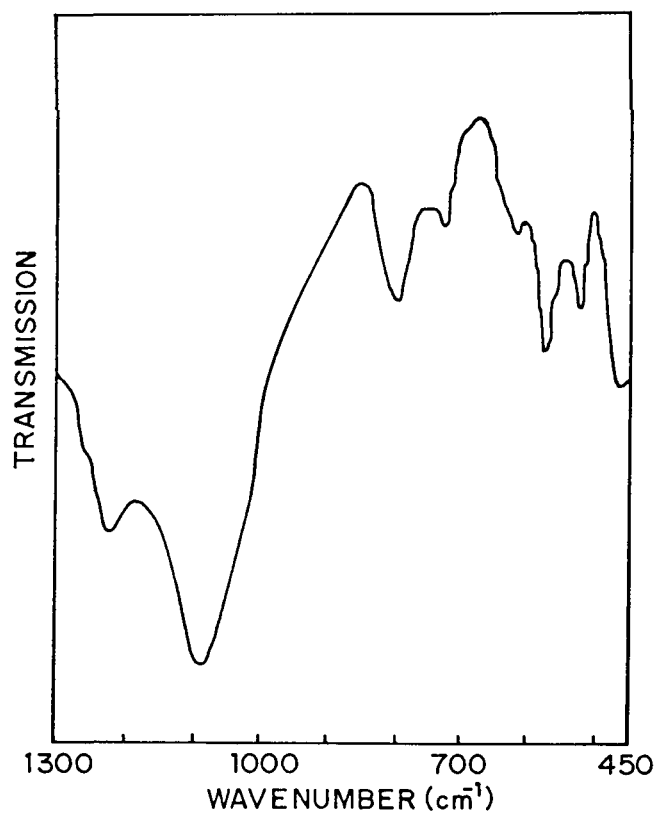
Fig. 2.10   Framework IR spectra of zeolite Beta

50
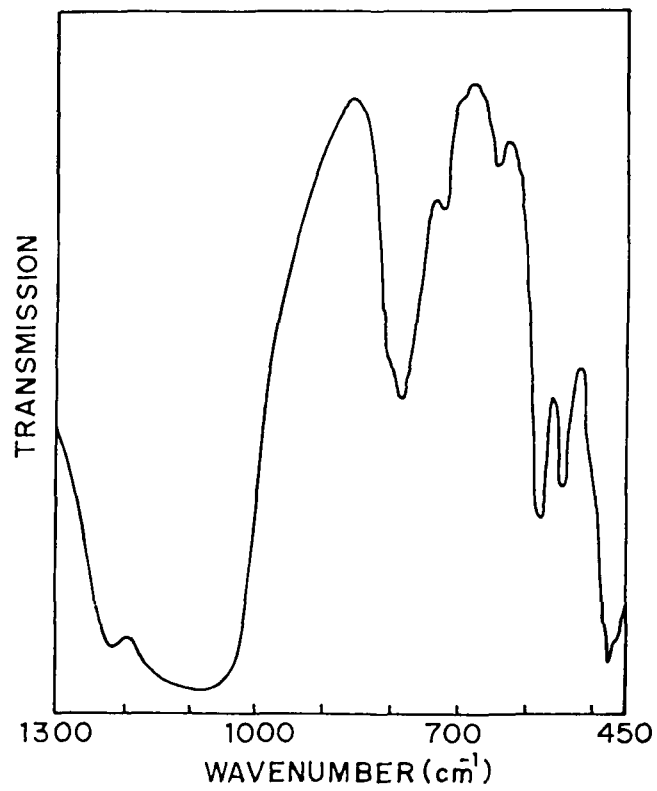
Fig. 2.11   Framework IR spectra of zeolite ZSM-12
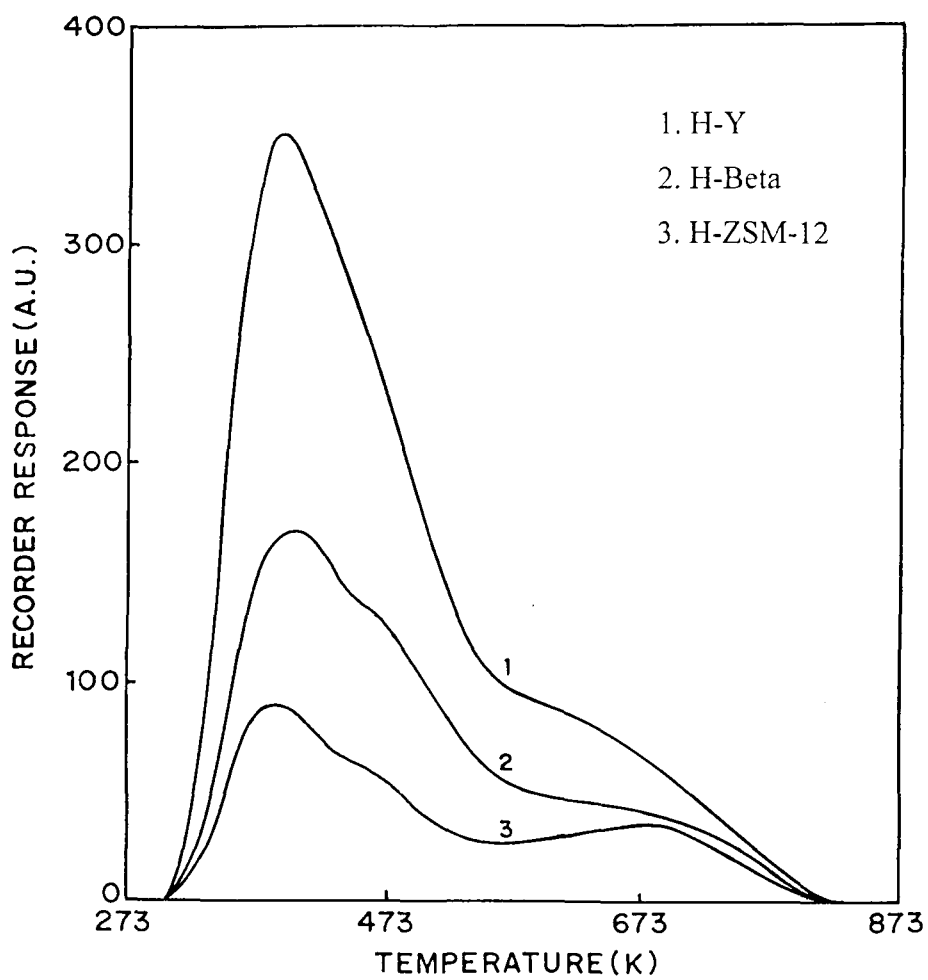
Fig. 2.12 NH₃-TPD profile of large pore zeolites
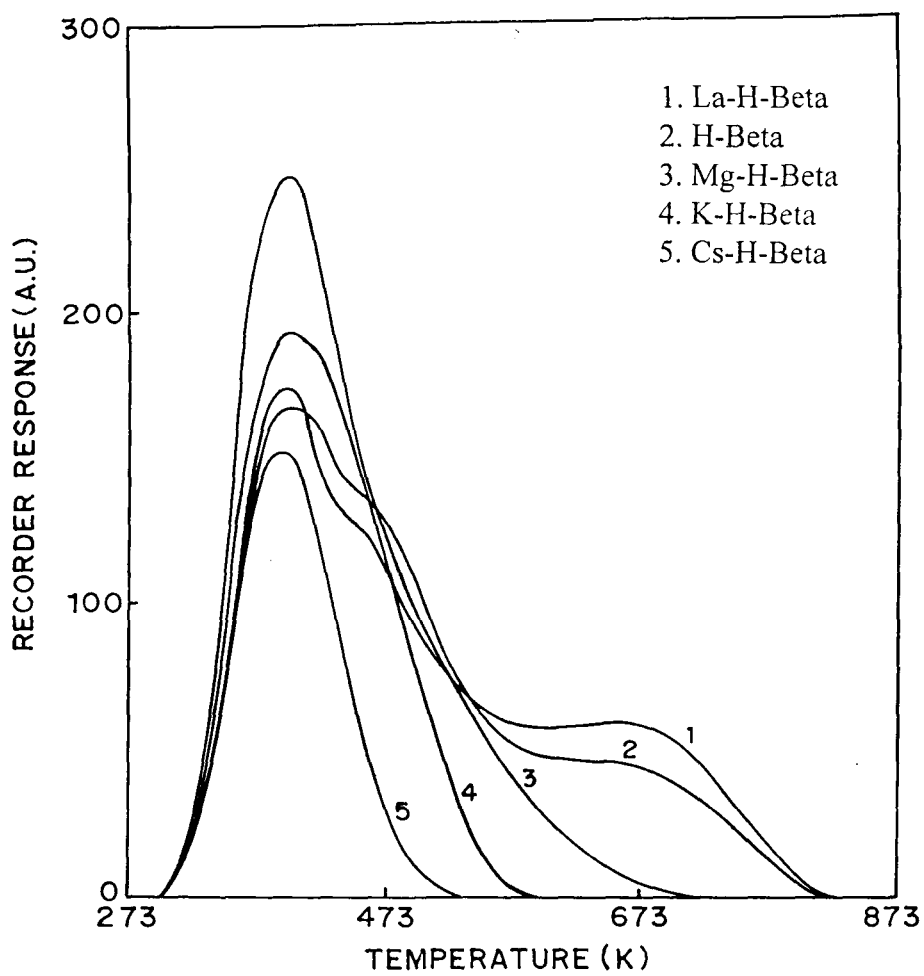
Fig. 2.13   NH$_3$-TPD profile of Beta and cation exchanged Beta zeolites

53

case of Cs-, K-, and Mg-exchanged Beta, which indicates their suppressed acidity. In La-H-Beta, the second NH3-TPD peak is lower than that of H-Beta, whereas the intensity of third peak is enhanced compared to H-beta, indicating the presence of stronger acid sites. Jacobs[36] has suggested that enhancement may be due to the hydrolysis of the water associated with the lanthanum ions to form species of the type as shown below, where the H^+ ion in the structure is believed to be responsible for the acidity

$$-Si-O-Al-O-Si-$$
$$La^{2+} (OH) H^+$$
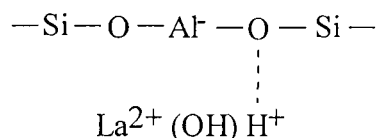
2.5 Conclusion

For the present study, large pore zeolites Beta and ZSM-12 were synthesized, and commercially obtained NH_4-Y was converted to its H-form. All the samples were characterized by various physico-chemical techniques. XRD patterns of the zeolites confirmed their high crystallinity and phase purity. Scanning electron micrographs of the zeolites revealed their crystal size and morphology, and confirmed their phase purity. IR analysis of the samples produced characteristic absorption bands which were well-matched with earlier studies. Thermal analysis of the samples showed their high thermal stability and provided other information such as the energetics and weight loss due to the desorption of water and organic template material. In the forthcoming chapters, the application of these samples to alkylation and transalkylation reactions for the syntheses of industrially important intermediates is discussed. Zeolites employed in this study differ principally in their framework structures and acidity. These differences described in this chapter will be shown to play a major role in the reactions mentioned above.

Zeolite Beta was modified by ion exchange with cations such as La^{3+}, Mg^{2+}, Cs^+ and K^+. The TPD analyses revealed that La^{3+} exchange created some distinct acidic

center, and Mg^{2+}, Cs^+ and K^+ exchanges reduced the acidity. Acidity differences due to La^{3+} and Mg^{2+} exchange in the H-Beta will be shown in the next chapter to influence the alkylation reactions. Basic centers created by alkali cations (e.g., Cs^+ or K^+) in H-Beta will be shown to influence the product patterns and catalytic performance in the transalkylation of aniline with N,N-dimethylaniline in Chapter 5.

2.6 References

1.   R.L. Wadlinger, G.T. Kerr and E.J. Rosinski, *US Pat.*, 3,308,069 (1969).

2.   J. Pérez-Pariente, J.A. Martens and P.A. Jacobs, *Appl. Catal.*, 31 (1987) 35.

3.   M.M.J. Treacy and J.M. Newsam, *Nature*, 332 (1988) 249.

4.   J.M. Newsam, M.M.J. Treacy, W.T. Koetsier and C.B. de Gruyter, *Proc. Royal Soc. Lond. A.*, 420 (1988) 375.

5.   R. Szostak, in *Handbook of Molecular Sieves*, Van Nostrand Reinhold, New York, (1992) 92.

6.   E.J. Rosinski and M.K. Rubin, *U.S. Pat.*, 3,832,449 (1974).

7.   P. Chu and G.H. Kuehl, *Eur. Pat. Appl.*, 18,089 (1980).

8.   G.H. Kuehl, *Eur. Pat. Appl.*, 14,795,2 (1985).

10.   M. K. Rubin, *Eur. Pat. Appl.*, 16,651,3 (1985).

11.   M. K. Rubin, *Eur. Pat. Appl.*, 16,723,2 (1985).

12.   E.J. Rosinski and M.K. Rubin, *US Pat.*, 4,391,785 (1983).

13.   X. Shou-He and L. Hexuan, *7th Int. Zeol. Conf.*, Tokyo, Japan, Preprints, Japan Association for Zeolites, (1986) 25.

14.   S. Ernst, P.A. Jacobs J.A. Martens and J. Weitkamp, *Zeolites*, 7 (1987) 458.

15.   D.W. Breck, *US Pat.*, 3,130,007 (1964).

16.   R.M. Barrer, *Proc. Royal Soc.*, A167 (1938) 392.

17.   R.M. Barrer and D.W. Riley, *Trans Faraday Soc.*, 46 (1950) 853.

18.   R.M. Barrer and A.B. Robins, *Trans Faraday Soc.*, 49 (1953) 1049.

19.   R.M. Barrer, *Pure Appl. Chem.*, 52 (1980) 2143.

20.   R.J. Neddenriep, *J. Colloid Interface Sci.*, 28 (1968) 293.

21. J.I. Goldstein, A.D. Romig, Jr., D.E. Newbury, C.E. Lyman, P.Echlin, C. Fiori, D.C. Joy and E. Lifshin, in *Scanning Electron Microscopy and X-Ray Microanalysis: A Text for Biologists, Material Scientists and Geologists*, 2nd Edn., Plenum Press, New York and London, (1992).

22. A. Nastro and L.B. Sand, *Zeolites*, 3 (1983) 57.

23. M. Ghamami and L.B. Sand, *Zeolites*, 3 (1983) 155.

24. G. Debras, A. Gourgue, J.B. Nagy and G.D. Clippeleir, *Zeolites*, 5 (1985) 369.

25. D. Demuth, G.D. Stucky, K.G. Unger, F. Schüth, *Microporous Mater.*, 3 (1995) 473.

26. S.J. Gregg and K.S.W. Sing, in *Adsorption, Surface Area and Porosity*, Academic Press, New York, 2nd Edn., (1982).

27. K.S.W. Sing in *Characterization of Catalysts*, J.M. Thomas and R.M. Lambert (Eds.), John Wiley and Sons, Chichester, (1980) 12.

28. D.H. Everett and J.C. Powl, *J. Chem. Soc. Faraday Trans.*, I, 72 (1976) 619.

29. E.G. Derouane, J.M. Andre and A.A. Lucas, *Chem. Phys. Lett.*, 137 (1987) 336.

30. A. Saito and H.C. Foley, *Microporous Mater.*, 3 (1995) 531.

31. P.W. Atkins, in *Physical Chemistry*, ELBS, London, (1978).

32. P.A. Gokhale and M.R. Wuensche, in *Advances in X-Ray Analysis*, C.S. Barrett *et al.* (Eds.), Plenum Press, New York, 33 (1990) 679.

33. E.M. Flanigen, H. Khatami and H.A. Szymanski, *Adv. Chem. Ser.*, 101 (1971) 201.

34. R. Szostak, in *Molecular Sieves, Principles of Synthesis and Modification*, Van Nostrand Reinhold, New York, (1989).

35. B.M. Lok, B.K, Marcus and C.L. Angel, *Zeolites*, 6 (1986) 185.

36. P.A. Jacobs, in *Carboniogenic Activity of Zeolites*, Elsevier, Amsterdam, (1977) 46.

CHAPTER 3

ALKYLATION REACTIONS OVER ZEOLITE BETA

3.1 Introduction

Zeolites have attracted considerable attention as catalysts as a result of their high activity and unusual selectivity for acid catalyzed reactions.[1-3] Due to the long operational time, ease of regeneration, and eco-friendly nature, zeolite catalysts find applications in many industrial alkylation reactions in the preparation of intermediates and end products such as ethylbenzene, isopropylbenzene and *para*-diethylbenzene.[4-12] A variety of reactants such as olefins, alcohols, ethers and alkyl halides have been used as alkylating agents for alkylation of aromatic hydrocarbons.[5,10,13-21] The acid catalyzed alkylation of aromatics is basically governed by electrophilic aromatic substitution which involves attack of an electron deficient species, $E^{\oplus}$ on an aromatic, ARH to form a larger aromatic product, AR-E.

$$E^{\oplus} + ARH \rightarrow Ar\text{-}E + H^{\oplus}$$
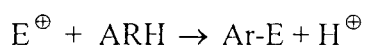
Here the aromatic ring may be viewed as a nucleophile, and in classical organic chemistry the reaction is believed to go through two steps. In the first step, the approaching electrophile interacts with the π orbitals of the aromatic to form a π complex, and the second step involves localized attack of the electrophile to form a σ complex or arenium ion.[22,23] Early studies on the alkylation of benzene and related aromatics with olefins on large pore zeolites revealed that a Langmuir-Rideal-type mechanistic pattern can correlate the chemical process.[24,25] In this mechanism (Fig. 3.1), it is proposed that an anionic lattice-associated carbenium ion is formed by attack of a proton on an olefin, and this carbenium ion is then attacked by a free or weakly adsorbed aromatic. There are several references which cite the carbenium ion-type mechanism for Friedel-Crafts type alkylations over large pore zeolites.[14,24,26-29] Zeolite catalyzed alkylation involving Langmuir-Rideal type mechanism has also been suggested by Coughlan et al.,[30] Weitkamp[31] and Ren et al.[32] However, studies in the alkylation of benzene with ethylene

R-CH=CH-CH3 ← RCH2CH=CH2 → oligomerization

RCH2CHCH3
      +

RCH2CH=CH2

H+   Ō-Zeol

CH3
CH-CH2R
H

CH3CH-CH2R
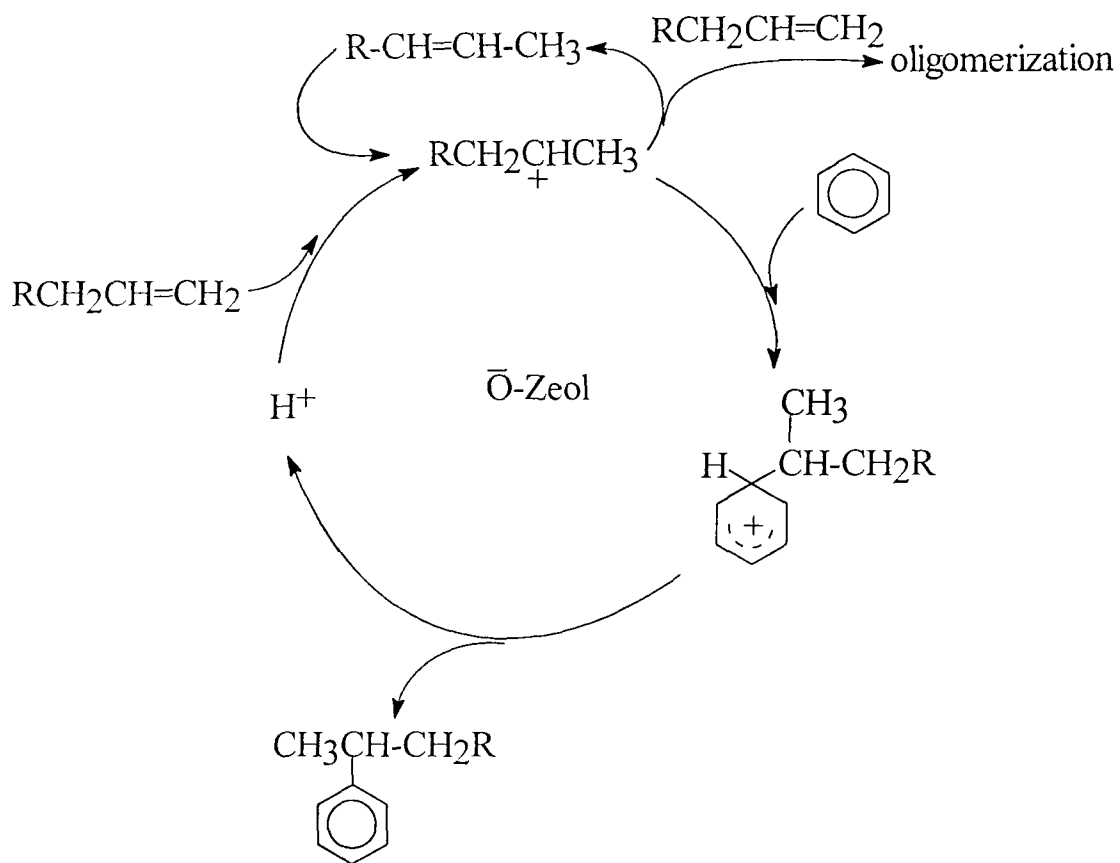
Fig. 3.1 Schematic representation of Langmuir-Rideal-type mechanism for aromatic alkylation with olefins over acidic zeolites

over H-Mordenite[5] and faujasite[33] revealed that no molecule within zeolite pores can really escape the field of sorption potential of the surrounding lattice, and thus, it is difficult to assume a Langmuir-Rideal-type mechanism in the strict sense i.e., adsorbed olefin and aromatic in the "gas phase", since any molecule within the zeolite pores is going to be subjected to the electric field gradients.[13] Thus, at least some degree of weak chemical adsorption of the aromatic through π bonding or hydrogen bonding via phenolic OH should be taken into account. The carbenium ion formed by the alcohols may lead to the formation of side products. The carbenium ion can undergo proton loss leading to olefin formation or intermolecular hydride abstraction leading to a paraffin formation. It can also undergo 1,2-shift involving either hydrogen or alkyl group to form a new ion.[34]

Zeolite Beta is a high silica zeolite, first synthesized by Wadlinger, Kerr and Rosinski.[35] It possesses a three dimensional 12-MR ring pore system. It was Treacy and Newsam[36] and Newsam et al.[37] who revealed that zeolite Beta is a disordered intergrowth of two isomorphs which are permeated by a tridimensional network of 12-membered ring channels. Both isomorphs result from the same centrosymmetrical tertiary building units arranged in layers. There is a high density of stacking faults in the zeolite structure, because successive layers must interconnect in either in a left or right handed fashion. The dimensions of the pores are 7.5 × 5.7 Å along the linear channels and 6.5 × 5.6 Å along the tortuous channels.[38] The pore dimensions of Beta are slightly smaller than Y but larger than Mordenite. Zeolite Beta can be synthesized in a wide range of silica to alumina ratios using TEA$^+$ as a template, and very small (<1 μm) crystallites are usually formed.[35,39,40]

Beta zeolite has high catalytic potential compared to the faujasite type zeolite by virtue of its high silica content, acid site distribution and stacking faults.[41] It has been widely studied as a Brönsted acid catalyst and has been shown to be active for reactions such as alkylation and acylation.[42,43] It is a strong acid catalyst for reactions such as

cracking of paraffins and gas oil.[44,45] In addition, zeolite Beta has been used for catalytic hydrodewaxing of petroleum oil, isomerization of m-xylene,[49] disproportionation and methylation of toluene.[50] Recent inventions disclose zeolite Beta to be a highly promising catalyst for the synthesis of cumene[51] using benzene and propylene. It is also reported to be used in the isomerization of n-hexane to dimethylbutanes.[52]

Cymenes (isopropyl toluene), especially the *meta* and *para* isomers are important intermediates for the production of cresols.[53] They are also used as raw materials for plasticizers. Moreover, *para*-cymene is also used as a heat transfer medium[54] and a starting material for many organic syntheses. Cymenes are important constituents in the production of polymers, fungicides, pesticides, perfumery, pharmaceuticals and special solvents.[55,56]

The main aim of this chapter is to study the catalytic applications of zeolite Beta in the formation of cymenes by isopropylation of toluene and methylation of cumene. The catalytic results are compared with that obtained from the cation-exchanged Beta zeolites, La-H-Beta and Mg-H-Beta.

3.2 Experimental

3.2.1 Catalyst Preparation

Zeolite Beta was synthesized hydrothermally from a $(TEA)_2O-Al_2O_3-Na_2O-H_2O$ system at 423 K. The general procedure of the synthesis is as follows. Appropriate amount of tetraethylammonium hydroxide, sodium hydroxide, sodium aluminate and distilled water were mixed together and stirred vigorously to get a homogeneous mixture. This mixture was then added slowly to a calculated amount of silica sol and the resulting gel was stirred vigorously for another one hour. This final gel was transferred to a teflon-lined stainless steel autoclave and treated at 423 K for 7 days. The as-synthesized zeolite was filtered, washed with deionized water and dried at 393 K. Crystalline sample

thus obtained was calcined in presence of air at 773 K for 24 hours to decompose the organic matter. The protonic form of the zeolite was obtained by repeated ion exchange with ammonium acetate solution (10 wt.%) at 353 K followed by calcination at 773 K for 24 hours in a flow of dry air.

La-H-Beta and Mg-H-Beta were prepared by treating 5 g of the calcined zeolite with 100 ml of 2 wt.% solution of lanthanum chloride and magnesium acetate respectively. After the repeated cation exchange the samples were thoroughly washed with deionized water until the filtrate was free from chloride or acetate ions. All the synthesis and modification procedures are described in detail in Chapter 2.

3.2.2 Catalyst Characterization

Crystalline phase purity, chemical composition and other physical properties were established by using techniques like XRD, SEM, TG-DTA, atomic absorption and X-ray fluorescence spectroscopy. Acidity of the samples were measured by temperature programmed desorption (TPD) of ammonia. Detail procedures of the characterization are described in Chapter 2.

3.2.3 Catalytic Reactions

Catalytic experiments were performed at atmospheric pressure in a fixed-bed, vertical, down-flow, integral silica reactor placed inside a double-zone furnace (géomécanique, France). Schematic diagram of a reactor setup is shown in Fig. 3.2. The catalysts were pressed, pelleted and sieved to obtain catalyst particles of ca. 10-20 mesh. The amount of catalyst taken each time was 2 g, the height of the catalyst bed being about 3 cm. The catalyst was charged in the center of the reactor in such way that the catalyst was sandwiched between the layers of inert porcelain beads. The upper portion of the reactor served as a vaporizer cum pre-heater. All heating and temperature measurements were carried out using 'Aplab' temperature controller and indicator instruments. The

1. Syringe pump
2. Gas inlet
3. Furnace
4. Silica reactor
5. Thermocouple
6. Condenser
7. Sample container
8. Gas outlet
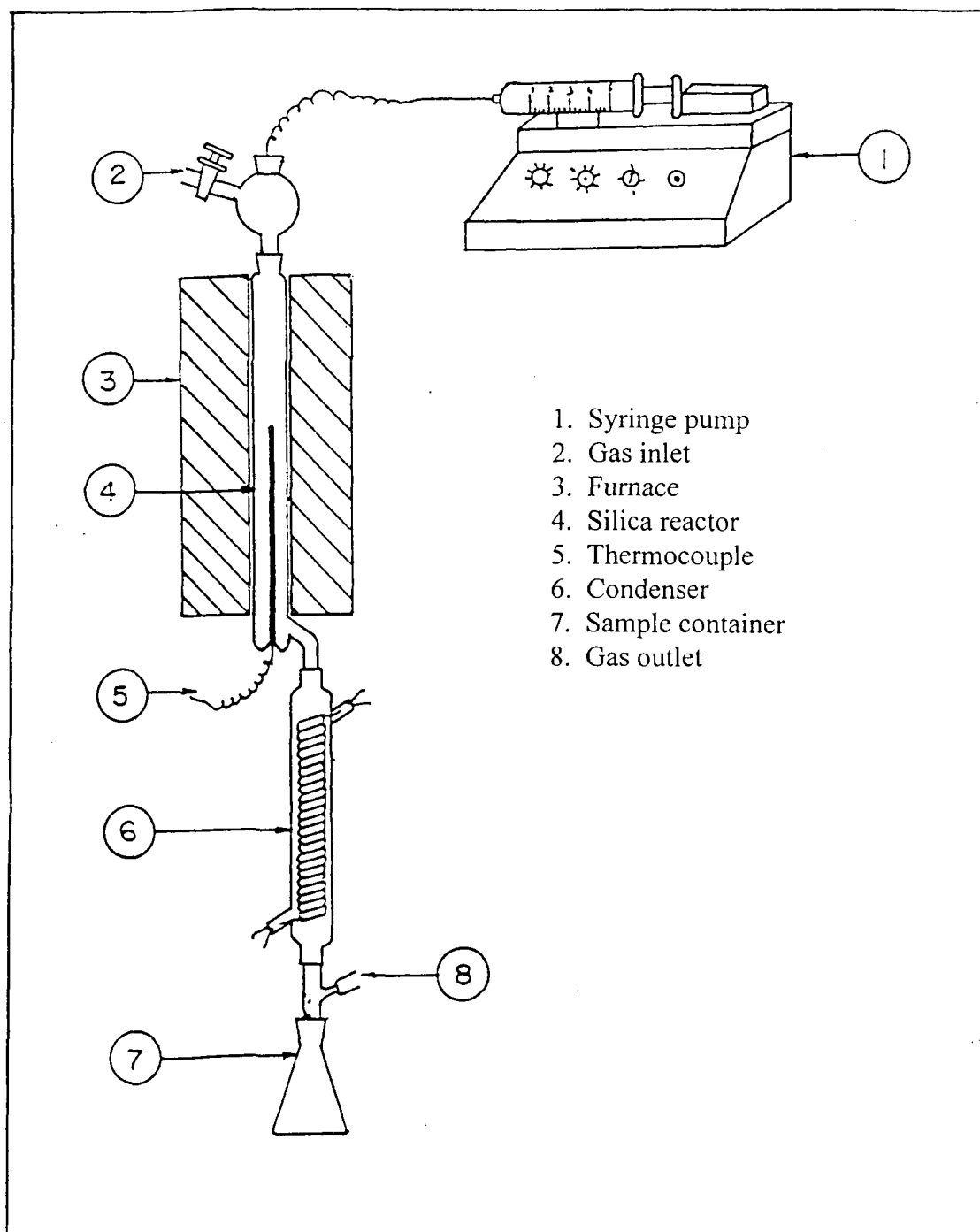
Fig. 3.2   Reactor set-up for reactions carried out at atmospheric pressure

exact temperature of the catalyst bed was obtained by inserting a thermocouple inside the thermowell in the lower portion of the reactor. The catalyst was activated at 773 K for at least 6 hours in a flow of dry air before each run. The reactor was then cooled to the desired reaction temperature in presence of nitrogen. The liquid reactant mixture was fed by a syringe pump (SAGE Instruments, Model 352, USA). The products of the reaction were collected downstream from the reactor in a receiver connected through a cold water circulating condenser. Products were collected at various time intervals and analyzed by gas chromatography (Shimadzu, Model 15A, connected with FID detector) and GC-MS (Shimadzu, Model QP 2000A, SE-52 capillary column, non polar silicon fluid). Liquid products were analyzed using a Xylene Master capillary column (Shinwa Chemical Industries Ltd., Japan), and the gaseous products were analyzed using a packed stainless steel Porapak Q column. The mass balance was of the order of 99.5 %.

Toluene, cumene, isopropanol and methanol used were AnalaR grade.

3.3 Results and Discussion

The crystallinity and phase purity of the samples were first ensured. All samples were highly crystalline as revealed by XRD patterns. SEM photographs showed the absence of any amorphous material adhered to zeolite samples.

Table 3.1 presents the unit cell compositions (calculated on anhydrous basis) and equilibrium sorption capacities obtained from sorption measurements of different sorbents for H-Beta, La-H-Beta and Mg-H-Beta at p/p_o 0.5 and 298 K. In general, the equilibrium sorption capacities of hydrocarbons remain nearly same for all samples. However, specific surface area (BET) obtained at lower temperature (liquid N_2 temperature) nitrogen sorption decreases from H-Beta to La-H-Beta to Mg-H-Beta. A decrease in cation density but an increase in cation size on account of monovalent proton by multivalent cations are expected to give rise to a small change in the void volume of

Table 3.1

Unit cell composition (anhydrous basis) and sorption capacities of Beta zeolites.

Sample	Unit Cell Composition	Amount adsorbed (g/100g)[a]			Surface area (m^2/g)
		$n\text{-}C_6H_{14}$	C_6H_{12}	C_6H_6	
H-Beta	$H_{3.4}Na_{0.1}Al_{3.5}Si_{60.5}O_{128}$	19.0	19.8	21.9	745
La-H-Beta	$H_{0.5}Na_{0.1}La_{0.9}Al_{3.3}Si_{60.7}O_{128}$	19.6	20.3	22.3	697
Mg-H-Beta	$H_{2.1}Na_{0.1}Mg_{0.6}Al_{3.4}Si_{60.6}O_{128}$	20.1	20.0	22.4	672

[a] $p/p_0 = 0.5$, T = 298 K

cation exchanged zeolites. The difference observed in low temperature nitrogen sorption may result from weak repulsive interaction of nonpolar cylindrical shaped N_2 molecule with extra-framework cations.[57]

The result of acidity of the samples measured by temperature programmed desorption of ammonia is presented in Fig. 3.3. It is clear from the TPD curves that H-Beta and La-H-Beta show three peaks of ammonia desorption whereas Mg-H-Beta shows only one peak. According to Lok et al.,[58] the first NH_3-TPD peak is associated with the weakly adsorbed NH_3 molecules on the external surface sites, or to the interaction of NH_3 molecules with surface oxide or hydroxyl groups by non-specific H-bonds or to extraneous material. The second NH_3-TPD peak is associated with the chemisorbed molecules of NH_3 to less acidic OH groups, and the third NH_3-TPD peak is associated with the strongly chemisorbed NH_3 molecules which corresponds to strong Brönsted acid sites and/or Lewis acid sites. The absence of the second and third peaks in Mg-H-Beta clearly indicates that exchange of Mg^{2+} in H-Beta suppresses the acidity in the sample. The enhancement of intensity in the first peak may be due to the formation of some defect sites with the exchanged cations which adsorbs some of the NH_3 molecules. Exchange of La^{3+} in H-Beta results in the decrease in the intensity of the second peak and enhancement in the intensity of the third peak. This indicates that weaker acidic sites are decreased and stronger acid sites are increased due to the La^{3+} exchange. The creation of stronger acid sites in La-H-Beta may be due to the hydrolysis of the water associated with the lanthanum ion[59,60] to form species of the type shown below:

$$-Si-O-Al-O-Si-$$
$$La^{2+} \text{ (OH) } H^+$$
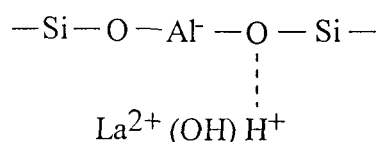
The H^+ ion in the structure is assumed to be responsible for the acidity.
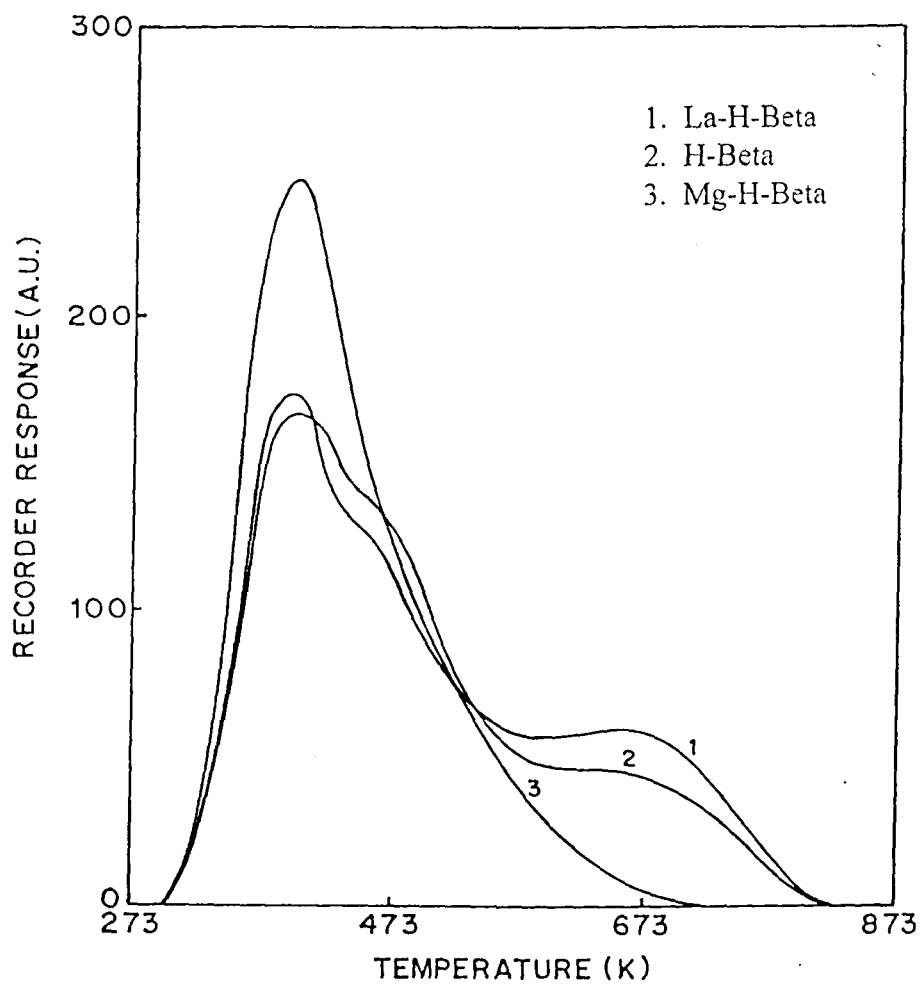
Fig. 3.3   NH$_3$-TPD profile of Beta zeolites

3.3.1 Isopropylation of toluene

Under the reaction conditions of the alkylation, protonation of the isopropanol to form the carbenium ion is proposed as the initial step. This is followed by transfer of the isopropyl group to the aromatic ring and transfer of a proton back to the catalyst site.[34]

$$(CH_3)_2CH\text{-}OH + H\text{-}Zeol \rightleftharpoons (CH_3)_2CH\text{-}\overset{+}{O}H_2\text{-}\overset{-}{Z}eol$$
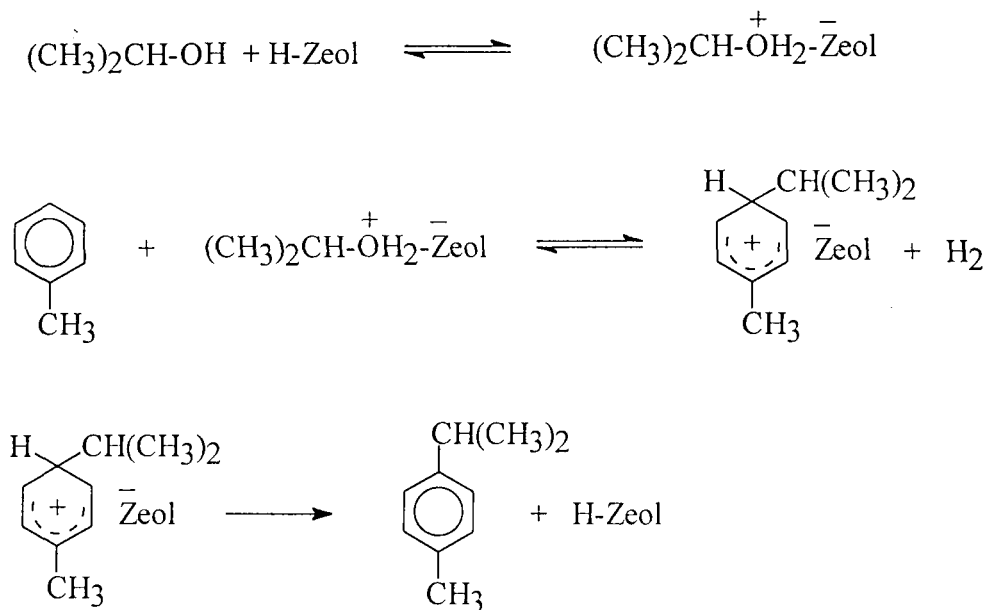
However, the same acid sites can also rapidly isomerize the cymene formed initially as it diffuses out of the zeolite, especially in the larger space in the pore to give *m*-isomer.
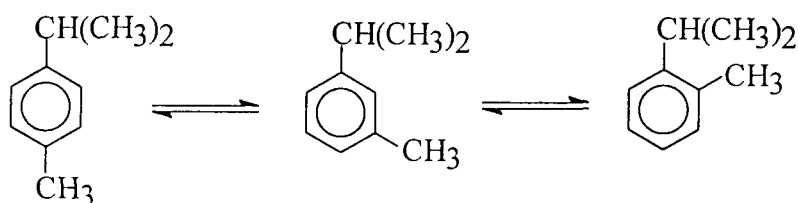
Based on the reaction products obtained, the main reaction scheme of isopropylation of toluene can be represented as:

Toluene + Isopropanol → Cymene + water

2 Toluene → Benzene + Xylene

Isopropanol → Propylene + water
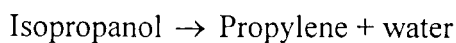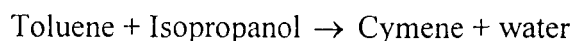
The reaction is known to proceed through the activation of propylene formed by the dehydration of isopropanol over acid sites of zeolite. The activated propylene (C_3-carbenuim ion) then reacts with toluene in the gas phase to produce cymene. It is also assumed that isopropanol and toluene are adsorbed on the adjacent sites and the protonated propylene formed by the dehydration of isopropanol can react with the activated toluene molecule. The cymenes formed do not undergo disproportionation and transalkylation reactions at lower temperature as these reactions need higher activation energies, and according to the selectivity relationships developed by Stock and Brown[61] for the non-specific catalysts, the relative rate constant for alkylation, $K_{toluene}$ / $K_{benzene}$ should be about 1.4. Hence, toluene alkylation is more probable than the dealkylation at these temperatures. Benzene and xylenes are formed due to disproportionation of toluene. Negligible amount of diisopropyltoluene (DIPT) and diisopropylbenzene (DIPB) are formed at higher temperature due to further isopropylation of cymene or cumene. Benzene may also be formed due to dealkylation of cumene. Dealkylation of toluene is less probable as it needs higher activation energy. A small amount of benzene formation is also possible due to disproportionation of cumene or dealkylation of DIPB at higher temperature.

Propylene and propane are formed as major aliphatic products. Nearly 5 % isobutane and trace amounts of methane, ethylene, ethane, n-butane, 1-butene, *cis*- and *trans*-2-butene are also formed. Among the aromatic impurities formed, ethyl and butyl substituted benzene and toluene are negligible. n-Propylbenzene or toluene are not formed in the reaction as the CH_3-CH^+-CH_3 carbenium ion formed through dehydration of isopropanol is not isomerized to CH_3-CH_2-CH_2^+. As there is no steric hindrance in large pore zeolites, n-propyl toluene is not formed. The formation of n-propyl substituted toluene in the isopropylation of toluene is already ascribed due to steric hindrance induced isomerization of cymenes inside the channels of MFI type of zeolites.[62]

3.3.1.1 Effect of temperature

Effect of temperature on isopropylation of toluene over H-Beta is shown in Table 3.2. Increase of temperature increases the rate of chemical reaction, and the thermodynamic equilibrium of the reaction depends on the temperature of the reaction. Usually the energy of the reacting molecule reaches the necessary activation energy and the activated complex is formed either with the catalyst surface or by colliding with the other reactants, then decomposes or reacts further. In the isopropylation of toluene, even though the main reaction is the cymene formation, numerous side reactions as discussed below are possible.

As described earlier, in the main reaction, the isopropyl carbenium ion reacts with toluene in the gas phase to form cymene. But the isopropyl ion can undergo dimerisation followed by decomposition to form ethyl or butyl groups or it can form propylene and diffuse out. During this process, the propylene can be adsorbed on the active sites and deactivate the sites. From the mass balance studies, and gas and liquid products obtained, the following reactions are assumed.

The conversion of toluene selectively towards alkylation is more at lower temperature (423 K - 483 K). At higher temperature (513 K), dealkylation and disproportionation reactions are enhanced leading to the formation of undesired products. Consequently, cymene selectivity decreases with the increase of temperature. Formation of cumene is also increased at higher temperatures along with trace amounts of ethyl and butyl-substituted benzenes. The increase of xylenes occurs with the increase of temperature due to disproportionation of toluene, which is observed in other zeolites also.[63]

3.3.1.2 Effect of W.H.S.V.

Contact time or space velocity is the parameter other than temperature which influences the activity of the catalyst and selectivity of the products. The product pattern

Table 3.2

Isopropylation of toluene over zeolite H-Beta
Effect of Temperature

Temperature (K)	423	453	483	513
Toluene Conv. (Wt.%)[a]	6.45	6.03	6.66	3.88
Isopropanol Conv. (Wt.%)	100	100	100	100
Product Selectivity (Wt. %)				
Aliphatics	0.82	0.74	1.94	5.21
Benzene	1.03	1.70	2.13	9.09
Σ Xylene	1.23	2.76	3.33	11.13
Ethylbenzene	-	-	0.18	0.48
Cumene	0.51	1.49	1.94	2.21
Σ Cymene	96.41	93.31	89.65	68.49
Σ Diethyl+butylbenzene	-	-	0.83	3.39

Reaction Codition : Toluene/Isopropanol (mol/mol) = 12 : 1, W.H.S.V. = 6.45 h^{-1}, Time On Stream (TOS) = 3 h.

[a]Toluene conversion selectively towards alkylation

71

Table 3.3

Isopropylation of toluene over zeolite H-Beta
Effect of Space Velocity

W.H.S.V. (h^{-1})	0.50	1.70	3.44	6.45
Toluene Conv. (Wt.%)	1.36	1.61	3.1	6.03
Isopropanol Conv. (Wt.%)	100	100	100	100
Product Selectivity (Wt. %)				
Aliphatics	8.59	5.74	2.18	0.74
Benzene	16.27	10.36	6.26	1.70
Σ Xylene	18.28	11.48	7.82	2.76
Ethylbenzene	-	-	-	-
Cumene	2.01	1.72	1.55	1.49
Σ Cymene	54.85	70.69	82.18	93.31
Σ Diethyl+butylbenzene	-	-	-	-

Reaction Codition : Toluene/Isopropanol (mol/mol) = 12 : 1, Temperature = 453 K, TOS = 3 h.

in majority of the catalytic reactions with diffusivity of reactants and products is governed by contact time. Higher contact time (lower space velocity) influence the secondary and successive reactions whereas, here, lower contact time selectively facilitates the main reaction. As can be seen from Table 3.3, aliphatics are formed more at lower W.H.S.V. or higher contact time. At lower W.H.S.V., dealkylation and disproportionation reaction rates are enhanced, resulting in the formation of more other aromatic impurities such as benzene, xylene and cumene. Conversion of isopropanol is complete at all W.H.S.V.s, and conversion of toluene selectively towards alkylation and cymene selectivity steadily increase with the increase in W.H.S.V.

3.3.1.3 Effect of toluene to isopropanol molar ratio

The results of the influence of reactant molar ratio on product distribution in the isopropylation of toluene over H-Beta is presented in Table 3.4. Conversion of isopropanol is complete at all toluene to isopropanol molar ratios (from 6 to 18) studied in the present work. The conversion of toluene selectively towards alkylation is maximum at 9:1 ratio. Selectivity of cymene is not much varied with the molar ratio variation. Gaseous products are more at lower molar ratio. Benzene to xylene ratio in the product remains more or less same at lower molar ratio (6:1-12:1) which are formed by disproportionation, whereas this ratio is higher at higher toluene/ispropanol molar ratio (15:1-18:1). The additional benzene is formed by the dealkylation of cymene or cumene.

3.3.1.4 Effect of cation exchange in H-Beta

Table 3.5 shows the comparison of results of the isopropylation of toluene between H-Beta, La-H-Beta and Mg-H-Beta zeolites. The maximum selectivity of cymene and conversion of toluene at the expense of minimum yield of impurities can be obtained in the reaction catalyzed by La-H-Beta. This may be due to the formation of stronger acid sites in La-H-Beta. Selectivity of cymene is maximum in La-H-Beta and lowest in

Table 3.4

Isopropylation of toluene over zeolite H-Beta
Effect of Feed Ratio

Toluene/Isopropanol (mol/mol)	6:1	9:1	12:1	15:1	18:1
Toluene Conv. (Wt.%)	6.85	7.64	6.03	4.94	4.51
Isopropanol Conv. (Wt.%)	100	100	100	100	100
Product Selectivity (Wt. %)					
Aliphatics	1.53	1.19	0.74	0.65	0.60
Benzene	0.95	1.19	1.70	2.22	2.41
Σ Xylene	1.43	1.70	2.76	2.35	2.01
Ethylbenzene	-	-	-	-	-
Cumene	0.95	1.36	1.49	1.04	0.57
Σ Cymene	95.14	94.56	93.31	93.74	94.40
Σ Diethyl+butylbenzene	-	-	-	-	-

Reaction Codition : Temperature = 453 K, W.H.S.V. = 6.45 h^{-1}, TOS = 3 h.

Table 3.5

Isopropylation of toluene over Beta and cation exchanged Beta zeolites.

Catalyst	H-Beta	La-H-Beta	Mg-H-Beta
Toluene Conv. (Wt.%)	6.03	6.56	1.80
Isopropanol Conv. (Wt.%)	100	100	98.90
Product Sel. (Wt. %)			
Aliphatics	0.74	0.57	6.38
Benzene	1.70	0.41	1.34
Σ Xylene	2.76	0.82	3.69
Ethylbenzene	-	-	0.33
Cumene	1.49	-	-
Σ Cymene	93.31	98.23	87.93
Σ Diethyl+butylbenzene	-	-	0.33

Reaction Codition : Toluene/Isopropanol (mol/mol) = 12 : 1, Temperature = 453 K, W.H.S.V. = 6.45 h^{-1}, TOS = 3h.
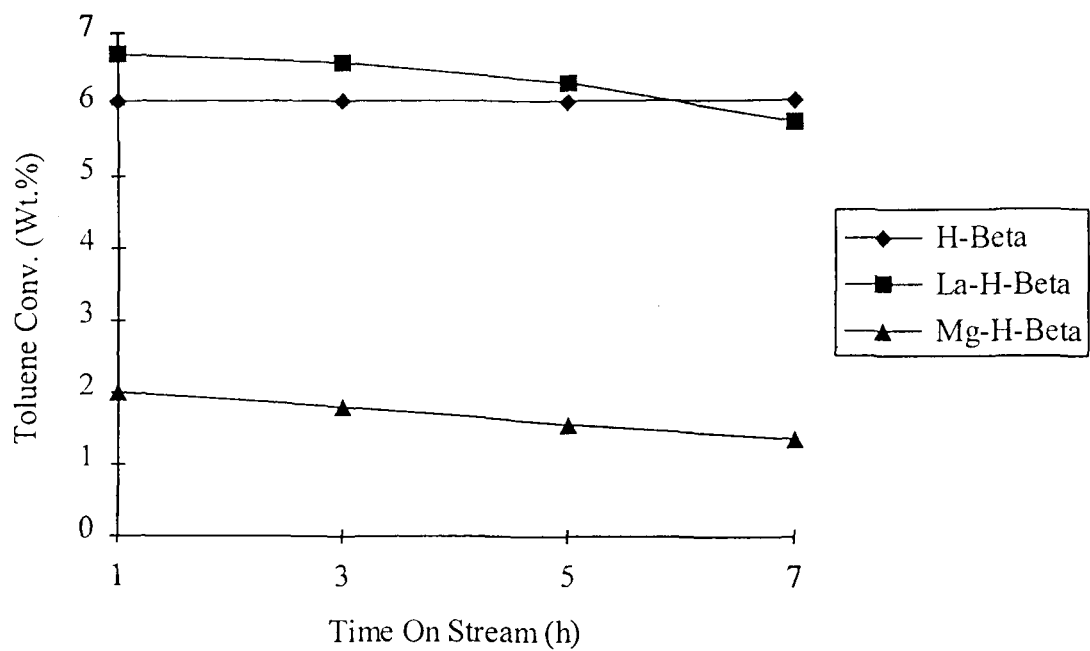
Fig. 3.4 Catalytic performance of Beta and cation exchanged Beta zeolites for the isopropylation of toluene; Temperature: 453K, WHSV: 6.45 h^{-1}, Toluene/Isopropanol (mol/mol): 12

Mg-H-Beta. As far as conversion of toluene selectively towards alkylation is concerned, La-H-Beta and H-Beta are comparable but Mg-H-Beta gives much lower conversion. The catalytic activity of Mg-H-Beta can be correlated with its lower acidity. H-Beta shows better stable activity than the cation exchanged samples. The cation exchanged Beta zeolites deactivate faster than H-Beta (Fig. 3.4) since La^{3+} or Mg^{2+} ions are not tightly bound to the framework and acidity induced by La in the extra framework cationic species is not fairly stable. The stable activity of H-Beta is due to its stable acidity, generated due to uniform distribution of tetrahedral framework silicon and aluminium.

3.3.2 Methylation of cumene

Aromatic alkylation using methanol is reported by several authors, particularly methylation of toluene to p-xylene.[64,65] Usually methylation reactions are much slower compared to ethylation or propylation. For example, relative rate of alkylation of toluene with isopropanol is 20,000 times faster than that with methanol.[34] To enhance the rate of methylation, higher temperature is needed, but at the same time at high temperatures, side reactions are more likely to compete with the main reaction.

Based on the products obtained, the main reaction scheme of methylation of cumene can be represented as follows:

$$Cumene + Methanol \rightarrow Cymene$$

$$2\ Cumene \rightarrow Diisopropylbenzene + Benzene$$

$$Cumene \rightarrow Benzene + Propylene$$
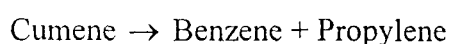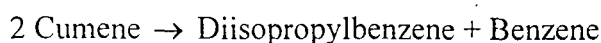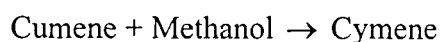
Among the aliphatic products, propylene and propane are formed as major products. Moderate amount of C_1 and C_4 hydrocarbons and small amounts of C_2 and C_5 hydrocarbons are also obtained. The formation of methane (C_1 hydrocarbon) increases with increasing reaction temperature at the expense of C_3 hydrocarbon. From ΔG values of the literature,[66] thermodynamically alkylation of cumene with methanol and alkylation

of toluene with isopropanol to form cymenes are equally feasible. However, the disproportionation and dealkylation of cumene are more energetically favored than that of toluene. Thus, selective alkylation of toluene with isopropylation is more favorable than the selective alkylation of cumene with methanol towards the formation of cymenes.

In the methylation of cumene, three major reaction products are cymene, diisopropylbenzene (DIPB) and benzene. The reactions involving cymene, DIPB and benzene are shown in Fig. 3.5 to Fig. 3.7. Cymene is produced from methylation of cumene. As the reaction is carried out at higher temperature, undesired reactions such as dealkylation, disproportionation and transalkylation of cumene are feasible. A fraction of cymene formed is dealkylated to cumene and toluene. DIPB is formed mainly due to the disproportionation of cumene and partly due to alkylation of cumene with propylene. A fraction of DIPB formed through the above reactions are transformed to propylene, benzene, cumene and diisopropyltoluene (DIPT) through dealkylation and transalkylation reactions. Benzene may also be formed due to disproportionation of cumene or dealkylation of cumene or DIPB. As alkylation is thermodynamically more feasible, a large portion of benzene is alkylated with olefins yielding substituted benzenes. Small fraction of benzene is transalkylated with cymene or DIPB yielding toluene or cumene.

Effect of temperature on methylation of cumene over H-Beta and cation exchanged Beta is presented in Table 3.6. Conversion of methanol is nearly complete at all temperatures. Benzene to DIPB molar ratio increases with increase in reaction temperature for all the catalysts. This reveals that at higher reaction temperature dealkylation of cumene is considerably increased. Cymene selectivity is lower at all temperatures. Impurities like ethyltoluenes, xylenes and butylbenzenes are formed by the alkylation with olefins formed by methanol reaction. As methanol to olefin conversion is high at higher temperatures, the formation of the impurities also enhances with the increase in temperature. Table 3.7 reflects the effect of W.H.S.V. on the reaction over H-Beta. At lowest W.H.S.V. (2.58 h^{-1}) benzene to DIPB ratio is higher and cymene

```
                    ┌─────────────────┐
                    │ Cumene + Methanol│
                    └─────────────────┘
                             │
                             │ Alkylation
                             ▼
┌──────────────────┐              ┌──────────┐              ┌──────────────────────┐
│ Toluene, Cumene  │  Dealkylation│          │Transalkylation│ Toluene, Cumene      │
│ Propylene, Ethylene│◄───────────│  Cymene  │──────────────►│ Diisopropylbenzene   │
└──────────────────┘              └──────────┘              │ Diisopropyltoluene   │
                                       │                     └──────────────────────┘
                                       │ Disprportionation
                                       ▼
                             ┌──────────────────────┐
                             │ Toluene, Xylene       │
                             │ Diisopropylbenzene    │
                             │ Diisopropyltoluene    │
                             └──────────────────────┘
```
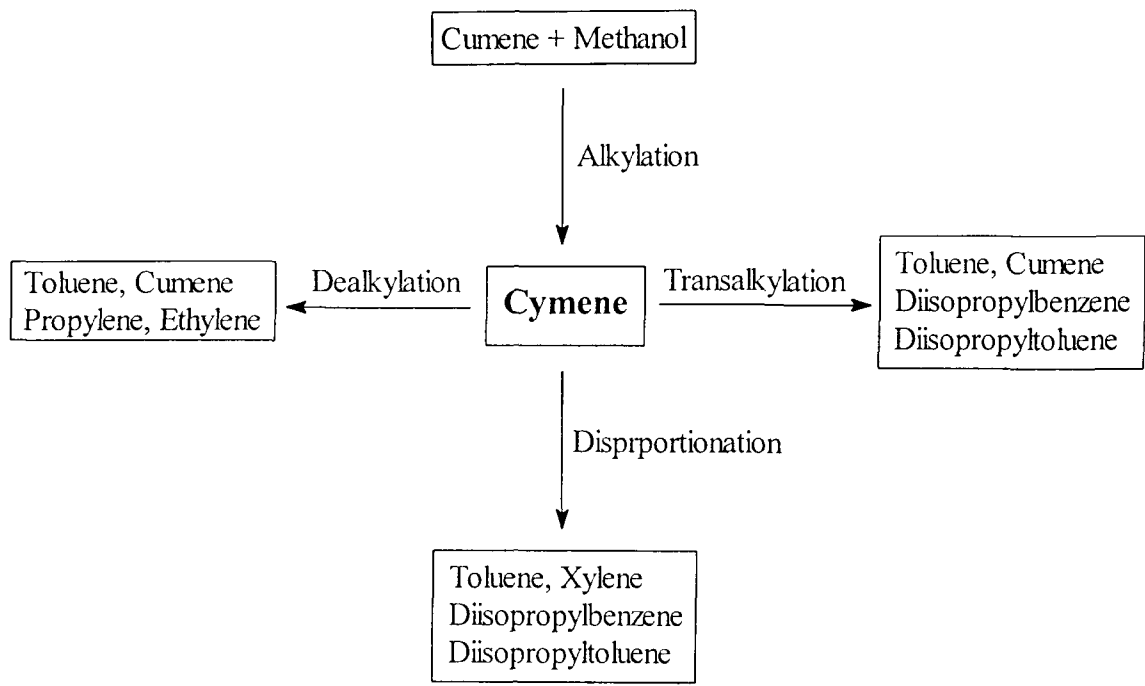
Fig. 3.5   Reaction involving 'cymene' in the methylation of cumene over Beta zeolite

```
                        ┌──────────┐
                        │ Cumene   │
                        │ Cymene   │
                        └──────────┘
                             │
                             │ Disprportionation
                             ▼
┌──────────┐  Alkylation  ┌──────────────────────┐  Transalkylation  ┌──────────┐
│ Cumene   │ ───────────▶ │ Diisopropylbenzene    │ ◀─────────────── │ Cumene   │
│ Propylene│              └──────────────────────┘                   │ Cymene   │
└──────────┘                         │                               └──────────┘

        Transalkylation    │    Dealkylation
              ▼                        ▼
┌─────────────────────┐      ┌──────────────────────┐
│ Cumene              │      │ Benzene, Cumene       │
│ Diisopropyltoluene  │      │ Propylene             │
└─────────────────────┘      └──────────────────────┘
```
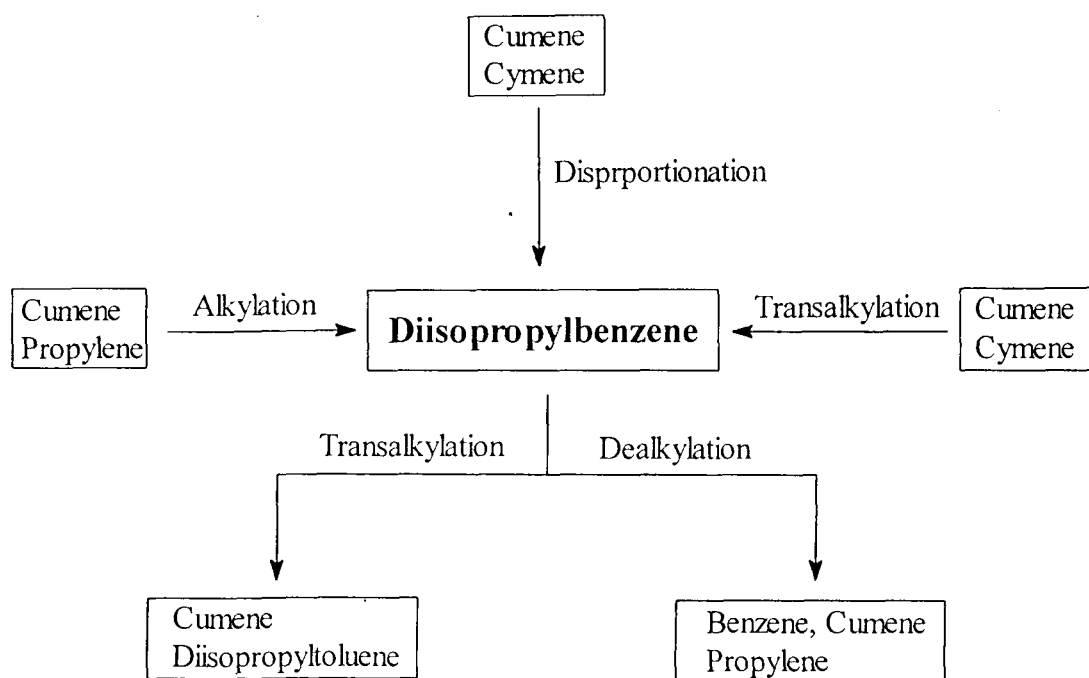
Fig. 3.6   Reaction involving 'DIPB' in the methylation of cumene over Beta zeolite

```
                        ┌─────────┐
                        │ Cumene  │
                        └─────────┘
                             │
                             │ Disprportionation
                             ▼
┌──────────────────┐              ┌──────────┐              ┌─────────┐
│ Cumene           │ Dealkylation │ Benzene  │ Transalkylation│ Cumene │
│ Diisopropylbenzene├────────────▶│          ├──────────────▶│ Toluene │
└──────────────────┘              └──────────┘              └─────────┘
                             │
                             │ Alkylation
                             ▼
                   ┌─────────────────────┐
                   │ Substituted benzenes │
                   └─────────────────────┘
```

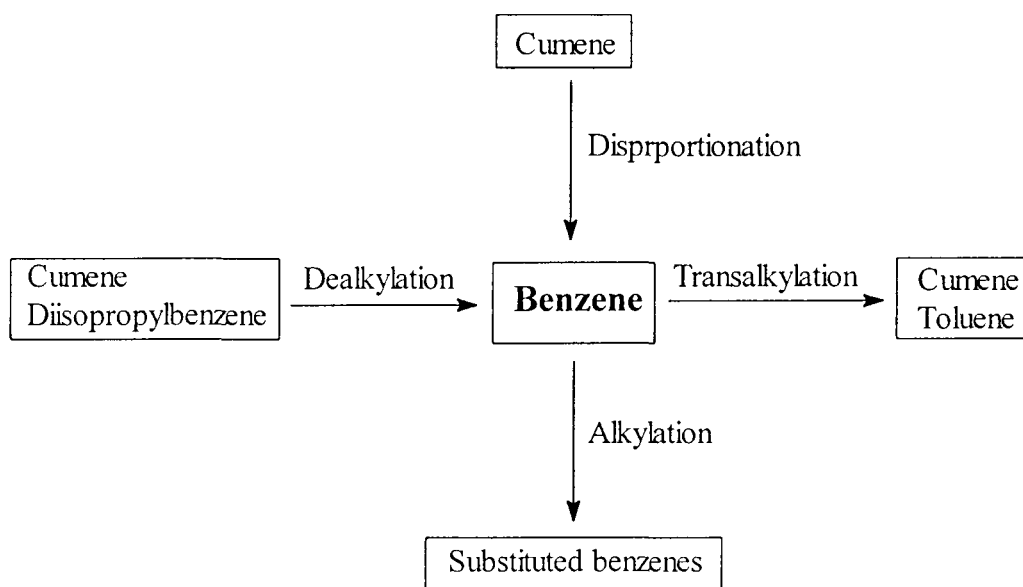**Fig. 3.7**   Reaction involving 'benzene' in the methylation of cumene over Beta zeolite

Table 3.6

Methylation of cumene over Beta and cation exchanged Beta zeolites.

Catalyst	H-Beta			La-H-Beta			Mg-H-Beta		
Temperature (K)	453	543	593	453	543	593	453	543	593
Cumene Conv. (Wt.%)	36.90	45.60	47.50	24.20	34.90	35.70	13.10	26.50	29.90
Benzene / DIPB (mol/mol)	3.15	4.46	18.13	1.07	1.75	6.76	1.18	1.84	6.55
Prod. Sel. (Wt. %)									
Aliphatics	5.40	7.33	10.12	0.09	3.87	7.36	3.95	1.02	10.42
Benzene	48.86	46.81	63.74	33.30	32.75	54.56	25.16	37.75	54.47
Toluene	3.79	7.75	1.47	0.32	5.84	6.53	3.16	4.07	4.99
Σ Xylene	0.69	1.33	1.54	0.04	1.03	1.14	0.79	0.59	0.69
Ethylbenzene	3.45	3.32	3.35	0.81	1.21	1.29	1.74	1.40	1.28
n-propylbenzene	1.64	1.80	2.04	0.45	0.94	1.26	0.79	0.97	1.04
Σ Ethyltoluene	-	0.26	0.23	-	0.18	0.23	-	0.13	0.10
Butylbenzene	0.78	1.00	1.15	0.09	0.54	0.73	2.53	0.51	0.59
Σ Cymene	-	6.49	4.86	-	11.62	7.24	15.98	9.07	6.65
Σ Diethylbenzene	1.12	1.38	1.42	0.04	0.57	0.61	0.08	0.38	0.73
Σ Ethylcumene	2.04	0.47	1.97	0.45	1.94	1.79	0.79	1.48	1.35
Σ DIPB[a]	32.23	21.78	7.86	64.37	38.91	16.76	44.32	42.34	17.28
Σ DIPT[b]	-	0.28	0.25	0.04	0.60	0.50	0.71	0.59	0.41

Reaction Codition : Cumene/Methanol (mol/mol) = 3 : 1, W.H.S.V. = 2.58 h^{-1}, TOS = 1h.
[a]Diisopropylbenzene, [b]Diisopropyltoluene

Table 3.7

Methylation of cumene over zeolite H-Beta
Effect of Space Velocity

W.H.S.V. (h^{-1})	2.58	4.30	7.45
Cumene Conv. (Wt.%)	45.60	17.43	15.62
Benzene/DIPB (mol/mol)	4.46	2.20	3.45
Product Selectivity (Wt.%)			
Aliphatics	7.33	5.47	12.80
Benzene	46.81	28.04	29.26
Toluene	7.75	5.59	5.72
Σ Xylene	1.33	1.29	4.36
Ethylbenzene	3.32	3.54	1.36
n-propylbenzene	1.80	1.35	1.50
Σ Ethyltoluene	0.26	0.77	0.86
n-butylbenzene	1.00	0.96	1.07
Σ Cymene	6.49	21.48	19.96
Σ Diethylbenzene	1.38	0.51	0.57
Σ Ethylcumene	0.47	3.73	3.86
Σ DIPB	21.78	26.50	17.60
Σ DIPT	0.28	0.77	1.07

Reaction Codition : Cumene/Methanol (mol/mol) = 3 : 1, Temperature = 543 K, TOS = 1 h.

Table 3.8

Methylation of cumene over zeolite H-Beta
Effect of Feed Ratio

Cumene/Methanol (mol/mol)	1:1	2:1	3:1	4:1
Cumene Conv. (Wt.%)	35.90	31.33	45.60	47.04
Benzene/DIPB (mol/mol)	0.88	2.06	4.46	5.77
Product Selectivity (Wt.%)				
Aliphatics	10.67	5.45	7.33	7.06
Benzene	23.65	33.12	46.81	52.07
Toluene	0.69	6.46	7.75	7.22
Σ Xylene	0.24	1.38	1.33	1.00
Ethylbenzene	2.07	1.28	3.32	3.34
n-propylbenzene	1.32	0.87	1.80	2.52
Σ Ethyltoluene	-	0.27	0.26	0.51
n-butylbenzene	1.02	0.81	1.00	0.78
Σ Cymene	0.96	14.09	6.49	3.85
Σ Diethylbenzene	0.24	0.67	1.38	0.91
Σ Ethylcumene	2.70	1.75	0.47	1.74
Σ DIPB	56.08	33.45	21.78	18.73
Σ DIPT	0.36	0.40	0.28	0.27

Reaction Codition : Temperature = 543 K, W.H.S.V. = 2.58 h^{-1}, TOS = 1 h.

selectivity is lower which indicates enhancement of dealkylation and disproportionation reactions yielding more undesired products. Effect of methanol to cumene feed ratio (mol/mol) over H-Beta reflects (Table 3.8) that selectivity of cymene is maximum at cumene to methanol ratio of 2:1. Benzene to DIPB ratio increases steadily with the increase in the feed ratio. Both dealkylation and disproportionation reactions predominate over alkylation reaction at higher cumene to methanol molar ratio yielding more side products.

3.4 Conclusion

Alkylation reactions using Beta zeolite are very promising due to the structural and acidic properties of the zeolite. Even though cymene can be obtained by the alkylation of toluene with isopropanol, and cumene with methanol, the former reaction is more favorable, and the selectivity of cymene is high in this reaction. In the methylation of cumene, higher reaction temperature is required to form cymenes, and at the same time, impurities are formed more at higher temperatures due to the dealkylation and disproportionation of cumene as well as olefin formation from methanol. In the isopropylation of toluene, La-H-beta shows better selectivity towards cymene but deactivates faster compared to H-Beta. Enhancement of selectivity can be correlated to the formation of stronger acid sites induced by the La^{3+} ion whereas faster deactivation of the catalyst is possible due to the fact that La^{3+} ions are not tightly bound to the framework and acidity induced by this ion is not fairly stable.

3.5 References

1. W. Hölderich, *Proc. 7th. Int. Zeol. Conf.*, Y. Murakami, A. Ijima, J.W. Ward (Eds.), Tokyo, 1986, Kodansha-Elsevier, Tokyo, (1986) 827.

2. N.Y. Chen, W.E. Garwood and F.G. Dwyer, in *Shape Selective Catalysis in Industrial Applications*, Marcel Dekker Inc., New York and Basel, (1989) 65.

3. W. Hölderich, M. Hesse and F. Naumana, *Angew. Chem. Int. Ed. Engl.*, 27 (1988) 226.

4. J.J. Wise, *US Pat.*, 3,215,897 (1966).

5. K.A. Becker, H.G. Karge and W.D. Streubel, *J. Catal.*, 28 (1973) 403.

6. J.A. Brennan, W.E. Garwood, S. Yurchuk and W. Lee, *Proc. Int. Sem. on Alternate Fuels*, A. Germain (Ed.), Liege, Belgium, May, (1981) 19.1.

7. L.B. Young, *US Pat.*, 4,310,317 (1981).

8. P.E. Keown, C.C. Meyers and R.G. Wetherold, *US Pat.*, 3,751,504 (1973).

9. P.J. Lewis and F.G. Dwyer, *Oil Gas J.*, 75 (1977) 55.

10. F.G. Dwyer, in *Catalysis of Organic Reactions*, W.R. Moser (Ed.), Marcel Dekker Inc., New York, (1981) 39.

11. W.W. Kaeding, C. Chu, L.B. Young, B. Weinstein and S.A. Butter, *J. Catal.*, 67 (1981) 159.

12. W.W. Kaeding, L.B. Young and A.G. Prapas, *Chemtech*, 12 (1982) 556.

13. P.B. Venuto, *Microporous Mater.*, 2 (1994) 297.

14. P.B. Venuto, L.A. Hamilton, P.S. Landis and J.J. Wise, *J. Catal.*, 5 (1966) 81.

15. Kh.M. Minachev, Ya.I. Isakov and V.J. Garanin, *Neftekhimiya*, 6 (1966) 53; *Chem Abstr.*, 64 (1966) 19452.

16. F.G. Dwyer, P.J. Lewis and F.H. Schneider, *Chem. Eng.*, 83 (1976) 90.

17. I.I. Ivanova, O.E. Ivashkina, E.V. Dmitruk, N.Dumont, Z. Gabelica, E.G. Derouane, J.B. Nagy, B.V. Romanovsky and A. Smirnov, *Proc. 9th Int. Zeol. Conf.*, J.B. Higgins, R. von Balmoos and M.M.J. Treacy (Eds.), Butterworth-Heinemann, Boston, MA, (1992) B43 (abstracts).

18. A.R. Pradhan, A.N. Kotasthane and B.S. Rao, *Appl. Catal.*, 72 (1991) 311.

19. W.W. Kaeding, L.B. Young and C. Chu, *J. Catal.*, 89 (1984) 267.

20. W.W. Kaeding, M.M. Wu, L.B. Young and G.T. Burres, *US Pat.* 4,197,413 (1980).

21. F.G. Dwyer and D.J. Klocke, *US Pat.*, 4,049,737 (1977).

22. J. March, in *Advanced Organic Chemistry*, John Wiley and Sons, New York, NY, 3rd Edn., (1985) 445.

23. P. Sykes, in *A Guidebook to Mechanism in Organic Chemistry*, John Wiley and Sons, New York, NY, (1986) 130.

24. P.B. Venuto and P.S. Landis, *Adv. Catal.*, Academic, New York, NY, 18 (1968) 259.

25. P.B. Venuto, *Chemtech*, April (1971) 215.

26. P.B. Venuto, L.A. Hamilton and P.S. Landis, *J. Catal.*, 5 (1966) 484.

27. P.B. Venuto and E.L. Wu, *J. Catal.*, 15 (1969) 205.

28. P.B. Venuto, E.L. Wu and J. Cattanach, *Molecular Sieves*, Society of Chemical Industry, London, (1968) 117.

29. P.B. Venuto, *J. Org. Chem.*, 32 (1967) 1272.

30. B. Coughlan and M.A. Keane, *J. Catal.*, 138 (1992) 164.

31. J. Weitkamp, *Acta Phys. Chem.*, 31 (1985) 271.

32. C.F. Ren, G. Coudurier and C. Naccache, *Stud. Surf. Sci. Catal.*, 28 (1986) 733.

33. R.M. Barrer, F. Bultitude and J.W. Sutherland, *Trans. Faraday Soc.*, 53 (1957) 1111.

34. A. Schriesheim, in *Friedel-Crafts and Related Reactions*, G.A. Olah, (Ed.), Wiley, New York, (1964) 476.

35. R.L. Wadlinger, G.T. Kerr and E.J. Rosinski, *US Pat.*, 3,308,069 (1967).

36. M.M.J. Treacy and J.M. Newsam, *Nature*, 332 (1988) 249.

37. J.M. Newsam, M.M.J. Treacy, W.T. Koetsier and C.B. de Gruyter, *Proc. Royal Soc. Lond. A.*, 420 (1988) 375.

38. R. Szostak, in *Handbook of Molecular Sieves*, Van Nostrand Reinhold, New York, (1992) 92.

39. M.A. Camblor and J. Pérez-Pariente, *Zeolites*, 11 (1991) 202.

40. J. Pérez-Pariente, J.A. Martens and P.A. Jacobs, *Appl. Catal.*, 31 (1987) 35.

41. S.G. Hegde, R. Kumar, R.N. Bhat and P. Ratnasamy, *Zeolites*, 9 (1989) 232.

42. A.R. Pradhan and B.S. Rao, *Appl. Catal.*, 106 (1993) 143.

43. G. Harvey and G. Mäder, *Coll. Czech. Chem. Commun.*, 57 (1992) 673.

44. A. Corma, V. Fornés, J.B. Montón and A.V. Orchillés, *J. Catal.*, 107 (1987) 288.

45. L. Bonetto, M.A. Camblor A. Corma and J. Pérez-Pariente, *Appl. Catal.*, 82 (1992) 37.

46. R.B. Lapierre and R.D. Partridge, *Eur. Pat. Appl.*, 94,827 (1983).

47. R.B. Lapierre, R.D. Partridge, N.Y. Chen and S.S. Wong, *Eur. Pat. Appl.*, 95,203 (1983).

48. R.B. Lapierre, R.D. Partridge, N.Y. Chen and S.S. Wong, *US Pat.*, 4,501,926 (1986).

49. J.A. Martens, J. Pérez-Pariente, E. Sastre, A. Corma and P.A. Jacobs, *Appl. Catal.*, 45 (1988) 85.

50. P. Ratnasamy, R.N. Bhat, S.K. Pokhriyal, S.G. Hegde and R. Kumar, *J. Catal.*, 119 (1989) 65.

51. (a) B.S. Rao, A.R. Pradhan and P. Ratnasamy, 1233/Del/1989; (b) T.C. Tsai, C.I. Ay and A. Wang, *Appl. Catal.*, 77 (1991) 199.

52. L.J. Leu, L.Y. Hou, B.C. Kang, C. Li, S.T. Wu and J.C. Wu, *Appl. Catal.*, 69 (1991) 49.

53. K. Ito, *Hydrocarbon Processing*, 52 (1973) 89.

54. J.M. Derfer and M.M. Derfer, in *Kirk-Othmer Encyclopedia of Chemical Technology*, 22 (1978) 709.

55. W.J. Welstead, Jr., in *Kirk-Othmer Encyclopedia of Chemical Technology*, 9 (1978) 544.

56. D. Frankel and M. Levy, *J. Catal.*, 118 (1989) 10.

57. K.S.N. Reddy, M.J. Eapen, H.S. Soni and V.P. Shiralkar, *J. Phys. Chem.*, 96 (1992) 7923.

58. B.M. Lok, B.K, Marcus and C.L. Angel, *Zeolites*, 6 (1986) 185.

59 P.A. Jacobs, in *Carboniogenic Activity of Zeolites*, Elsevier, Amsterdam, (1977) 46.

60. S. Sivasanker, S.G. Hegde, S.V. Awate, S.R. Padalkar and S.B. Kulkarni, *React. Kinet. Catal. Lett.*, 36 (1988) 173.

61. L.M. Stock and H.C. Brown, *J. Am. Chem. Soc.*, 81 (1959) 3323.

62. P.A. Parikh, N. Subrahmanyam, Y.S. Bhat and A.B. Halgeri, *Appl. Catal.*, 90 (1992) 1.

63. B. Wichterlová and J. Cejka, *J. Catal.*, 146 (1994) 523.

64. W.W. Kaeding, C.Chu, L.B. Young, B.Weinstein and S.A. Butter, *J. Catal.*, 67 (1981) 159.

65. N.Y. Chen, W.W. Kaeding and F.G. Dwyer, *J. Am. Chem. Soc.*, 101 (1979) 6783.

66. D.R. Stull, E.F. Westrum, Jr. and G.C. Sinke, in *The Chemical Thermodynamics of Organic Compounds*, John Wiley and Sons, (1969).

CHAPTER 4

## TRANSALKYLATION REACTIONS OF ALKYL AROMATICS OVER LARGE PORE ZEOLITES

4.1 Introduction

Transfer of an alkyl group between two similar or dissimilar molecules is known as transalkylation reaction. This reaction is industrially important since many low valued by-products like diethyl or diisopropyl benzenes can be converted to their monoalkyl homologs. In this field, early research work was carried out to convert toluene to benzene and xylenes.[1] Later the work was extended to the transalkylation of trimethylbenzenes with toluene to xylenes.[2] Transalkylation reactions are normally carried out in vapor phase over acid catalysts such as Friedel-Crafts catalysts, silica alumina and zeolites at elevated temperatures and pressures.[3-6] Zeolites are superior to the other catalysts due to their activity, selectivity, ease of regeneration and environmentally friendly nature. Today processes like Mobil toluene disproportionation process (MTDP) and liquid phase toluene disproportionation (LDP) are widely used to convert toluene to mixtures of xylene isomers and benzene using ZSM-5 based catalysts.[7,8] Similar to the transfer of methyl group, processes have also been developed for the transalkylation of diethylbenzene with benzene to ethylbenzene and diisopropylbenzene with benzene to cumene.[9,10] In recent years, many zeolite based catalysts such as Mordenite, LaX, LaY, ZSM-5 and Beta have been reported for different transalkylation reactions.[5,10-15]

Transalkylation reactions over zeolites are catalyzed by Brönsted acid sites.[16] The first step of the reaction is the adsorption of aromatic molecules on the acidic sites of the zeolites followed by carbenium ion formation. Two different reaction mechanisms (S_{N1} and S_{N2}) are proposed by Tsai and Wang[17] for this type of disproportionation (for same molecule) or transalkylation reaction (for different molecules). In the S_{N1} mechanism (monomolecular reaction), alkylbenzene first dissociates into an alkyl ion and a benzene molecule. The former then attacks another alkylbenzene and forms dialkylbenzene.

H2C—R

[scheme: reaction mechanism diagram]
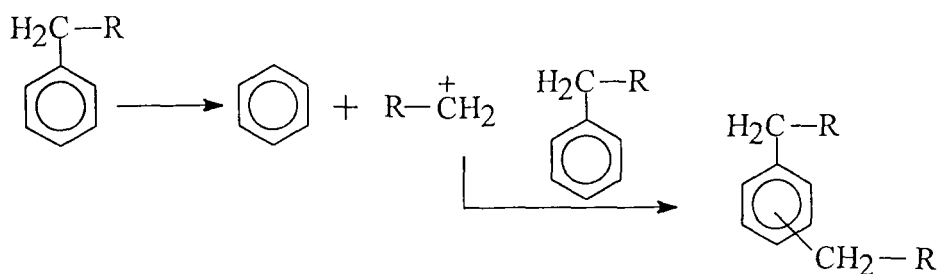
In the S_{N2} mechanism (bimolecular reaction), alkylbenzene first forms a carbenium ion, then it reacts with another alkylbenzene to form a biphenylmethane-type intermediate which finally dissociates into dialkylbenzene and benzene.[12,18,19]

[scheme: reaction mechanism diagram]
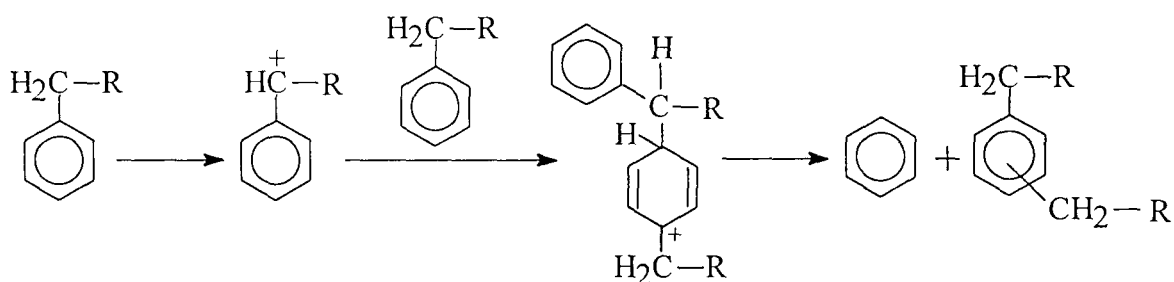
In general S_{N2} mechanism dominates at lower reaction temperatures, while S_{N1} mechanism dominates at higher reaction temperatures.[20,21]

Cymenes and cumene are two industrially important intermediates. Cumene is important for the production of phenol and acetone, and cymenes, specially *para* and *meta* isomers are useful raw materials for the production of cresols, pesticides, pharmaceuticals, perfumery, heat transfer media, polymers and special solvents.[22-25] The present chapter describes the formation of cymenes and cumene by transalkylation reactions over large pore zeolites. In the first section of this chapter, selective formation of cymenes by transalkylation of toluene with cumene over zeolite Beta is studied. The catalytic performance is compared with another two large pore zeolites, Y and ZSM-12. In the second section of this chapter, simultaneous formation of cymenes and cumene by transalkylation of toluene with diisopropylbenzene is studied over large pore zeolites. In

the last section, the same reaction i.e., transalkylation of toluene with diisopropylbenzene is studied at high pressure over REY zeolite.

4.2 Experimental

4.2.1 Catalyst Preparation

Zeolite Beta was synthesized hydrothermally from a system $(TEA)_2O$- Na_2O-SiO_2-Al_2O_3-H_2O at 423 K and ZSM-12 was synthesized from a system $(MTEA)_2O$- Na_2O-SiO_2-Al_2O_3-H_2O at 423 K. The as synthesized zeolites were converted to their protonic forms by usual method of ammonium exchange followed by calcination. NH_4-Y zeolite commercially obtained from Union Carbide, was converted to its protonic form by calcining the catalyst at 773 K for 24 h in a flow of dry air. The H-Y obtained by this way was further modified by exchanging with rare earth salt solution to get REY zeolite. The detailed procedure of the synthesis of zeolite Beta and ZSM-12 and the modification of Y zeolite are described in chapter 2.

4.2.2 Catalyst Characterization

Prior to the catalytic runs, all the samples were characterized by using techniques like XRD, SEM, TG-DTA, atomic absorption and X-ray fluorescence spectroscopy. Acidity of the samples were measured by temperature programmed desorption (TPD) of ammonia. The detailed procedures for the characterization are described in Chapter 2.

4.2.3 Catalytic Reactions

For the transalkylation of toluene with cumene and diisopropylbenzene over H-Beta, H-Y and H-ZSM-12, catalytic experiments were performed at atmospheric pressure in a fixed bed, vertical, down flow integral silica reactor. The reactor set up and reaction procedure are as those discussed in Chapter 3. The catalysts (2g) were pressed, pelleted

and sieved to 10-20 mesh size and charged in the center of the reactor The catalyst was activated at 773 K for at least 6 hours in a flow of dry air before each run. The reactor was then cooled to the desired reaction temperature in presence of nitrogen. The liquid reactant mixture (toluene and cumene or 1,4-diisopropylbenzene) was fed by a syringe pump (SAGE Instruments, Model 352, USA). The products of the reaction were collected downstream from the reactor in a cold trap, and analyzed by gas chromatography, Shimadzu 15A, connected with Xylene Master column and FID detector.

Transalkylation of toluene with diisopropylbenzene over REY zeolite was carried out at high pressure in a catatest unit reaction set up (géomécanique, France). About 5 g of catalyst (REY) was taken, mixed with equal amount of alumina binder and loaded in the form of extrudates in the stainless steel reactor. The catalyst was activated at 773 K for at least 5 h and cooled down to the desired temperature prior to the catalytic reaction. An industrial cumene bottom fraction consisting mainly diisopropylbenzene (DIPB) isomers with some impurities like 2-methyl,3-phenylhexane obtained from an operating commercial plant was mixed with toluene in desired molar ratio to prepare the commercial transalkylation feed. The mixture was pumped using an automated digital metering pump (Model 500D, ISCO, USA). Hydrogen was used as the carrier gas. Products of the reaction were collected at an hourly interval and analyzed by gas chromatograph, Shimadzu 15A, using an Apiezon L column for liquids and Porapak Q column for gaseous samples. High pressure reactor set up is shown in Fig. 4.1.

4.3 Results and Discussion

4.3.1 Transalkylation of toluene with cumene over large pore zeolites

High intensity of the peaks and absence of baseline drift in the XRD patterns reveal that the zeolite samples were highly crystalline. SEM photographs showed well defined
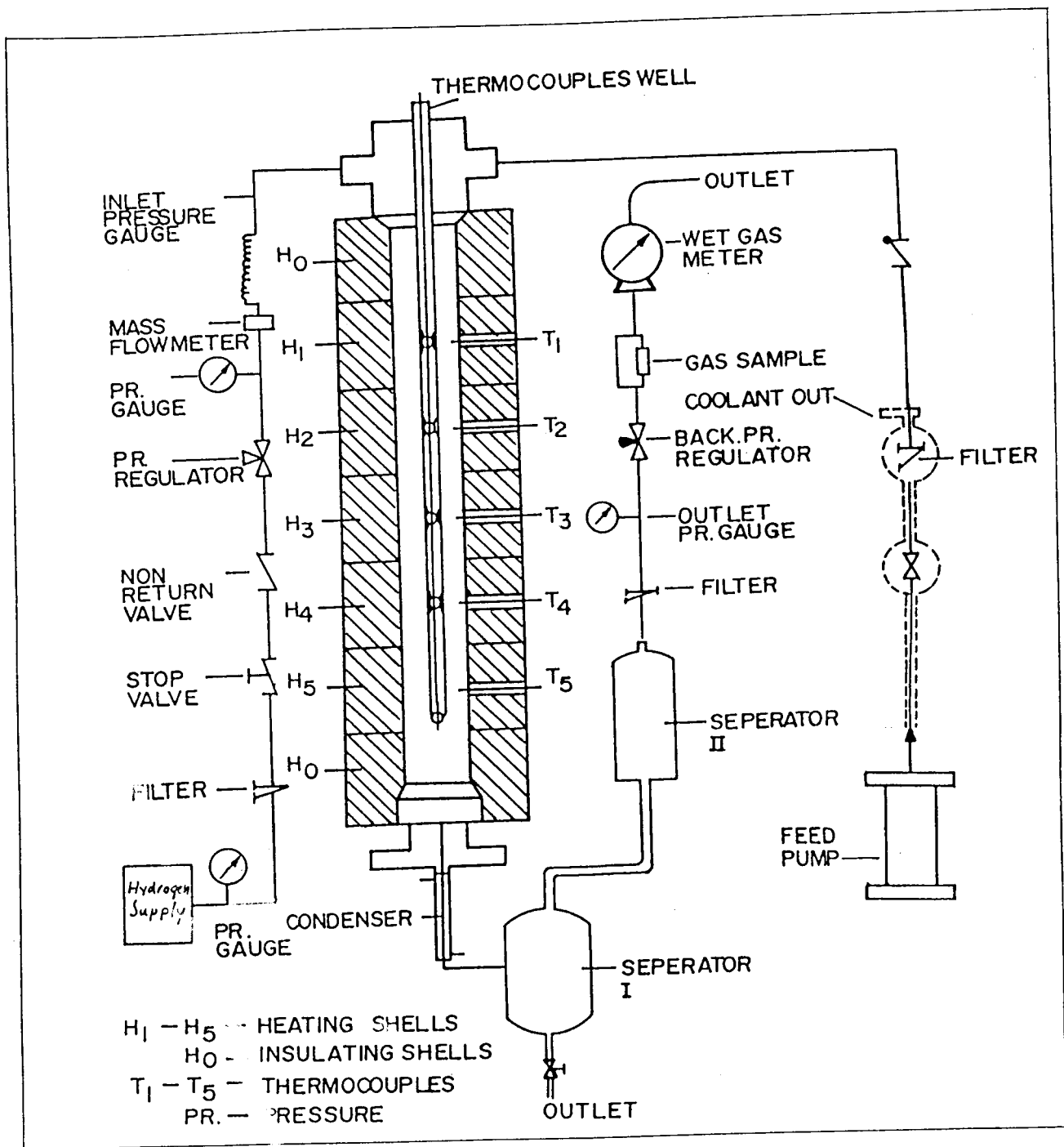
Fig. 4.1   High-pressure reactor set-up for transalkyaltion of toluene with DIPB over REY zeolite

materials without any occluded samples in the zeolites. TG-DTA-DTG results indicated thermal resistance of the samples.

A possible reaction scheme for the transalkylation reaction of toluene with cumene as well as the possible side reactions is presented in Fig 4.2. One mole of toluene reacts with one mole of cumene to yield equimolar quantities of cymene and benzene. The other possible reaction is the disproportionation of cumene yielding diisopropylbenzene (DIPB). Benzene is also formed by the dealkylation of cumene. Disproportionation of toluene and cymene also occur simultaneously to form xylene and diisopropyltoluene (DIPT) respectively but the amounts are too low. The secondary isomerization of p-cymene to m-cymene is also favorable. Possible reaction mechanism of the transalkylation reaction is shown in Fig. 4.3. According to S_{N1} mechanism (monomolecular reaction), cumene first dissociates into isopropyl ion and a benzene molecule. The former then reacts with toluene to form cymene. In S_{N2} mechanism (bimolecular reaction), cumene first forms a cumyl or isopropyl benzyl ion, then reacts with toluene to form a 2,2'-diphenylpropane-type intermediate which finally dissociates into cymene and benzene. The reaction mechanism depends on the reaction temperature as well as the internal pore structure of the zeolite. According to Tsai et al.,[17] only the zeolites with 12-membered rings and open structures undergo a bimolecular reaction mechanism. The S_{N2} mechanism prevails in large pore zeolites like Beta and Y due to the adequate pore space required for the formation of biphenylmethane or biphenylpropane-type intermediates whereas both S_{N1} and S_{N2} mechanisms prevail in the unidimensional pore systems like ZSM-12 and mordenite, depending upon the reaction temperature.

4.3.1.1 Effect of feed ratio

The influence of toluene to cumene molar ratio on the transalkylation reaction is shown in Table 4.1. Cumene conversion as well as selectivity of cymenes reach a
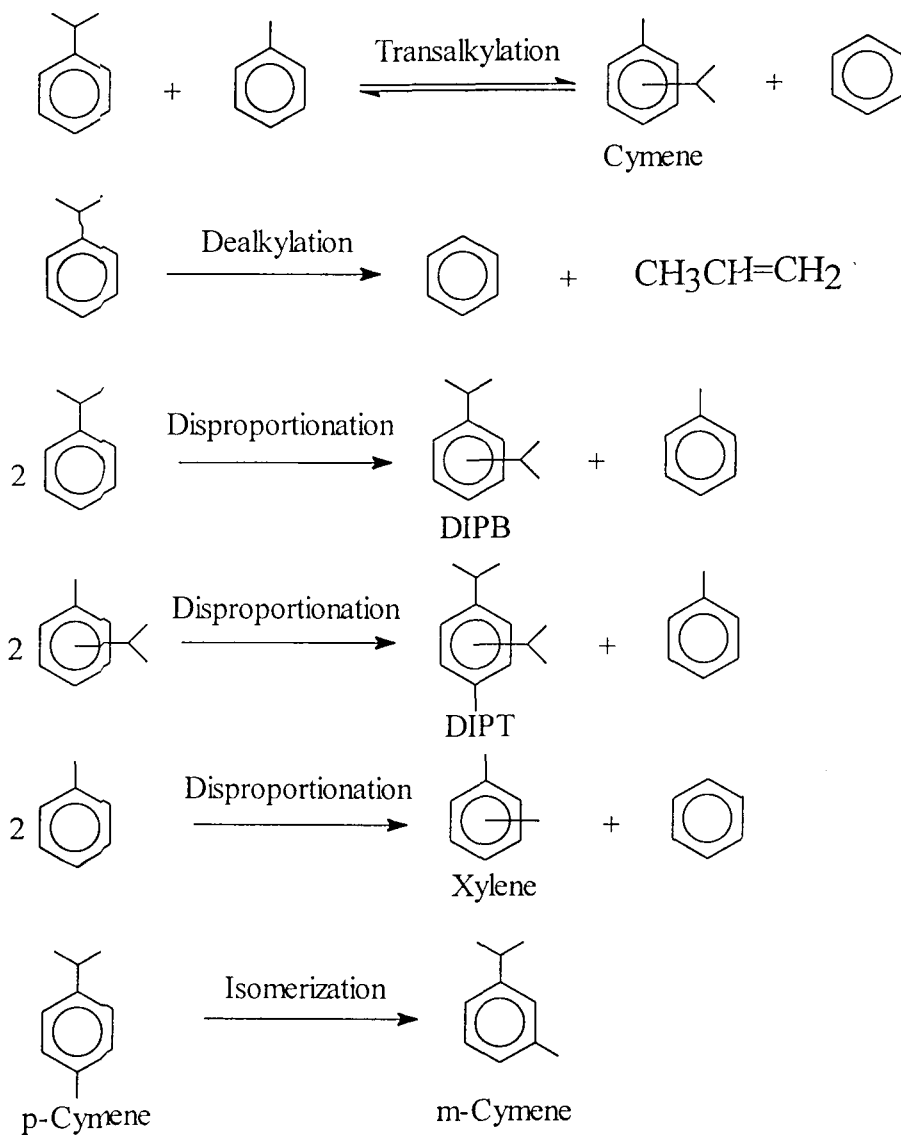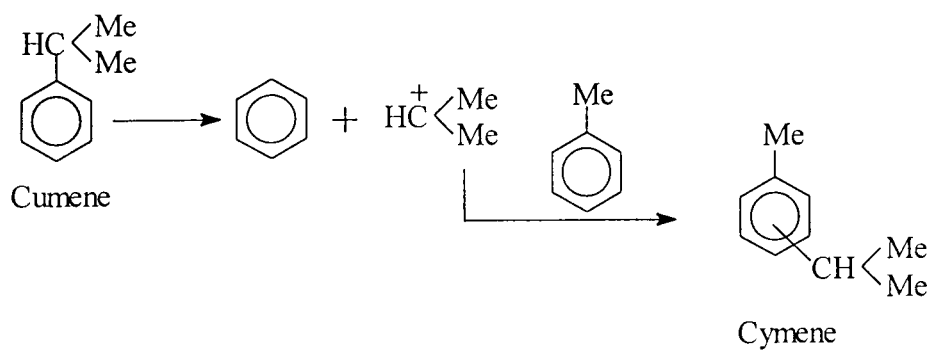
Fig. 4.2   Reaction scheme for transalkylation of toluene with cumene and side reactions

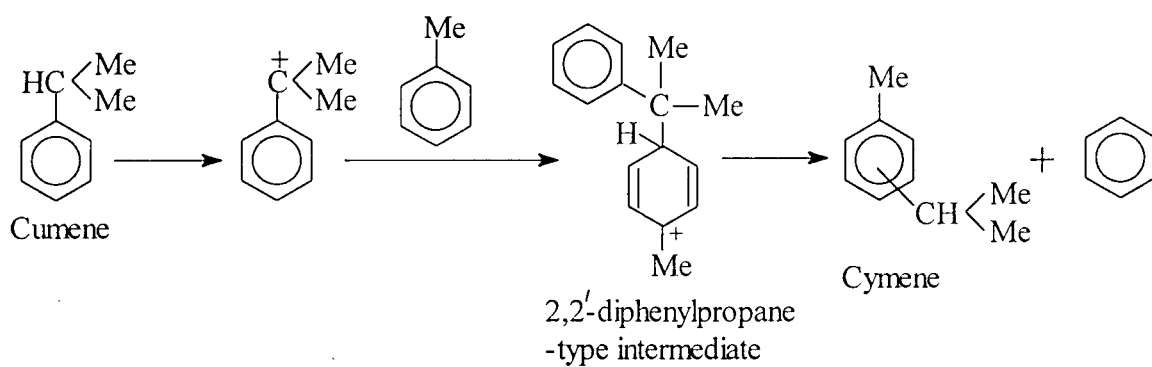## S_N1 Mechanism

S_N2 Mechanism

Fig. 4.3   Reaction mechanism for transalkylation of toluene with cumene

Table 4.1

Transalkylation of toluene with cumene over H-Beta
Effect of Toluene/Cumene molar ratio on catalytic activity

Product distribution (Wt.%)	Tolune/Cumene (mol/mol)				
	6	10	14	18	22
Aliphatics	0.04	0.03	0.02	0.02	0.01
Benzene	5.33	4.51	2.92	2.24	1.78
Toluene	76.54	83.14	88.83	90.96	92.62
Σ Xylene	0.26	0.26	0.19	0.17	0.14
Cumene	9.14	5.05	3.34	3.11	2.70
p-Cymene	2.39	1.98	1.35	1.01	0.80
m-Cymene	5.12	4.38	2.99	2.24	1.77
o-Cymene	0.37	0.31	0.21	0.16	0.13
Σ Cymene	7.88	6.67	4.55	3.41	2.70
Σ DIPB	0.66	0.25	0.11	0.07	0.04
Σ DIPT	0.15	0.09	0.04	0.02	0.01
p/m Cymene	46.68	45.21	45.15	45.09	45.19
Performance					
% Cumene conversion	44.88	52.75	58.42	50.68	48.27
% Cymenes selectivity	87.65	91.37	92.67	92.41	93.10

Reaction condition : Temperature = 473 K, W.H.S.V. = 4.2 h^{-1}, Time on stream (TOS) = 2 h

maximum value at toluene to cumene molar ratio of 14. Further increase in molar ratio lowers the conversion of cumene without affecting cymene selectivity.

4.3.1.2 Effect of temperature

The reaction was performed over a range of temperatures from 453 K to 513 K using H-Beta catalyst (Table 4.2). Conversion of cumene increases with the increase in temperature. Cymene selectivity does not vary much. However, side products such as xylenes and DIPT are observed at higher temperature. The conversion of cumene as a function of time on stream with the variation in temperature is shown in Fig. 4.4. Slow deactivation of the catalyst is observed at all temperatures with a faster deactivation at higher temperatures. This may be attributed to the formation of more coke precursors at higher temperatures due to the dealkylation of cumene and formation of olefins.

4.3.1.3 Effect of space velocity

The transalkylation reaction was also studied as a function of space velocity ranging from 1.2 h^{-1} to 8.2 h^{-1} at 473 K (Table 4.3). Conversion of cumene decreases sharply with the increase in WHSV (i.e., decrease in contact time), the selectivity of cymenes remaining almost constant. With variation of contact time/space velocity (about 7 times), the p/m cymene ratio varied from 45 to 49.5 which indicates that the secondary isomerization process in H-Beta is not important in spite of being a unimolecular reaction. The optimum conditions for selective transalkylation over zeolite H-Beta at atmospheric pressure was found to be: temperature 473 K- 493 K, WHSV 4.2 h^{-1} and toluene to cumene molar ratio 14. The zeolite showed a stable performance for longer time.

4.3.1.4 Comparison of catalysts

The catalytic performance of H-Beta in the transalkylation of toluene with cumene was compared with other two large pore zeolites, namely H-Y and H-ZSM-12. The

Table 4.2

Transalkylation of toluene with cumene over H-Beta
Effect of temperature on catalytic activity

Product distribution (Wt.%)	Temperature (K)			
	453	473	493	513
Aliphatics	0.01	0.02	0.02	0.07
Benzene	1.74	2.92	3.47	4.35
Toluene	90.26	88.83	87.66	88.12
Σ Xylene	0.12	0.19	0.24	0.33
Cumene	5.04	3.34	3.23	1.87
p-Cymene	0.82	1.35	1.54	1.52
m-Cymene	1.77	2.99	3.43	3.37
o-Cymene	0.13	0.21	0.25	0.26
Σ Cymene	2.72	4.55	5.22	5.15
Σ DIPB	0.10	0.11	0.10	0.04
Σ DIPT	0.01	0.04	0.06	0.07
p/m Cymene	46.33	45.15	44.90	45.10
Performance				
% Cumene conversion	30.69	58.42	58.90	75.44
% Cymenes selectivity	91.89	92.67	92.55	90.99

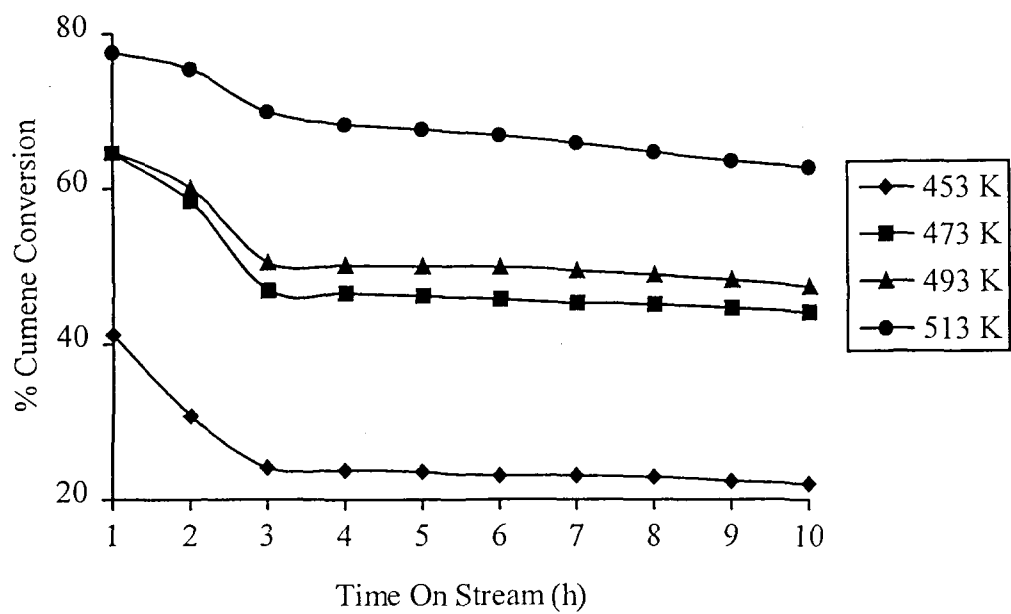Reaction condition : Toluene/Cumene (mol/mol) = 14, W.H.S.V. = 4.2 h^{-1}, TOS = 2h

Th 8454

Fig. 4.4 Transalkylation of toluene with cumene over H-Beta: effect of temperature on cumene conversion; toluene/cumene (mol) = 14, WHSV = 4.2 h^{-1}

Table 4.3

Transalkylation of toluene with cumene over H-Beta
Effect of W.H.S.V. on catalytic activity

Product distribution (Wt.%)	W.H.S.V. (h⁻¹)				
	1.2	2.5	4.2	6.2	8.2
Aliphatics	0.05	0.03	0.02	0.01	0.01
Benzene	3.71	3.09	2.92	1.62	1.15
Toluene	87.63	88.75	88.83	90.10	90.83
Σ Xylene	0.36	0.26	0.19	0.12	0.11
Cumene	2.61	3.05	3.34	5.58	6.11
p-Cymene	1.63	1.39	1.35	0.74	0.52
m-Cymene	3.63	3.09	2.99	1.56	1.05
o-Cymene	0.25	0.22	0.21	0.13	0.10
Σ Cymene	5.51	4.70	4.55	2.43	1.67
Σ DIPB	0.09	0.09	0.11	0.13	0.11
Σ DIPT	0.04	0.03	0.04	0.01	0.01
p/m Cymene	44.90	44.98	45.15	47.64	49.52
Performance					
% Cumene conversion	66.69	62.15	58.42	27.62	21.32
% Cymenes selectivity	91.09	92.44	92.67	90.00	87.43

Reaction condition : Temperature = 473 K, Toluene/Cumene (mol/mol) = 14, TOS = 2h

comparison of the zeolites are presented in Table 4.4, Fig. 4.5 and Fig. 4.6. Both cumene conversion and cymene selectivity are much higher in H-Beta than H-Y and H-ZSM-12. All three catalysts deactivate with time, but deactivation is faster in H-Y and H-ZSM-12. During the period of study, H-Beta did not show any appreciable drop in cumene conversion. In H-Beta, p/m cymene ratio does not vary much with the variation in space velocity. However, with the increase in space velocity from 1.2 h^{-1} to 8.2 h^{-1}, p/m cymene ratio (wt.%) increases from 59% to 92% in HY and from 48% to 88% in H-ZSM-12 (Fig. 4.7). This indicates that secondary isomerization of p-cymene to m-cymene is favorable in these two samples.

H-Y possesses an open type structure, and the deactivation is faster mainly due to coke formation. Similarly, in H-ZSM-12, due to its unidimensional pore structure, the coking is appreciable. Due to coking, the cumene conversion and cymene yield are reduced and a variation in the distribution of cymenes is observed. Thus, p-cymene concentration increases in the products while m-cymene concentration decreases in spite of the decrease in total activity. However, no appreciable change in the cymene isomers is observed with H-Beta (Fig 4.8). The products, in the transalkylation reaction, are favored by *ortho/para* orientation depending on the thermodynamic equilibrium. In the initial stage of the reaction, the primary *para* isomers are converted to *meta* isomers by a secondary isomerization process which reduces with coking of the active sites exhibiting high *para* selectivity. Due to the coking both inside and outside, the active sites are reduced leading to reduction in activity and modifying the channels or the pore openings. The dimensions, length, breadth and width for *para* and *meta* were computed using Silicon Graphics as described in literature.[26] The values are: a = 7.14 Å, b = 6.66 Å, and c = 2.95 Å for m-cymene and a = 7.87 Å, b = 4.28 Å, and c = 2.95 Å for p-cymene. Cymenes are formed in equilibrium concentrations inside the pores of zeolites, and p-cymene, in particular, due to its smaller dimensions diffuses faster through the pores which are partially coked. Thus p-cymene concentration in the product increases.

Table 4.4

Transalkylation of toluene with cumene over large pore zeolites

Product distribution (Wt.%)	Catalyst		
	H-Y	H-ZSM-12	H-Beta
Aliphatics	0.01	0.01	0.04
Benzene	1.07	1.47	5.33
Toluene	81.51	80.47	76.54
Σ Xylene	0.15	0.14	0.26
Cumene	15.52	15.43	9.14
p-Cymene	0.48	0.71	2.39
m-Cymene	0.78	1.13	5.12
o-Cymene	0.11	0.14	0.37
Σ Cymene	1.37	1.98	7.88
Σ DIPB	0.36	0.49	0.66
Σ DIPT	0.01	0.01	0.15
p/m Cymene	61.54	62.83	44.68
Performance			
% Cumene conversion	6.91	7.31	44.88
% Cymenes selectivity	72.11	75.29	87.65

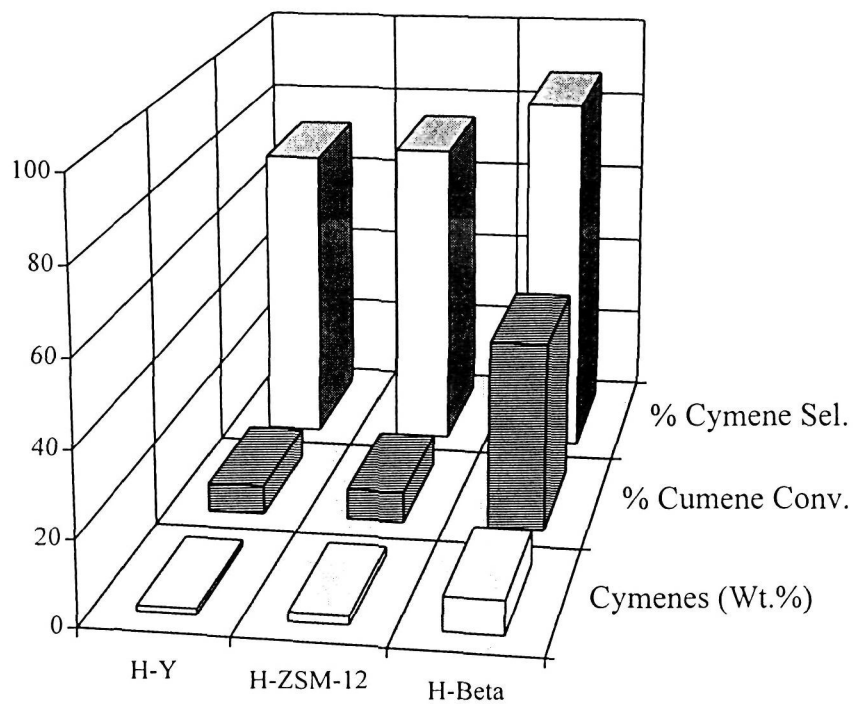Reaction condition : Temperature = 473 K, Toluene/Cumene (mol/mol) = 6, W.H.S.V. = 4.2 h^{-1}, TOS = 2 h

Fig. 4.5   Transalkylation of toluene with cumene: catalytic performance of large pore zeolites; toluene/cumene (mol) = 6, T = 473 K, WHSV = 4.2 h^{-1}
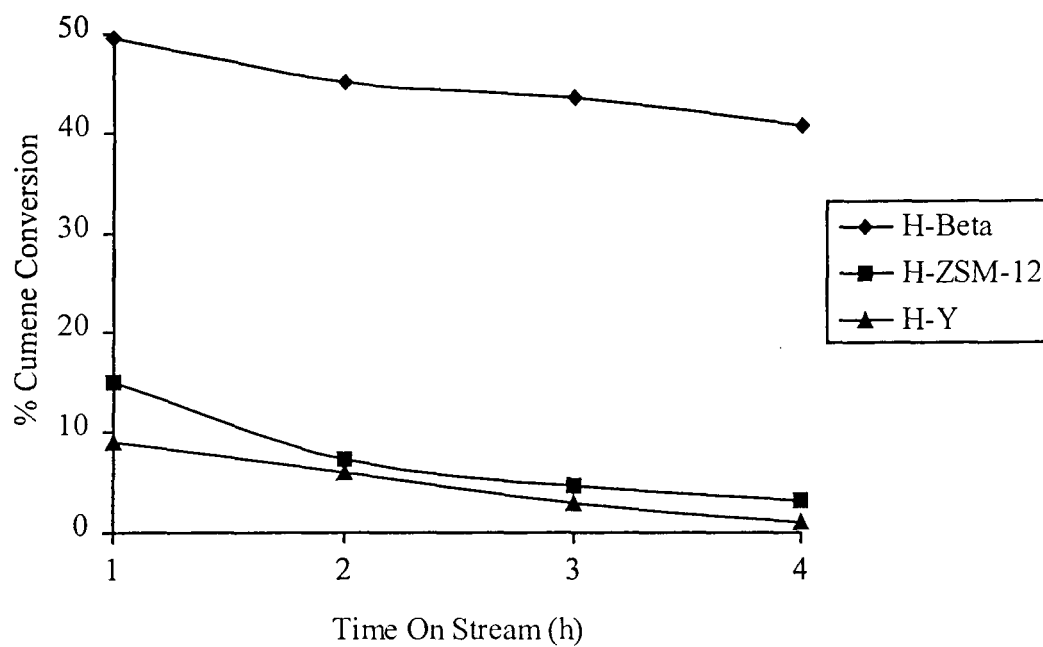
Fig. 4.6   Transalkylation of toluene with cumene over large pore zeolites: cumene conversion with time on stream; toluene/cumene (mol) = 6, T = 473 K, WHSV = 4.2 h^{-1}
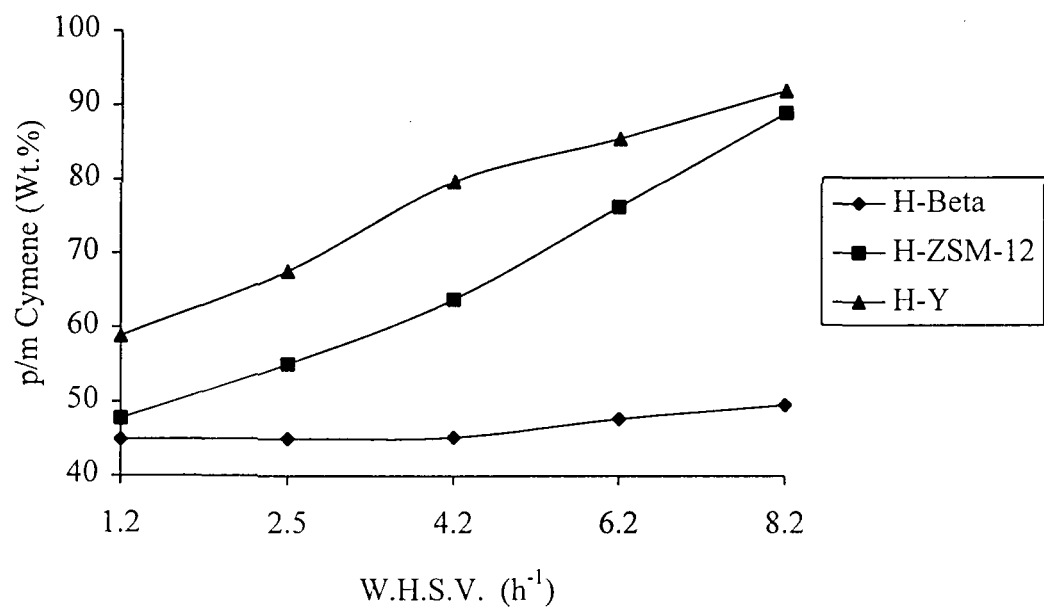
Fig. 4.7   Transalkylation of toluene with cumene over large pore zeolites: effect of
space velocity on p/m cymene ratio; toluene/cumene (mol) = 14,
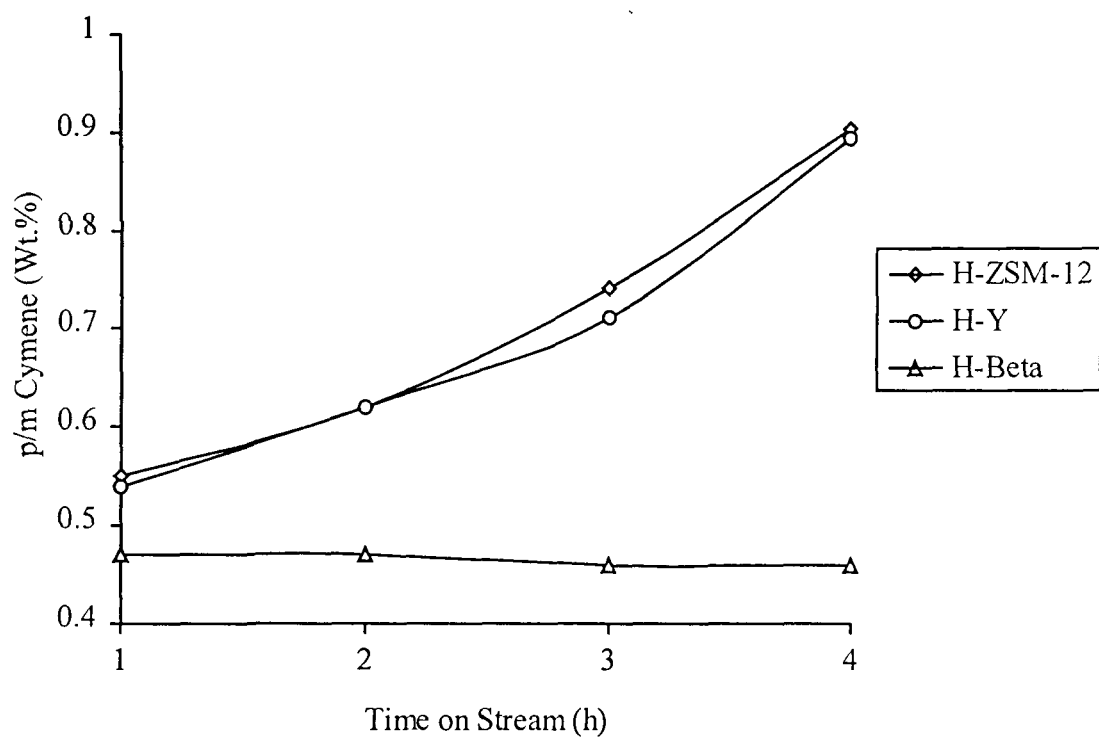T = 473 K, TOS = 2 h

Fig. 4.8   Transalkylation of toluene with cumene: formation of *para* cymene over large pore zeolites; toluene/cumene (mol) = 6, T = 473 K, WHSV = 4.2 h⁻¹

108

However, formation of *o*-cymene is less and the concentration remains more or less same. This type of coke induced shape selectivity is partially responsible for the higher *p/m* cymene ratio in H-Y and H-ZSM-12. H-Beta did not show any shape selectivity as deactivation in H-Beta is very less.

4.3.2 Transalkylation of toluene with 1,4-diisopropylbenzene (1,4-DIPB) over large pore zeolites

As mentioned earlier, cymene and cumene are two industrially important intermediates and raw materials for important end products. Both cymene and cumene can be simultaneously formed by the transalkylation of toluene with diisopropylbenzene. In this reaction, one of the isoprpyl group of DIPB is transferred to toluene yielding cymene and cumene. The reaction is studied over large pore zeolite H-Beta at atmospheric pressure and the catalytic performance is compared with H-ZSM-12 and H-Y.

The transalkylation of toluene with DIPB is a multi-step and sequential reaction. A possible reaction scheme is presented in Fig. 4.9 from the product analysis. One mole of toluene reacts with one mole of DIPB giving rise to equimolar cymene and cumene. DIPB first forms a carbenium ion (positive charge on the secondary carbon atom of one of the isopropyl groups), then reacts with toluene to form a 2,2'-diphenylpropane type intermediate and then dissociates into cymene and cumene. In addition to the main transalkylation reactions, there are another two side transalkylation reactions which can occur simultaneously. These are the transalkylation of benzene with DIPB to form cumene[10] and transalkylation of toluene with cumene to form cymene.[27] DIPB can dealkylate to cumene which consequently can dealkylate to form benzene. Besides, xylenes and diisopropyltoluene (DIPT) are formed from the disproportionation of toluene and cymene respectively, though these reactions are negligible at higher toluene to 1,4-DIPB molar ratio and lower temperatures. Simultaneously, 1,4-DIPB is isomerized to
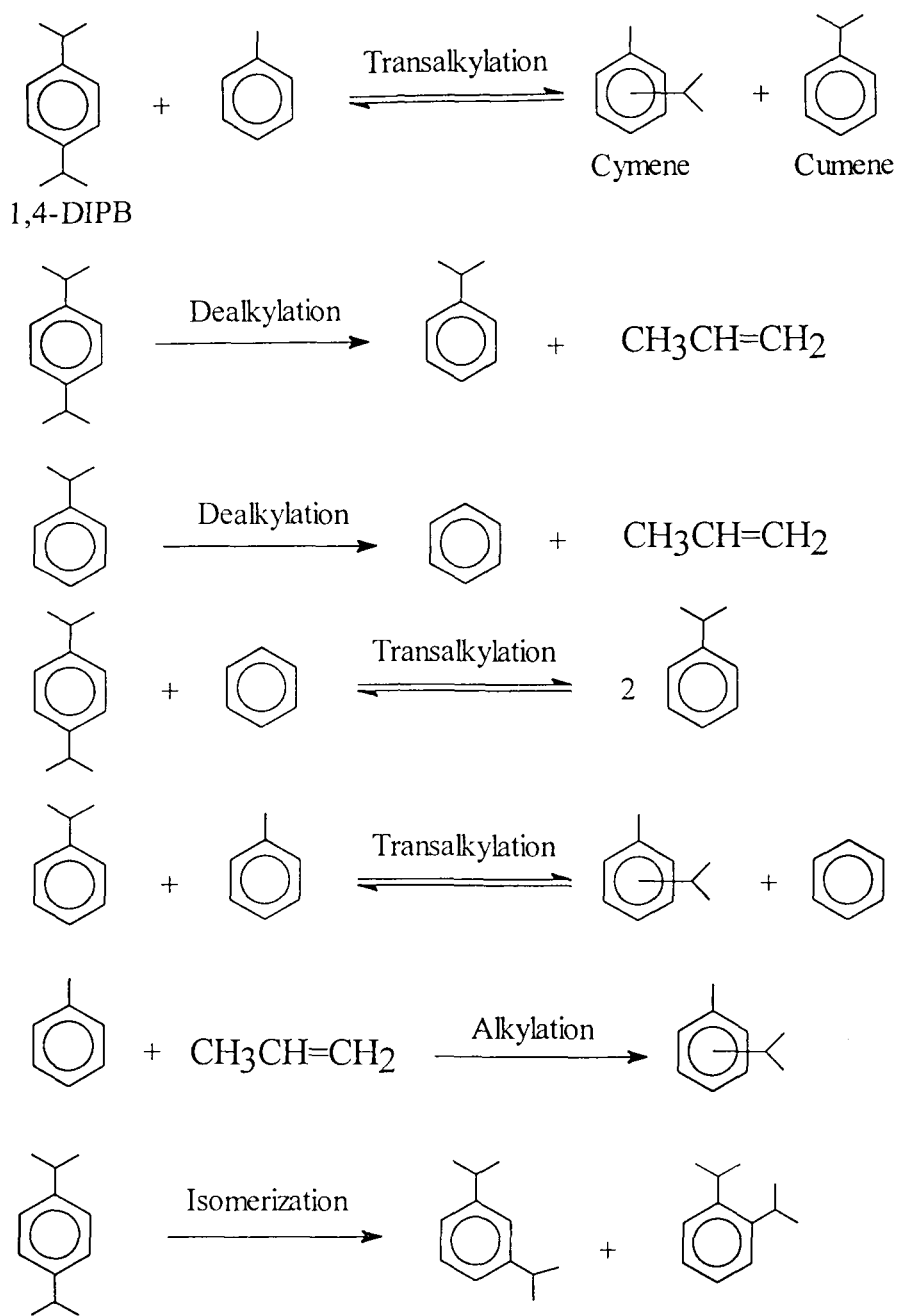
109

Fig. 4.9 Reaction scheme for transalkylation of toluene with DIPB

1,3- and 1,2-DIPBs, the amount of 1,2-DIPB being negligible due to its relatively high strain energy. The influence of various reaction parameters on catalytic activity of H-Beta and comparison of its performance with H-ZSM-12 and H-Y are discussed below.

4.3.2.1 Effect of temperature

The transalkylation of toluene with 1,4-DIPB has been studied over temperatures ranging from 453 K to 513 K. The influence of temperature on the activity and product selectivity over Beta is presented in Table 4.5. Conversion of 1,4-DIPB is more than 98% at all temperatures except at low temperature (353 K). Selectivity of cymene increases and that of cumene decreases steadily with increase in temperature. This is because at higher temperatures, dealkylation of cumene to benzene and propylene is enhanced, and cymene can be formed by the transalkylation of toluene with cumene and further alkylation of toluene with propylene at higher temperatures. Selectivity to 1,3- + 1,2-DIPB is more at lower temperature indicating favorable competition of isomerization of 1,4-DIPB with transalkylation reaction, though yield of 1,2-isomer is always negligible. However, at higher temperature transalkylation of 1,4-DIPB predominates over isomerization.

4.3.2.2 Effect of feed ratio (Toluene/1,4-DIPB)

The influence of toluene to 1,4-DIPB molar ratio in the feed on the conversion and product selectivity over H-Beta is shown in Table 4.6. Conversion of 1,4-DIPB increases with the increase in toluene to 1,4-DIPB molar ratio. Selectivity of cymene increases steadily with the increase in molar ratio. On the other hand, selectivity of 1,3 + 1,2-DIPB decreases with increase in the molar ratio indicating less isomerization of 1,4-DIPB at higher molar ratio. Selectivity of cumene does not vary to a greater extent with the increase in molar ratio. This may be due to the fact that, conversion of cumene by dealkylation to benzene and transalkylation with toluene to cymene is compensated by

Table 4.5

Transalkylation of toluene with 1,4-DIPB over H-Beta
Effect of temperature on catalytic activity

Product distribution (Wt.%)	Temperature (K)			
	453	473	493	513
Aliphatics	0.03	0.05	0.04	0.06
Benzene	0.16	0.68	1.01	1.86
Toluene	91.14	89.09	88.59	87.66
Σ Xylene	0.05	0.10	0.13	0.27
Cumene	3.16	3.90	3.53	2.56
Σ Cymene	3.37	5.71	6.34	7.36
1,3-DIPB	1.44	0.29	0.19	0.09
1,4-DIPB	0.59	0.11	0.09	0.04
1,2-DIPB	0.01	0.01	0.01	0.01
Σ DIPT	0.05	0.06	0.07	0.09
Performance				
% Conversion (1,4-DIPB)	90.77	98.20	98.63	99.05
% Selectivity Cymenes	40.75	52.87	55.96	59.84
% Selectivity Cumene	38.21	36.11	31.16	20.81
% Selectivity (1,3+1,2-DIPB)	17.53	1.85	1.77	0.81

Reaction condition : Toluene/1,4-DIPB (mol/mol) = 22, W.H.S.V. = 4.0 h^{-1}, TOS = 3 h

Table 4.6

Transalkylation of toluene with 1,4-DIPB over H-Beta
Effect of Toluene/1,4-DIPB on catalytic activity

Product distribution (Wt.%)	Tolune/1,4-DIPB (mol/mol)				
	6	10	14	18	22
Aliphatics	0.15	0.05	0.06	0.05	0.04
Benzene	0.27	0.57	0.60	0.91	0.82
Toluene	73.85	79.48	85.08	86.74	89.07
Σ Xylene	0.09	0.13	0.13	0.16	0.14
Cumene	7.78	7.58	5.61	4.59	3.63
Σ Cymene	7.97	9.10	7.10	7.00	5.91
1,3-DIPB	6.46	2.00	0.91	0.31	0.19
1,4-DIPB	2.94	0.82	0.37	0.14	0.08
1,2-DIPB	0.09	0.02	0.01	0.01	0.01
Σ DIPT	0.40	0.25	0.13	0.09	0.11
Performance					
% Conversion (1,4-DIPB)	85.47	93.83	96.30	98.19	98.69
% Selectivity Cymenes	34.34	46.19	48.80	53.35	54.47
% Selectivity Cumene	33.52	38.48	38.56	34.98	33.46
% Selectivity (1,3+1,2-DIPB)	28.22	10.25	6.32	2.39	1.84

Reaction condition : Temperature = 473 K, W.H.S.V. = 4.0 h^{-1}, TOS = 2 h

the dealkylation of DIPB and transalkylation of DIPB with benzene to form cumene further.

4.3.2.3 Effect of space velocity

With the increase in W.H.S.V., conversion of 1,4-DIPB decreases slowly. Selectivity of cymenes decreases (Fig. 4.10) and selectivity of cumene increases at higher space velocity (lower contact time) due to the simultaneous transalkylation of benzene with DIPB. Isomerization of 1,4-DIPB to 1,3- and 1,2- isomers also competes to some extent with transalkylation of 1,4-DIPB at higher W.H.S.V.

4.3.2.4 Comparison of catalysts

Transalkylation of toluene with 1,4-DIPB over zeolite H-Beta is compared with H-ZSM-12 and H-Y. The results are shown in Table 4.7 and Fig. 4.11. H-Beta shows high activity compared to the other two zeolites. In both H-ZSM-12 and H-Y, conversion of 1,4-DIPB decreases rapidly with time on stream indicating fast deactivation. The faster deactivation in these catalysts may be attributed to their structure types and formation of more coke precursors, as described earlier. In H-Beta, the conversion of 1,4-DIPB is much higher (>90 %) indicating stable activity of the catalyst and least deactivation. Selectivity towards cymenes is much higher in H-Beta, whereas selectivity towards cumene and 1,3 + 1,2-DIPB are much higher in H-ZSM-12 and H-Y than H-Beta. Dealkylation reaction is more in H-Beta than the other two zeolites as ensured by the benzene formation. There is least benzene formation in the other two catalysts.This is due to the structural differences of the zeolites.
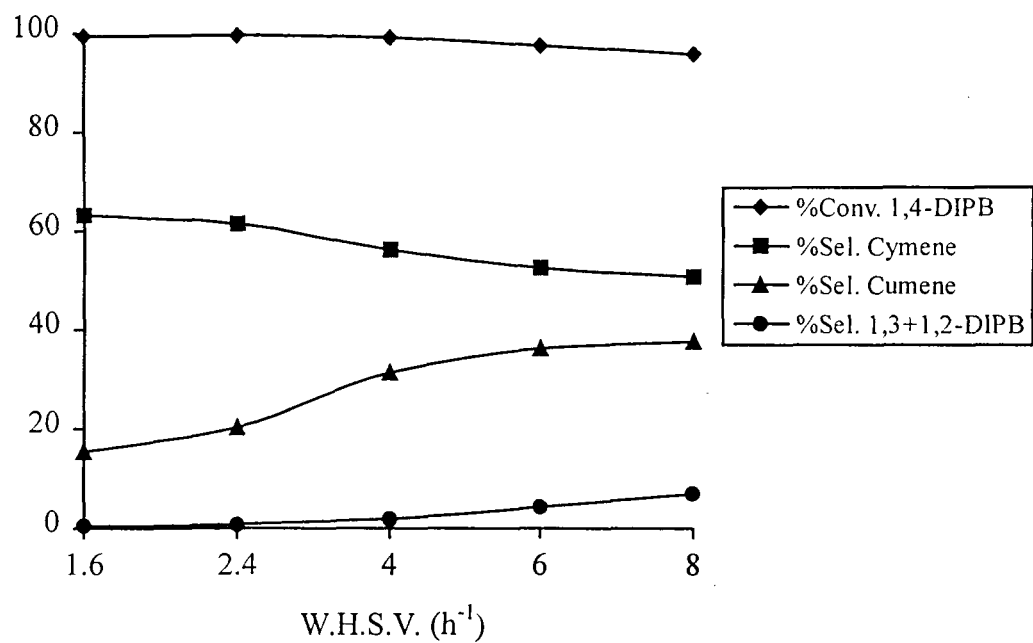
Fig. 4.10   Transalkylation of toluene with DIPB over H-Beta: catalytic performance
with space velocity; toluene/DIPB (mol) = 22, T = 493K, TOS = 3h

Table 4.7

Transalkylation of toluene with 1,4-DIPB over large pore zeolites

Product distribution (Wt.%)	Catalyst		
	H-Beta	H-ZSM-12	H-Y
Aliphatics	0.05	0.02	0.04
Benzene	1.15	0.19	0.12
Toluene	88.35	90.59	91.36
Σ Xylene	0.15	0.04	0.06
Cumene	3.26	2.80	2.63
Σ Cymene	6.72	3.34	2.69
1,3-DIPB	0.15	2.01	1.59
1,4-DIPB	0.08	0.98	1.44
1,2-DIPB	0.01	0.01	0.02
Σ DIPT	0.08	0.02	0.05
Performance			
% Conversion (1,4-DIPB)	98.78	84.24	76.85
% Selectivity Cymenes	56.93	36.62	37.36
% Selectivity Cumene	28.95	33.21	36.53
% Selectivity (1,3+1,2-DIPB)	1.42	23.96	22.36

Reaction condition : Toluene/1,4-DIPB (mol/mol) = 22, T = 493 K, W.H.S.V. = 4.0 h^{-1}, TOS = 2 h
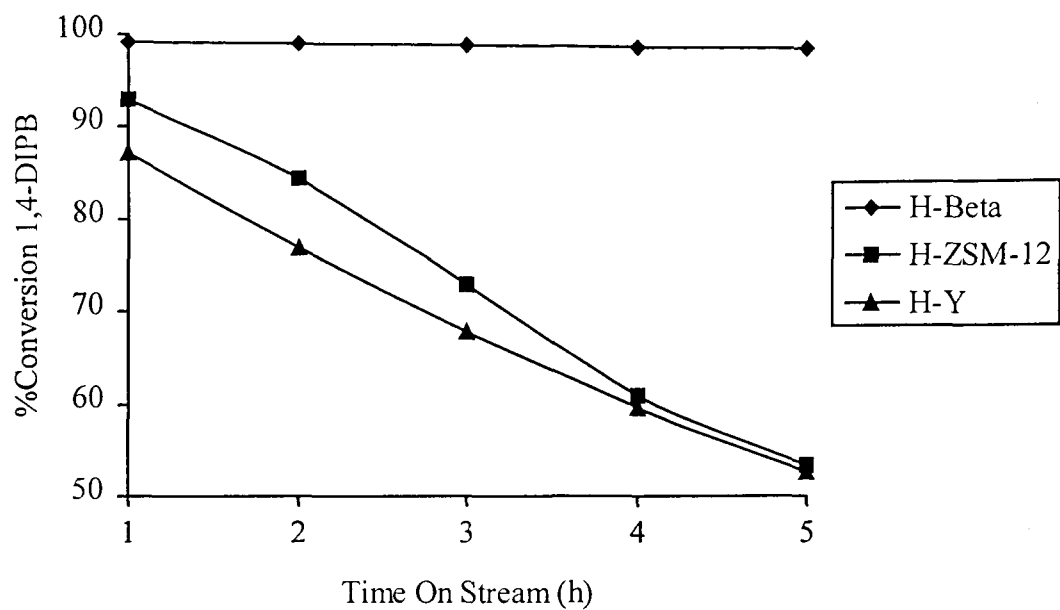
Fig. 4.11 Transalkylation of toluene with DIPB over large pore zeolites: conversion of 1,4-DIPB with time on stream; toluene/DIPB mol) = 22, T = 493K, WHSV = 4.0 h^{-1}

4.3.3 Transalkylation of toluene with diisopropylbenzene (DIPB) over zeolite REY at high pressure

Rare earth exchanged zeolites, due to their improved hydrothermal stability and superior catalytic properties, have been widely used in industries. The main advantages of carrying out reactions using hydrogen as carrier gas at high pressure is to improve the life of the catalyst, or in other words, to minimize the deactivation of the catalyst. The coke precursors, usually polynuclear unsaturated hydrocarbons formed within the pore of zeolites are hydrogenated in presence of hydrogen and diffuses out at high pressure.

Transalkylation of toluene with diisopropylbenzene was carried out over REY zeolite at high pressure taking commercial cumene bottom fraction from an operating plant, and consisting mainly DIPB isomers. The preparation of the catalyst and the reactant mixture, and the reaction procedure have been described earlier.

The possible reaction scheme for the transalkylation reaction is presented in Fig. 4.12. The reaction scheme is basically same as that over zeolite Beta at atmospheric pressure. Here instead of 1,4-DIPB, cumene bottom fraction is taken as the DIPB source which consists small amount of impurities mainly 2-methyl,3-phenylhexane. As mentioned earlier, the reaction goes through a 2,2'-diphenylpropane type intermediate which can be easily accommodated inside the cage of REY zeolite. Apart from the transalkylation reaction, cumene can be formed from the dealkylation of DIPB and cymenes can be formed from the alkylation of toluene or transalkylation of cumene. Benzene is formed from the dealkylation of cumene or 2-methyl,3-phenylhexane. Xylenes and diisopropyltoluene are also formed in negligible amounts. The effect of different parameters on the reaction is discussed in the next section.
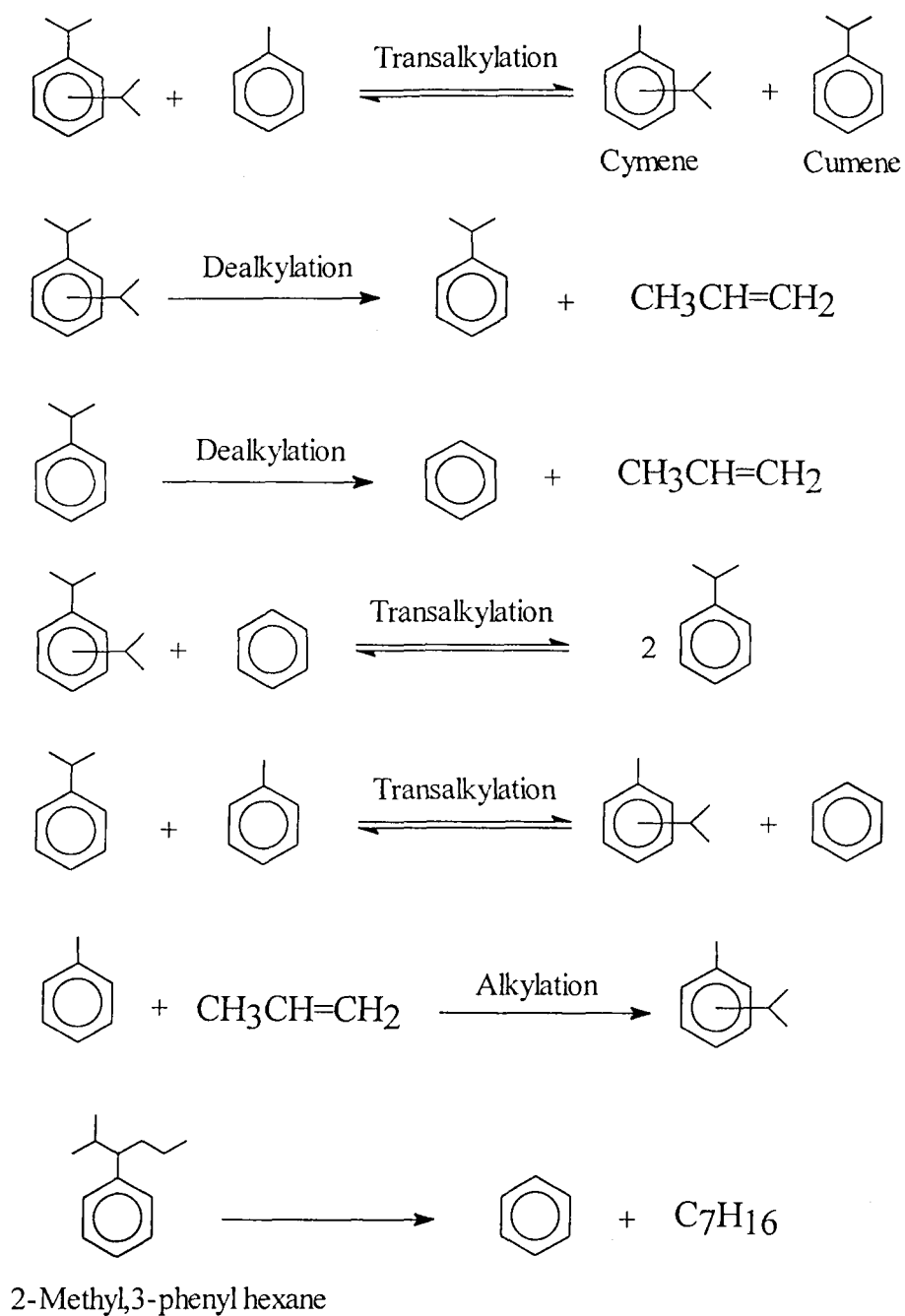
Fig. 4.12 Reaction scheme for transalkylation of toluene with DIPB at high pressure over REY zeolite

4.3.3.1 Effect of temperature

Conversion of DIPB increases from 61% to 98% with the increase in temperature from 503 K to 573 K (Table 4.8). As temperature increases, dealkylation of DIPB to cumene and further dealkylation of cumene to benzene increases, and consequently selectivity of cymene and cumene decreases. Amount of xylene is also increased with the increase in temperature indicating increase in disproportionation of toluene at higher temperatures. In the initial stage, depending on the concentration of hydrogen, dealkylation and hydrogenation of C_{12} compound takes place with high exothermicity. Unless the exothermicity is controlled, transalkylation reaction is overcome by dealkylation.

4.3.3.2 Effect of space velocity

As W.H.S.V. is increased from 4.8 h^{-1} to 24.0 h^{-1}, conversion of DIPB decreases steadily due to decrease in contact time (Table 4.9). Aliphatics, benzene and xylenes also decrease consequently. Selectivity of cymenes remains more or less same while that of cumene increases with the increase in W.H.S.V. The enhancement of cumene selectivity is probably due to lower disproportionation at higher W.H.S.V., and transalkylation of benzene with DIPB to form cumene further.

4.3.3.3 Effect of feed ratio

Toluene to DIPB molar ratio was varied from 4 to 18 during the reaction. With the increase in toluene/DIPB molar ratio, increase in the DIPB conversion is observed (Fig. 4.13). Selectivity of cymenes increaseas and selectivity of cumene remains more or less same with the increase in the molar ratio. The amount of aliphatics and benzene decrease with the increase in the molar ratio.

Table 4.8

Transalkylation of toluene with DIPB over REY zeolite
Effect of temperature on catalytic activity

Product distribution (Wt.%)	Temperature (K)			
	503	523	548	573
Aliphatics	1.39	1.70	2.22	1.92
Benzene	3.20	4.54	6.74	8.49
Toluene	77.60	75.81	76.26	74.87
Σ Xylene	0.07	0.18	0.44	1.27
Cumene	5.15	5.34	3.43	2.13
Σ Cymene	6.39	9.47	9.33	8.56
Σ DIPB	5.12	1.76	0.38	0.21
Σ DIPT	0.32	0.31	0.19	0.14
Others	0.76	0.89	1.01	2.41
Performance				
% Conversion (DIPB)	61.85	86.88	97.31	98.51
% Selectivity Cymenes	36.98	42.22	39.94	34.35
% Selectivity Cumene	29.80	23.81	14.68	8.55

Reaction condition : Toluene/DIPB (mol/mol) = 8, W.H.S.V. = 8.0 h^{-1}, P = 35 Bar,
TOS = 5 h

Table 4.9

Transalkylation of toluene with DIPB over REY zeolite
Effect of W.H.S.V. on catalytic activity

Product distribution (Wt.%)	W.H.S.V. (h^{-1})				
	4.8	8.0	12.8	16.0	24.0
Aliphatics	1.83	1.70	1.33	0.65	0.75
Benzene	4.77	4.54	3.03	2.20	1.96
Toluene	75.73	75.81	77.27	79.86	80.05
Σ Xylene	0.23	0.18	0.13	0.09	0.05
Cumene	5.03	5.34	5.68	4.92	4.30
Σ Cymene	9.97	9.47	8.32	6.92	5.69
Σ DIPB	0.90	1.76	3.19	4.05	6.01
Σ DIPT	0.27	0.31	0.35	0.34	0.32
Others	1.27	0.89	0.70	0.97	0.87
Performance					
% Conversion (DIPB)	93.63	86.88	77.40	64.35	47.10
% Selectivity Cymenes	42.66	42.22	42.58	43.00	40.82
% Selectivity Cumene	21.52	23.81	29.07	30.58	30.85

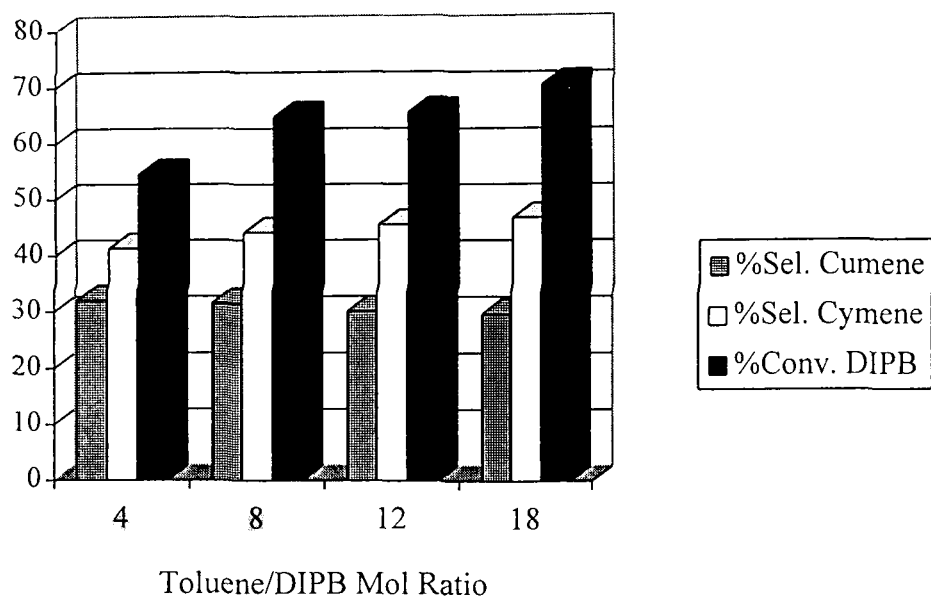Reaction condition : Toluene/DIPB (mol/mol) = 8, T = 523 K, P = 35 Bar, TOS = 5 h

Fig. 4.13   Transalkylation of toluene with DIPB over REY zeolite: influence of Toluene/DIPB mol ratio; T = 523K, P = 35 Bar, WHSV = 16 h^{-1}, TOS = 3 h

4.4 Conclusion

From the present chapter which describes the formation of cymene and cumene over large pore zeolites, the conclusions can be drawn are described below:

Under optimum conditions, toluene can be selectively transalkylated with cumene over large pore zeolites like H-Beta, H-Y and HZSM-12 to produce cymene. Due to secondary isomerization and partially due to coking, an increase in the *p/m* cymene ratio is observed over H-Y and H-ZSM-12. Both cymene and cumene can be simultaneously formed by the transalkylation of toluene with diisopropylbenzene over the large pore zeolites mentioned above. In both reactions, in terms of activity and selectivity, H-Beta shows better performance over H-Y and H-ZSM-12. The activity and coking of the catalysts are attributed to the acidic and structural properties of the zeolites. In industrial point of view, the formation of cymene and cumene can be performed over rare earth modified Y zeolite at high pressure to study for prolonged time with better performance and lesser deactivation of the catalyst.

4.5 References

1. H.C. Brown and K.L. Nelson, *J. Am. Chem. Soc.*, 75 (1953) 6292.

2. W.O. Haag and F.G. Dwyer, *Am. Inst. Chem. Eng.*, 8th Meeting, Boston, USA, (1979).

3. H.C. Brown and J.K. Hans, , *J. Am. Chem. Soc.*, 77 (1955) 3584.

4. H.A. Benesi, *J. Catal.*, 59 (1979) 26.

5. P.B. Venuto, L.A. Hamilton, P.S. Landis and J.J. Wise, *J. Catal.*, 5 (1966) 81.

6. L.J. Leu, B.C. Kang, S.T. Wu and J.C. Wu, *Appl. Catal.*, 63 (1990) 91.

7. D.H. Olson and W.O. Haag, *ACS Symp. Ser.*, 248 (1984) 275.

8. N.Y. Chen, W.E. Garwood and F.G. Dwyer, in *Shape Selective Catalysis in Industrial Applications*, Marcel Dekker, New York and Basel, (1989).

9. S.T. Bakas and P.T. Barger, *US Pat.*, 4,870,222 (1989).

10. A.R. Pradhan and B.S. Rao, *Appl. Catal.*, 106 (1993) 143.

11. R.M. Pitts, Jr., J.E. Connor and L.H. Leum, *Ind. Eng. Chem.*, 47 (1955) 770.

12. S.M. Csicsery, *J. Catal.*, 23 (1971) 124.

13. J.C. Wu and L.J. Leu, *Appl. Catal.*, 7 (1983) 283.

14. I. Wang, T.C. Tsai and S.T. Huang, *Ind. Eng. Chem. Res.*, 29 (1990) 2005.

15. L. Forni, G. Cremona, F. Missineo, G. Bellussi, C. Perego and G. Pazzuconi, *Appl. Catal.*, 121 (1995) 261.

16. J.W. Ward, *Prepr. Am. Chem. Soc. Div. Petrol. Chem.*, B6 (1971).

17. T. Tsai and I. Wang, *J. Catal.*, 133 (1992) 136.

18. H. Pines and O.T. Anigo, *J. Am. Chem. Soc.*, 80 (1958) 279.

19. R.M. Roberts, Y.L. Lin and G.P. Anderson, Jr., *Tetrahedron*, 25 (1969) 4173.

20. D.A. McCaule and A.P. Lien, *J. Am. Chem. Soc.*, 75 (1953) 241.

21. R.M. Roberts and S. Roengsumran, *J. Org. Chem.*, 46 (1981) 3689.

22. K. Ito, *Hydrocarbon Process.*, 52 (1973) 89.

23. W.J. Welsted, Jr., in *Kirk-Othmer Encyclopedia of Chemical Technology*, 9 (1978) 544.

24. D. Fraenkel and M. Levy, *J. Catal.*, 118 (1989) 10.

25. J.M. Derfer and M.M. Derfer, in *Kirk-Othmer Encyclopedia of Chemical Technology*, 22 (1978) 709.

26. A. Chatterjee and R. Vetrivel, *J. Chem. Soc. Faraday Trans.*, 91 (1995) 4313.

27. R. Bandyopadhyay, P.S. Singh and R.A.Shaikh, *Appl. Catal.*, 135 (1996) 249.

CHAPTER 5

TRANSALKYLATION REACTIONS OF N-CONTAINING AROMATICS OVER LARGE PORE ZEOLITES

5.1 Introduction

Methylation of aniline results in the formation of N-methylaniline (NMA), N,N-dimethylaniline (NNDMA) and toluidine (T) as major products. Aniline was alkylated with methanol in the liquid phase using acids or halides as catalysts.[1] The liquid phase alkylation process has been used in industries to prepare NNDMA.[2] However this process had severe corrosion problems due to the use of strong acid as a catalyst at high temperature and pressure. The use of oxide in the gas phase has also been reported for the reaction.[3,4] Methylation of aniline has been studied over zeolites[5-18] and aluminophosphate molecular sieves.[19,20] Most of the research in this field was carried out on NaY,[5] NaX or CaX[6] and ZSM-5.[7-11] Ione and Kiktyanin[9] studied the distribution of C-alkylated products on ZSM-5 zeolites and related the results to the formation of complexes between the aniline molecule and zeolite active sites and their orientation on the surface and channels. Woo et al.[10] used borosilicates as catalysts and correlated their catalytic and acidic data obtained from TPDA studies. The effect of alkali cation exchange in zeolites on the methylation of aniline has been reported by Rao et al.,[12,13] Su and Barthomeuf.[15]

One major feature of methylation of aniline is that, in addition to the N-methylation, the reaction usually accompanies the ring methylation (i.e., C-alkylation) leading to the formation of toluidines.[3,7,17] Moreover, in this reaction, formation of primary product, i.e., NMA is always associated with the formation of N,N-dialkylated product, i.e., NNDMA. Selectivity towards C-alkylation or N-alkylation depends on experimental conditions (temperature and space velocity) and nature of the catalyst. For example, using ZSM-5, the N-alkylation decreases from 100 to 0.3 % when the reaction temperature increases from 548 to 723 K.[9] In general, strong protonic zeolites tend to give more C-alkylation.[7,9,10] Woo et al.[10] suggested that strong acid sites, medium acid

sites and weak acid sites are active sites to produce C-alkylate and coke, NNDMA and N-methyltoluidine (NMT), and NMA respectively.

Studies on the selective mono-methylation of aniline to form N-methylaniline is limited, though interest in this area is growing in recent years.[13,14,16,17] Takamiya et al.[16] reported that, NMA was obtained in a 30% yield over MgO at 753 K while Henkel et al.[17] claimed that a 27.9% yield of NMA was obtained with a 85% selectivity over a high silica zeolite at 573 K. The use of dimethylcarbonate as the alkylating agent to get NMA selectively is reported by several authors.[13,14,21]

Preparation of N-alkylaniline is possible by transalkylation of aniline with N,N-dialkylaniline over zeolite catalysts and this type of reaction is reported by Klug et al.[22] in a German patent.

$R^1 = C_{1-4}$ alkyl, $R^2, R^3 = H, C_{1-4}$ alkyl or alkoxy, F, Cl, Br
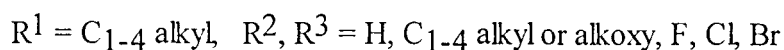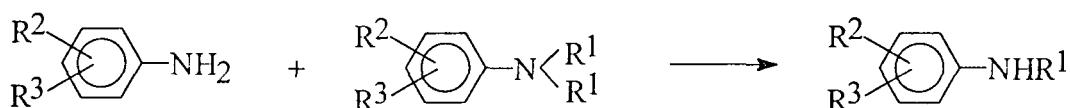
21 and 49% yield of NMA is reported over HZSM-5 and HY zeolites respectively at 573 K using 0.5 mol of aniline and 0.5 mol of NNDMA autoclaved for 3 h.

Keeping the aim of the selective N-monomethylation, this chapter describes the formation of N-methylaniline (NMA) by transalkylation of aniline with N,N-dimethylaniline over H-Beta zeolite. The catalytic results are compared with other two large pore zeolites H-Y and H-ZSM-12. The formation and selectivity of different N-alkylated and C-alkylated products are often governed by the acido-basic properties of the zeolites. H-Beta is exchanged with alkali cations and the effect of this cation exchange on the reaction is also studied in this chapter.

5.2 Experimental

5.2.1 Catalyst Preparation

Zeolite Beta and ZSM-12 were synthesized according to the procedure described in detail in Chapter 2. The as synthesized zeolites were filtered, washed with distilled water and dried overnight at 393 K. The protonic forms of the zeolites were obtained by repeated ammonium exchange with ammonium acetate solution (10%) at 353 K followed by calcination at 773 K for 24 hours in a flow of dry air. NH_4-Y zeolite was obtained commercially from Union Carbide, USA, and converted to its protonic form by the method discussed above.

Cs-H-Beta and K-H-Beta were prepared by ion-exchange with 0.5M solution of cesium and potassium chloride respectively. 5 g of H-Beta was treated with 100 ml 0.5M of chloride solution of the corresponding metal-chloride salt at 353 K for 8 h. The material was then washed with distilled water until the filtrate was free from chloride ions followed by drying and calcining in the same manner described above.

5.2.2 Catalyst Characterization

All the samples were characterized by various physico-chemical techniques such as XRD, SEM, TG-DTA, atomic absorption and X-ray fluorescence spectroscopy. Acidity of the samples were measured by temperature programmed desorption (TPD) of ammonia. The detailed procedures for the characterization are described in Chapter 2.

5.2.3 Catalytic Reactions

The catalytic reactions were performed in a fixed-bed, downflow, silica reactor. The set-up of the reactor and reaction procedures are described in detail in Chapter 3. Taking the catalyst inside the reactor, it was activated at 773 K in a flow of air for 6 hours before each run. The reactor was then cooled to the desired reaction temperature in presence of nitrogen. Aniline and N,N-dimethylaniline (both AR grade) were mixed in the desired

ratio taking benzene as the solvent (reactant/benzene 1:10 mol) and the reactant mixture was fed by a syringe pump (SAGE Insruments, USA). The products of the reaction were collected downstream from the reactor in a cold trap and analyzed by gas chromatograph, Shimadzu 15A, connected with SE30 column and FID detector.

5.3. Results and Discussion

5.3.1 Reaction scheme and mechanism

The major product of the reaction of aniline (A) with N,N-dimethylaniline (NNDMA) is the transalkylated product, i.e., N-methylaniline (NMA). Equimolar amount of aniline and N,N-dimethylaniline react together to yield two moles of NMA. The other reaction products obtained in the reaction are Toluidine (T), N-methyltoluidine (NMT) and N,N-dimethyltoluidine (NNDMT) (Fig. 5.1). All these side products are formed from NMA or NNDMA via isomerization or rearrangement.[19] Fig. 5.2 shows the mechanism of formation of the primary product, NMA. Toluidine can be formed from NMA either by direct N-C shift or by carbocation formation (Fig 5.3). Similarly N-methyl toluidine (NMT) is formed from NNDMA either by intramolecular N-C shift or by carbocation mechanism (Fig. 5.4). On the other hand N,N-dimethyltoluidine is formed via disproportionation of NNDMA, or in other words, intermolecular reaction of two moles of NNDMA (Fig. 5.5). Formation of all the products (NMA, T, NMT and NNDMT) is dependent upon the reaction parameters such as temperature, A/NNDMA molar ratio as well as space velocity.

5.3.2 Effect of temperature

The transalkylation reaction is performed at different temperatures ranging from 473 K to 673 K. Table 5.1 shows the influence of temperature over the product distribution. Conversion of NNDMA increases with the increase in temperature and
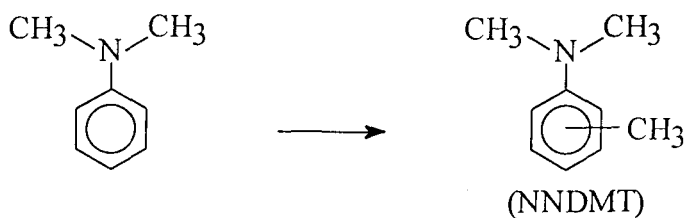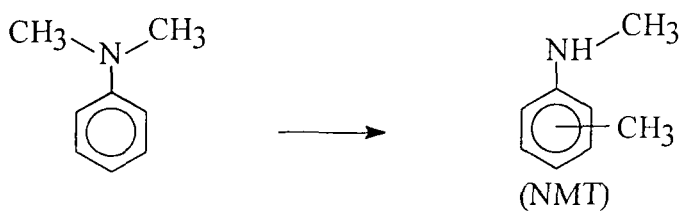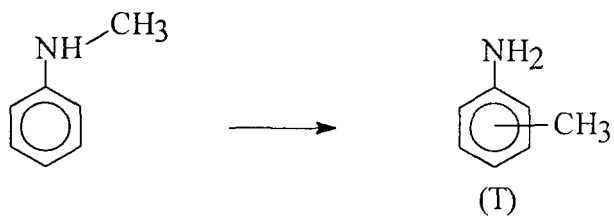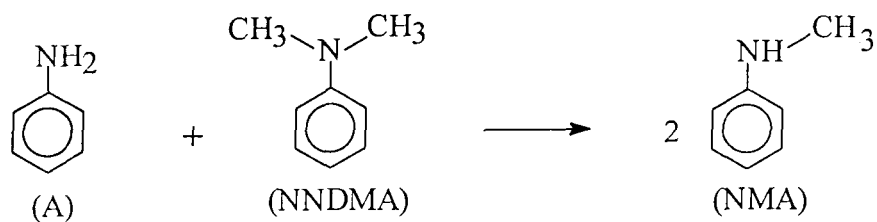
Fig. 5.1   Reaction scheme for transalkylation of aniline with NNDMA and other side reactions

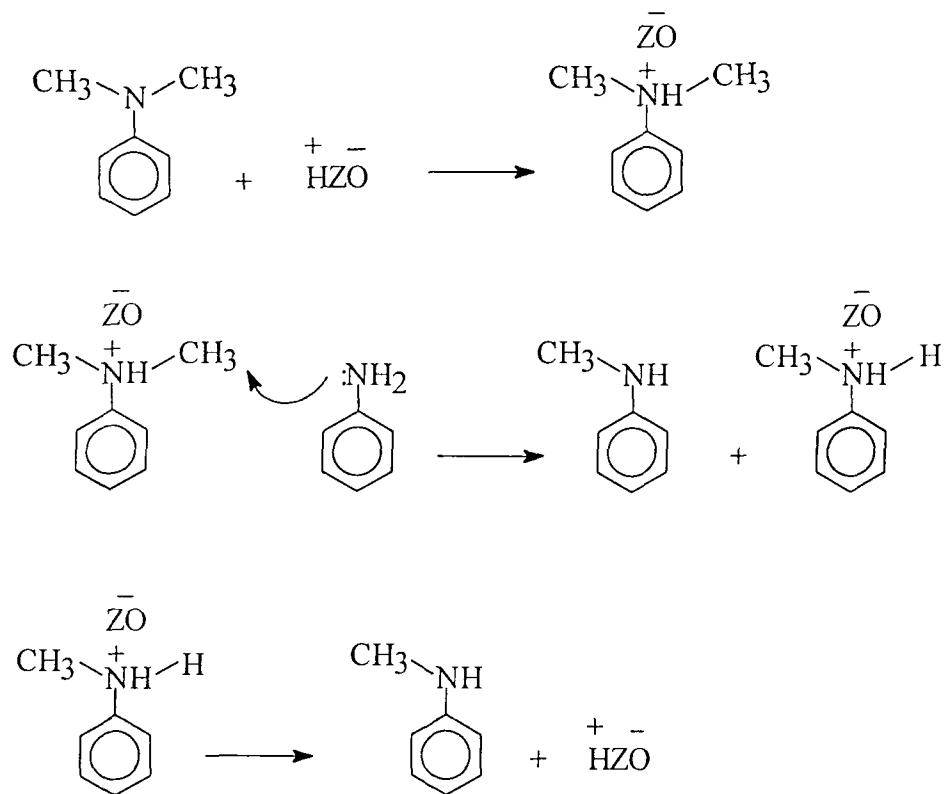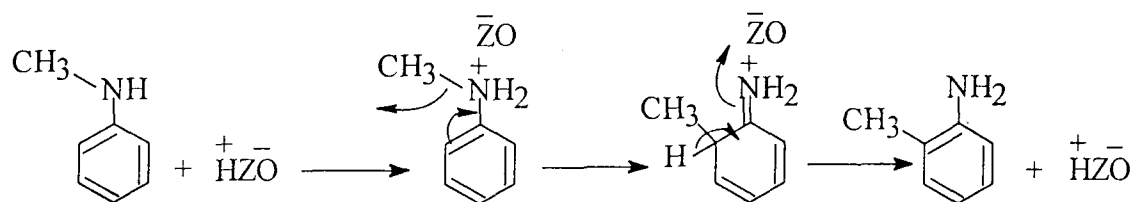**Fig. 5.2**   Formation of N-methylaniline (NMA)

(a) via intramolecular rearrangement

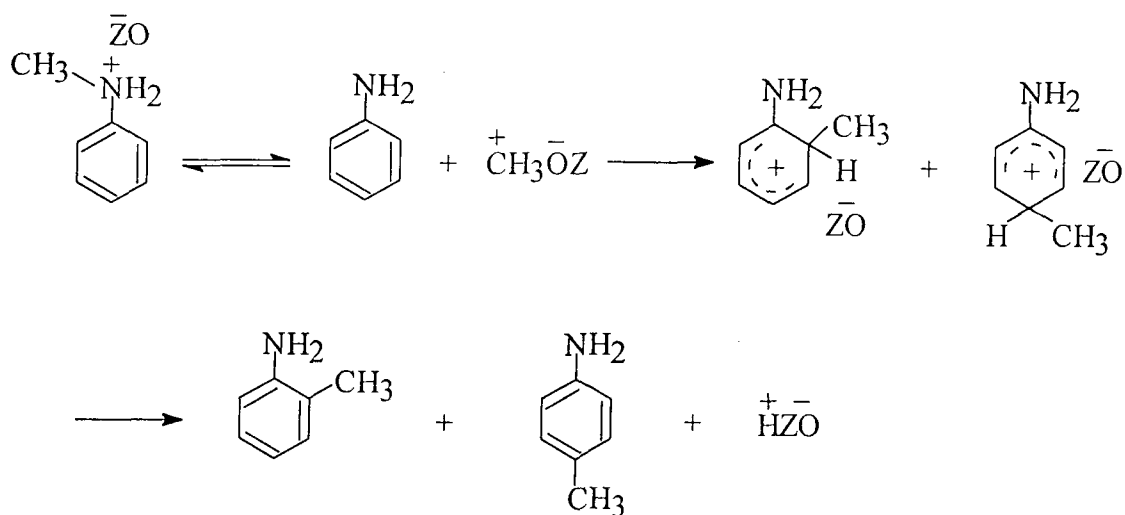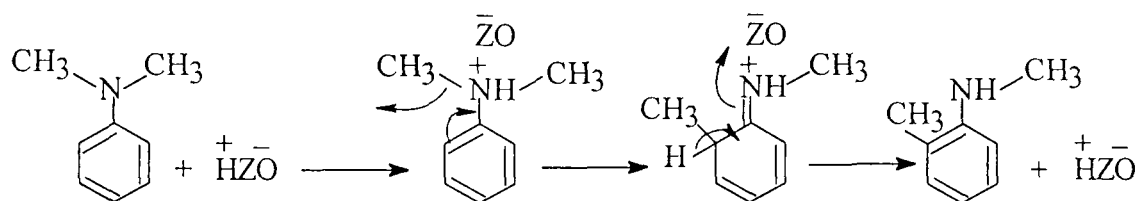**(b) via carbocation mechanism**

Fig. 5.3   Formation of Toluidine (T)

133

(a) via intramolecular rearrangement

(b) via carbocation mechanism
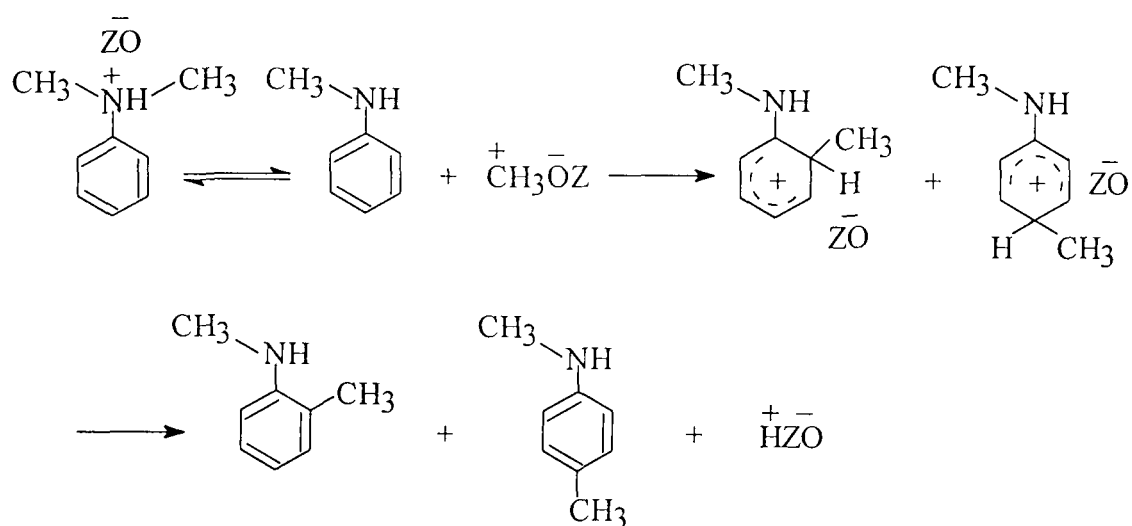
Fig. 5.4   Formation of N-methyltoluidine (NMT)

via intermolecular mechanism
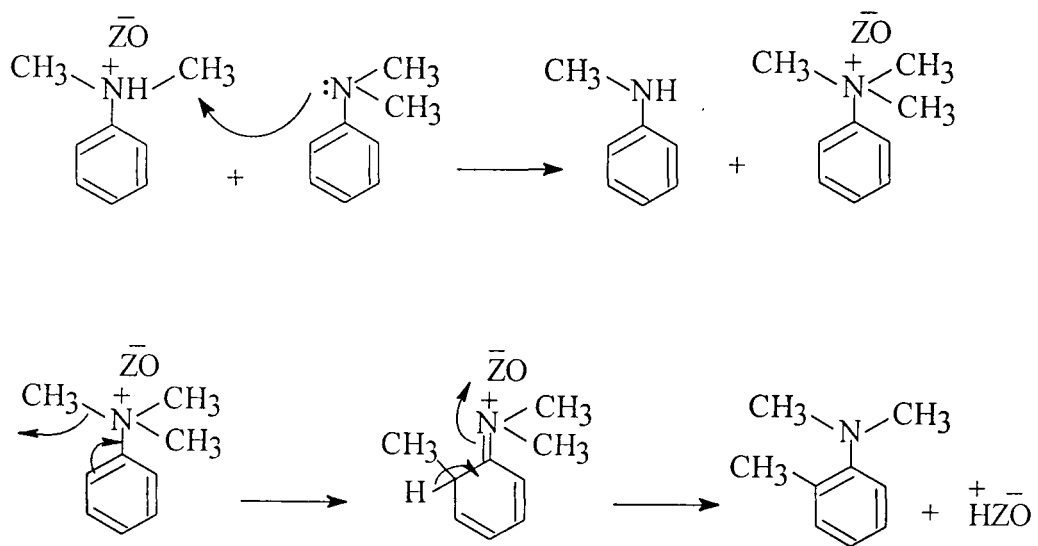
Fig. 5.5   Formation of N,N-dimethyltoluidine (NNDMT)

Table 5.1

Transalkylation of aniline with N,N-dimethylaniline over H-Beta
Effect of temperature

Product distribution (Wt. %)	Temperature (K)				
	473	523	573	623	673
Aniline	54.94	44.47	45.03	44.76	50.50
N-methylaniline	9.39	35.38	24.89	19.13	9.78
Toluidine	–	1.58	10.88	20.00	26.10
N,N-dimethylaniline	35.67	12.99	6.74	3.70	0.80
N-methyltoluidine	–	3.49	9.44	10.25	11.30
N,N-dimethyltoluidine	–	2.09	3.01	2.16	1.51
Performance					
% Conv. NNDMA	13.82	69.72	83.72	91.21	98.09
% Sel. NMA	100.00	83.17	51.62	37.12	20.09
% Sel. T	–	3.71	22.56	38.80	53.60
% Sel. NMT	–	8.20	19.58	19.89	23.21
% Sel. NNDMT	–	4.91	6.24	4.19	3.10

Reaction condition : A/NNDMA (mol) = 2:1, Solvent = benzene, W.H.S.V. = 1.76 h^{-1}, Time on stream (TOS) = 5 h

conversion is almost complete at 673 K. At lowest reaction temperature (473 K) only transalkylation reaction takes place and NMA is formed exclusively at a low conversion level of NNDMA. NMA is formed by the transalkylation reaction. As temperature increases from 523 K onwards, selectivity towards Toluidine and NMT increases. Toluidine and NMT are formed by either intramolecular rearrangement or carbocation mechanism from NMA and NNDMA respectively, as depicted in Fig. 5.3 and Fig. 5.4. At higher temperatures selectivity of toluidine exceeds that of NMA. NNDMT is formed via disproportionation or intermolecular mechanism of NNDMA (Fig. 5.5). The selectivity of NNDMT remains more or less unaltered with the increase in temperature. It is notable that since toluidine is formed from NMA only, whenever selectivity towards NMA decreases the selectivity towards toluidine increases consequently and *vice versa*. The gas fraction was analyzed in which only trace amount of benzene was found.

5.3.3 Effect of feed ratio (A/NNDMA molar ratio)

The effect of A/NNDMA molar ratio on the reaction is shown in Table 5.2. At any particular temperature and time on stream, conversion of NNDMA remains almost unchanged with the increase in A/NNDMA molar ratio. Selectivity towards NMA increases with the increase in molar ratio whereas selectivity towards NMT and NNDMT decreases with the increase in molar ratio. This indicates that at lower A/NNDMA ratio, i.e., at higher concentration of NNDMA in the feed, formation of side products are more due to the reactions of NNDMA according to the reaction scheme shown in Fig. 5.1.

5.3.4 Effect of space velocity

The effect of W.H.S.V. over the reaction is presented in Fig. 5.6. As W.H.S.V. is increased from 1.76 h^{-1} to 6.60 h^{-1}, conversion of NNDMA decreases linearly due to decrease in the contact time which indicates that there are no external mass transfer limitations. Selectivity towards NMA increases and consequently selectivity towards

Table 3.2

Transalkylation of aniline with N,N-dimethylaniline over H-Beta
Effect of feed ratio

Product distribution (Wt. %)	Aniline/NNDMA (mol/mol)		
	1:1	2:1	3:1
Aniline	29.39	45.01	57.39
N-methylaniline	21.98	22.42	22.12
Toluidine	19.74	14.72	9.06
N,N-dimethylaniline	8.04	4.98	4.22
N-methyltoluidine	16.31	10.15	5.87
N,N-dimethyltoluidine	4.53	2.72	1.34
Performance			
% Conv. NNDMA	86.42	87.97	86.99
% Sel. NMA	35.13	44.83	57.62
% Sel. T	31.55	29.43	23.60
% Sel. NMT	26.07	20.30	15.29
% Sel. NNDMT	7.24	5.44	3.49

Reaction condition : Temperature = 573 K, Solvent = benzene, W.H.S.V. = 1.76 h^{-1}, TOS = 4 h
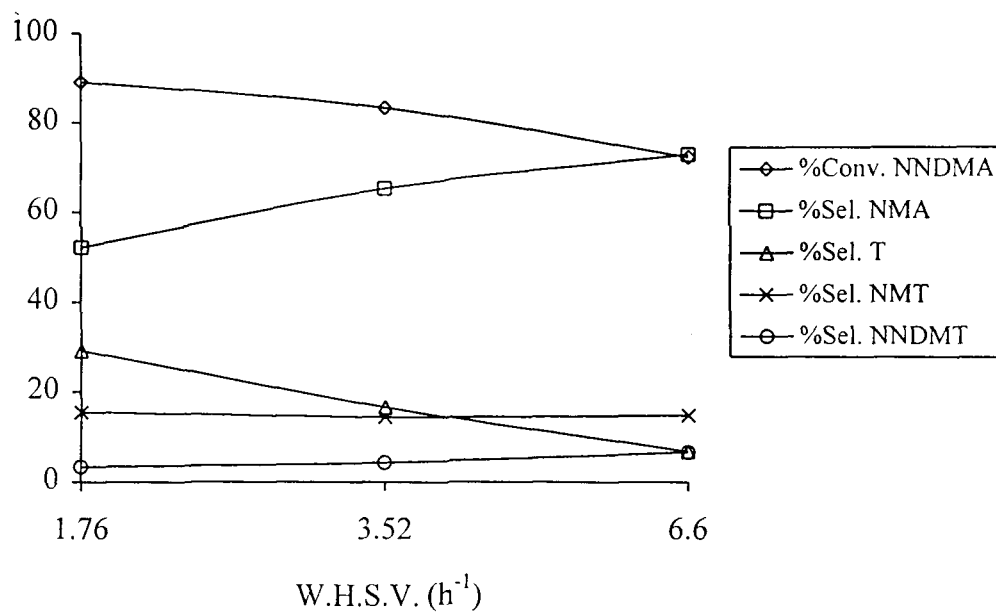
Fig. 5.6   Transalkylation of aniline with N,N-dimethylaniline over H-Beta: effect of space velocity; A/NNDMA = 3:1 mol, T = 573 K, TOS = 3h

139

toluidine decreases with the increase in W.H.S.V. As contact time is decreased by increasing W.H.S.V., NMA is the only product formed in the transalkylation reaction. However selectivity towards NMT and NNDMT does not vary much with the variation in W.H.S.V.

5.3.5 Effect of time on stream (TOS)

The activity of H-Beta and selectivity towards the products with time on stream is shown in Fig. 5.7. Conversion of NNDMA decreases slowly with time on stream in H-Beta. The catalyst is fairly stable even after 12 hours run. Selectivity towards NMA increases steadily with time on stream, i.e., as percent conversion decreases. Consequently selectivity towards toluidine decreases with time on stream. However, selectivity towards both NMT and NNDMT remains unaltered with time on stream.

5.3.6 Effect of alkali cation exchange

Table 5.3 shows the effect of alkaline cation exchange on the product distribution. Conversion of NNDMA is highest in the case of H-Beta and lowest in Cs-Beta. As the level of exchange of Cs and K is high in the samples, steric constraints would play a role and thus the activity would decline.[23] As basicity increase in the samples H-Beta < K-Beta < Cs-Beta, selectivity towards N-alkylated product i.e., NMA increases and C-alkylated product i.e., toluidine decreases. At lower temperature (523 K), Cs-Beta yields exclusively the N-alkylated product, i.e., NMA. As temperature increases, selectivity towards toluidine increases but still it follows the same order, i.e., toluidine formation is lowest in Cs-Beta. The difference for N-selectivity for protonic and alkaline zeolites indicates that formation of N-alkylated product, i.e., NMA is favored on active centers such as basic and/or Lewis acid sites whereas formation of C-alkylated product i.e., formation of toluidine from NMA via N-C shift or carbocation is favored on protonic sites.[13]
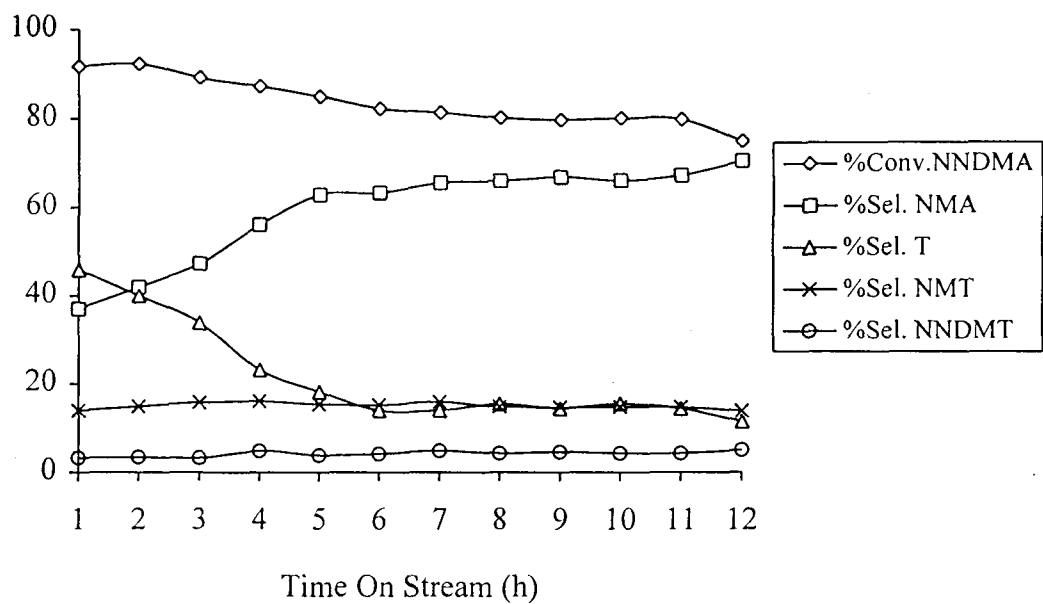
Fig. 5.7   Transalkylation of aniline with N,N-dimethylaniline over H-Beta: effect of time on stream; A/NNDMA = 3:1 mol, T = 573 K, WHSV = 1.76 h^{-1}

Table 5.3

Transalkylation of aniline with N,N-dimethylaniline over Beta zeolites
Effect of alkali cation exchange

Catalyst	H-Beta			K-Beta			Cs-Beta		
Temperature (K)	523	573	623	523	573	623	523	573	623
Prod. Dist. (Wt.%)									
Aniline	54.92	57.39	57.44	61.59	60.73	59.51	63.89	59.15	58.84
NMA	34.13	22.12	17.51	20.88	25.57	23.32	11.02	26.97	23.32
Toluidine	–	9.06	15.90	–	–	5.63	–	–	3.93
NNDMA	9.29	4.22	2.76	16.26	7.44	4.14	25.09	10.57	7.20
NMT	0.90	5.87	5.30	0.55	4.58	5.86	–	2.22	5.04
NNDMT	0.76	1.34	1.09	0.71	1.67	1.53	–	1.08	1.66
Performance									
% Conv. NNDMA	71.37	86.99	91.50	48.32	76.94	86.84	21.50	67.23	77.47
% Sel. NMA	95.36	57.62	43.99	94.31	80.35	64.17	100.0	89.10	68.69
% Sel. T	–	23.60	39.95	–	–	15.49	–	–	11.58
% Sel. NMT	2.51	15.29	13.32	2.48	14.39	16.13	–	7.33	14.84
% Sel. NNDMT	2.12	3.49	2.74	3.21	5.25	4.21	–	3.57	4.89

Reaction condition : A/NNDMA (mol) = 3:1, Solvent = benzene, W.H.S.V. = 1.76 h^{-1}, TOS = 5 h

Table 5.4

Transalkylation of aniline with N,N-dimethylaniline over large pore zeolites

Product distribution (Wt. %)	Catalyst		
	H-Beta	H-ZSM-12	H-Y
Aniline	55.18	62.36	64.36
N-methylaniline	33.87	17.03	15.99
Toluidine	–	–	2.72
N,N-dimethylaniline	9.63	18.44	12.90
N-methyltoluidine	0.62	0.92	3.11
N,N-dimethyltoluidine	0.70	1.25	0.91
Performance			
% Conv. NNDMA	70.32	41.99	59.60
% Sel. NMA	96.25	88.70	70.35
% Sel. T	–	–	11.97
% Sel. NMT	1.76	4.79	13.68
% Sel. NNDMT	1.99	6.51	4.00

Reaction condition : A/NNDMA = 3:1, Solvent = benzene, Temperature = 523 K, W.H.S.V. = 1.76 h^{-1}, TOS = 3 h
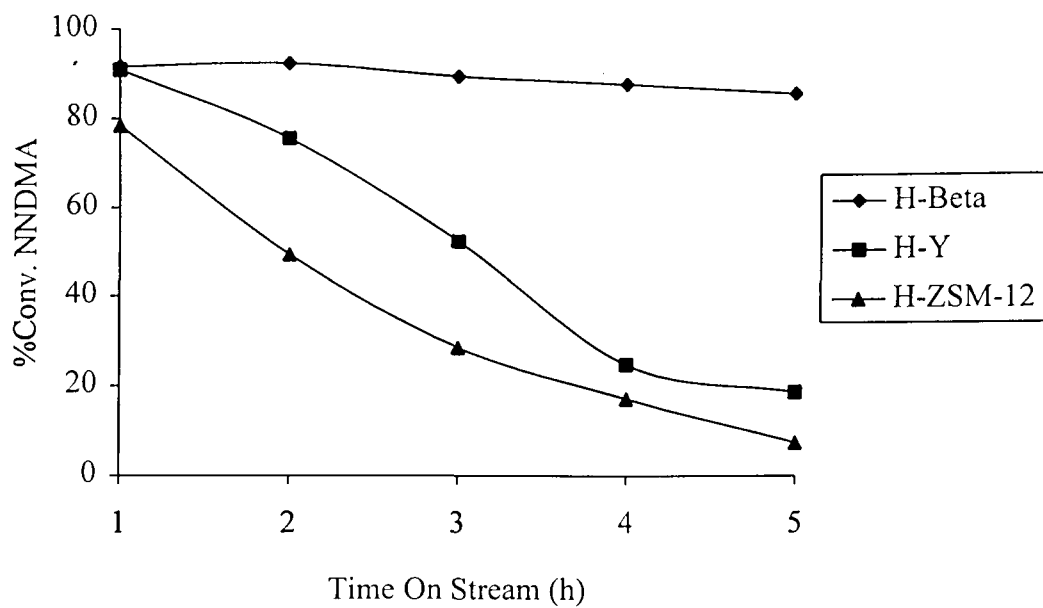
Fig. 5.8 Transalkylation of aniline with N,N-dimethylaniline over large pore zeolites: comparison of catalytic activity with time on stream; A/NNDMA = 3:1 mol; T = 573 K; WHSV = 1.76 h⁻¹

5.3.7 Comparison of catalysts

The catalytic performance of H-Beta is compared with two other large pore zeolites namely H-ZSM-12 and H-Y (Table 5.4). H-Beta shows much higher activity and selectivity compared to the other two catalysts. Selectivity towards NMA is maximum in H-Beta compared to H-ZSM-12 and H-Y. At 523 K toluidine is formed only in H-Y. Among these three catalysts H-Beta shows fairly stable activity whereas the other two deactivate faster with time on stream. Beta deactivates slowly, whereas the other two deactivate within 5 h. (Fig. 5.8). The faster deactivation of H-Y is attributed to its open type of structure, and H-ZSM-12 deactivates faster due to its unidimensional pore structure.

5.4 Conclusion

Under optimum conditions zeolite H-Beta can be used as a potential catalyst for the formation of N-methylaniline by transalkylation of aniline and N,N-dimethylaniline. Though at lower temperature (473 K) formation of N-methylaniline is exclusive and formation of side products increase with increasing temperature, it is desirable to use little higher temperature (ca. 523 K - 573 K) for a higher conversion of N,N-dimethylaniline. In terms of activity, stability and selectivity H-Beta shows better performance over H-Y and H-ZSM-12. Though alkali cation exchange in H-Beta increases selectivity towards N-methylaniline, the exchanged catalysts show less conversion of N,N-dimethylaniline.

5.5 References

1. A.B. Brown and E.E. Reid, *J. Am. Chem. Soc.*, 46 (1924) 1836.

2. L.K. Doraiswamy, G.R.V. Krishnan and S.P. Mukherjee, *Chem. Eng.*, 88 (1981) 78.

3. A.G. Hill, J.H. Shipp and A.J. Hill, *Ind. Eng. Chem.*, 43 (1951) 1679.

4. J.M. Parrera, A. Gonzalez and M.A. Barral, *Ind. Eng. Chem. Prod. Res. Dev.*, 7 (1968) 259.

5. K. Kunikata, *Japan Kokai*, 78,28,128.

6. G.O. Chivadze and L.Z. Chkheidze, *Izv. Acad. Nauk. Gruz. SSR., Ser. Khim.*, 10 (1984) 232.

7. P.Y. Chen, M.C. Chen, H.Y. Chu, N.S. Chang and T.K. Chuang, *Stud. Surf. Sci. Catal.*, 28 (1986) 739.

8. P.Y. Chen, S.J. Chu, N.S. Chang and T.K. Chuang, *Stud. Surf. Sci. Catal.*, 49 (1989) 1105.

9. K.G. Ione and O.V. Kiktyanin, *Stud. Surf. Sci. Catal.*, 49 (1989) 1073.

10. S.I Woo, J.K. Lee, S.B. Hong, Y.K. Park and Y.S. Uh, *Stud. Surf. Sci. Catal.*, 49 (1989) 1095.

11. Y.K. Park, K.Y. Park and S.I Woo, *Catal. Lett.*, 26 (1994) 169.

12. P.R.H.P. Rao, P. Massiani and D. Barthomeuf, *Stud. Surf. Sci. Catal.*, 84 (1994) 1449.

13. P.R.H.P. Rao, P. Massiani and D. Barthomeuf, *Catal. Lett.*, 31 (1995) 115.

14. Z. Fu and Y. Ono, *Catal. Lett.*, 22 (1993) 277.

15. B.L. Su and D. Barthomeuf, *Appl. Catal.*, 124 (1995) 73.

16. N. Takamiya, Y. Koinuma, K. Ando and S. Murai, *Nippon Kagaku Kaishi*, (1979) 1453.

17. G. Henkel, L. Feiler, W. Haenzel and D. Kottmann, *DE,* (1990) 4013613A1.

18. M. Onaka, K. Ishikawa and Y. Izumi, *Chem. Lett.,* (1982) 1983.

19. S. Prasad and B. S. Rao, *J. Mol. Catal.,* 62 (1990) L17.

20. P.S. Singh, R. Bandyopadhyay and B.S. Rao, *Appl. Catal.,* 136 (1996) 177.

21. F. Trotta, P. Tundo and G. Moragilo, *J. Org. Chem.,* 52 (1987) 1300.

22. G. Klug, H.J. Buysch and L. Pappe, *Ger. Offen. DE,* (1989) 3803662.

23. C.O. Veloso, J.F. Monterio, E.F. Sousa-Aguiar, *Stud. Surf. Sci. Catal.,* 84 (1994) 1931.

CHAPTER 6

CONCLUSION

6.1 Summary and Conclusions

Due to their unique properties that include well-defined microporous structure, high thermal stability, high internal surface area, ion exchange properties, ease of regeneration and an eco-friendly nature, zeolites and related molecular sieves are increasingly replacing conventional homogeneous and other heterogeneous catalysts. Today, zeolites are widely applied in diverse areas such as catalysis, separation, ion exchange and drying processes. The present thesis was devoted to the application of large pore zeolites with structural and aciditiy differences, namely Beta, Y and ZSM-12, in the formation of some industrially important intermediates by alkylation and transalkylation reactions. The first step or requirement to investigate the formation of industrially important intermediates was the synthesis and careful characterization of the large pore zeolites.

The catalysts used in this study have been synthesized, suitably modified and thoroughly characterized. Zeolite Beta and ZSM-12 have been synthesized and Beta has also been modified by ion exchange with La^{3+}, Mg^{2+}, Cs^+ and K^+. Commercially obtained NH_4-Y was converted to its protonic form and also modified to its rare-earth form. Characterization of all the samples by various physico-chemical techniques has also been described.

Cymene is an important intermediate for the production of many useful materials such as cresols, polymers, fungicides, pesticides and heat transfer media. The formation of cymenes has been studied over zeolite Beta by alkylation reactions. For this purpose, two different routes, namely isopropylation of toluene and methylation of cumene, have been employed. Beta zeolite has been modified with La^{3+} and Mg^{2+} cations and the effect of these exchanges on cymene synthesis has been discussed. La^{3+}-exchanged Beta was more selective for cymene than H-Beta and Mg-H-Beta, but it also deactivated faster than

148

H-Beta. In the methylation of cumene, the formation of undesired side products was enhanced due to dealkylation and disproportionation reactions.

Formation of cymenes has also been studied over large pore zeolites by transalkylation reactions. Three large pore zeolites with different structures and acidity have been used for this purpose, namely H-Beta, H-Y and H-ZSM-12. Toluene has been transalkylated with cumene. The reaction was proposed to proceed through a diphenylpropane-type intermediate (i.e., an S_{N2} mechanism) over Beta and Y zeolites, whereas both S_{N2} and carbocation formation (S_{N1}) mechanisms occur over ZSM-12, depending upon reaction temperature.

Cymene and cumene can simultaneously be formed by the transalkylation of toluene with diisopropylbenzene (DIPB), and this reaction has been studied over the same series of large pore zeolites. Isomerization of 1,4-DIPB competed to some extent with the transalkylation reaction. Y zeolite was modified to its rare-earth form and the same reaction has been studied over rare-earth Y at high pressure using a commercial cumene bottoms fraction as the DIPB source. Increase in reaction temperature resulted in the decrease in cymene and cumene selectivity due to dealkylation and disproportionation reactions.

During the methylation of aniline, formation of N-monomethylated product is often associated with the N,N-dialkylation and C-alkylation. Formation of N-methylaniline by transalkylation of aniline and N,N-dimethylaniline over large pore zeolites has been studied in the present investigation. Over H-Beta, formation of N-methylaniline is exclusive at lower temperature (473 K). The catalytic activity of H-Beta was compared with Cs and K-exchanged Beta as well as H-Y and H-ZSM-12. H-Y and H-ZSM-12 showed lower selectivity towards N-methylaniline and faster deactivation compared to H-Beta.

The major findings of the thesis include:

- La^{3+} exchange in zeolite H-Beta creates distinct acidic sites which are responsible for better selectivity towards cymenes during the isopropylation of toluene.

- Formation of cymenes over H-Beta is more feasible by isopropylation of toluene than methylation of cumene. Cumene methylation is not a suitable route for the formation of cymene, since it requires higher temperature which enhances the formation of undesired side products.

- Toluene can be selectively transalkylated with cumene over large pore zeolites. The optimum conditions for selective transalkylation over H-Beta are found to be: temperature 473 K - 493 K, WHSV 4.2 h^{-1} and toluene/cumene molar ratio 14.

- Cymene and cumene can be simultaneously generated by the transalkylation of toluene with DIPB over large pore zeolites at optimum conditions.

- Selective formation of N-methylaniline is possible by the transalkylation of aniline and N,N-dimethylaniline over large pore zeolites. At lower temperature (473 K) formation of N-methylaniline is exclusive over H-Beta, but higher temperature (523 - 573 K) is desired for a higher NNDMA conversion. Though alkali cation exchange in Beta increases the selectivity of N-methylaniline, the exchanged zeolites exhibit lower conversion of N,N-dimethylaniline.

- Among the large pore zeolites examined in present study, zeolite Beta exhibits the best results in terms of activity and selectivity for alkylation and transalkylation reactions. The faster deactivation of zeolite Y and ZSM-12 are attributed to the open type of structure of Y and unidimensional structure of ZSM-12.

6.2 Scope for further work

The present thesis describes the formation of cymene, cumene and N-methylaniline over large pore zeolites by alkylation and transalkylation reactions. These investigations

could be extended by choosing aromatic molecules with different substituents and examining their activity in other novel transalkylation reactions over large pore zeolites. For example, in Chapter 5, formation of N-methylaniline was studied by transalkylation of aniline with N,N-dimethylaniline. In a broader sense, N-alkylaniline can be formed by the transalkylation of aniline with N,N-dialkylaniline. This route has been reported by Klug et al.[1] and also described in Chapter 5. Hence, the formation of N-ethyl or higher alkyl aniline could be formed in the same manner and various zeolites could be tested for this purpose to determine the optimal combination of acidity and pore geometry.

The application of transalkylation reactions could be extended by reacting oxygen-containing aromatics, e.g., phenol. Agaev et al. have reported[2] that cresols can be formed by the transmethylation of phenol by pseudocumene (1,2,4-trimethylbenzene). Aromatics with methyl groups such as trimethylbenzenes and xylenes could be applied as transalkylating agents to form cresols, and various zeolites (e.g., Beta and Mordenite) might be useful for this purpose.

Finally, deactivation during the alkylation and transalkylation of toluene has not been deeply investigated in the present thesis. Foundations for such a study already have been published by the Rao research group in the case of the isopropylation of benzene.[3] Studying (i) the effect of coking on the product distribution, (ii) sorption kinetics of different substrates on fresh and coked catalysts, and (iii) measurement of nature and amount of coke in the zeolites could provide better insight into the deactivation mechanisms over large pore zeolites.

6.3 References

1.   G. Klug, H.J. Buysch and L. Pappe, *Ger. Offen. DE,* (1989) 3803662.

2.   A.A. Agaev, R.I. Mamedova and I.M. Gulieva, *Zh. Prikl. Khim.,* 67 (1994) 464.

3.   A.R. Pradhan and B.S. Rao, *J. Catal.,* 132 (1991) 79.

List of Publications

1.   Transalkylation of cumene with toluene over zeolite Beta.
      Rajib Bandyopadhyay, Puyam S. Singh and R. A. Shaikh.
      Applied Catalysis, 135 (1996) 249.

2.   Transalkylation of diisopropylbenzene with toluene over REY zeolite.
      Rajib Bandyopadhyay, Puyam S. Singh and B. S. Rao.
      Reaction Kinetics and Catalysis Letters (in press, 1996).

3.   Formation of N-methylaniline by transalkylation of aniline with N,N-dimethylaniline over zeolite Beta.
      Rajib Bandyopadhyay, Puyam S. Singh and B. S. Rao.
      Applied Catalysis (accepted, 1996).

4.   Alkylation of aniline with methanol over AEL type molecular sieve.
      Puyam S Singh, Rajib Bandyopadhyay and B. S. Rao.
      Applied Catalysis, 136 (1996) 177.

5.   Vapor phase Beckmann Rearrangements over SAPO-11 molecular sieves.
      Puyam S Singh, Rajib Bandyopadhyay, S. G. Hegde and B. S. Rao.
      Applied Catalysis, 136 (1996) 249.

6.   Characterization of SAPO-11 synthesized conventionally and in the presence of fluoride ions.
      Puyam S Singh, Rajib Bandyopadhyay and B. S. Rao.
      Journal of Chemical Society, Faraday Transactions, 92 (1996) 2017.

6.   Spectroscopic studies of vanadium incorporated SAPO-11 molecular sieve.
      Puyam S Singh, Rajib Bandyopadhyay and B. S. Rao. ›
      Journal of Molecular Catalysis, 104 (1995) 103.

8.   Synthesis of CoVPI-5 with bifunctional activity.
      Puyam S. Singh, R. A. Shaikh, Rajib Bandyopadhyay and B. S. Rao.
      Journal of Chemical Society, Chemical Communication, (1995) 2255.

9.   Selective acidic, oxidative and reductive reactions over AlPO-11 and Si or Metal substituted ALPO-11.
      Puyam S Singh, Rajib Bandyopadhyay, R. A. Saikh and B. S. Rao.
      Studies in Surface Science and Catalysis, 97 (1995) 343.

10.   Simultaneous production of cymenes and cumene through transalkylation reaction over zeolite REY.
      Rajib Bandyopadhyay
      Proceedings of National Workshop on Catalysis, CSMCRI, Bhavnagar, India, 20-22 Dec., 1995.

11.   Influence of physico-chemical parameters on n-hexane dehydrocyclization over Pt/LTL zeolites.
       P. N. Joshi, Rajib Bandyopadhyay , S. V. Awate, V. P. Shiralkar and B. S. Rao.
       Reaction Kinetics and Catalysis Letters, 53 (1994) 231.

12.   Aluminium gradient and the catalytic properties of ZSM-5 zeolites.
       R.A. Shaikh, Rajib Bandyopadhyay, P. S. Singh and B. S. Rao.
       Catalysis : Modern Trends, N. M. Gupta and D. K. Chakrabarty (Eds.), Narosa Publishing House, New Delhi, (1995) p 91, *Proceedings of the 12th National Symposium on Catalysis*, BARC, Bombay, India, 19-22 Dec., 1994.

13.   Coke induced shape selectivity over silynated ZSM-5.
       R. A. Shaikh, Rajib Bandyopadhyay, P. S. Singh and B. S. Rao.
       Catalysis : Present and Future, P. Kanta Rao and R. S. Beniwal (Eds.), Wiley Eastern Ltd., New Delhi, (1995) p 31, *Proceedings of the 11th National Symposium on Catalysis*, IICT, Hyderabad, India, 2-4 April, 1993.

14.   Formation of cymenes and cumene by transalkylation of toluene with diisopropylbenzene over zeolite Beta.
       Rajib Bandyopadhyay, Puyam S. Singh and B. S. Rao.
       Reaction Kinetics and Catalysis Letters (communicated, 1996).

15.   Formation of cymenes via isopropylation and methylation over cation exchanged Beta zeolites: effect of cation on alkylation activity.
       Rajib Bandyopadhyay and Puyam S. Singh.
       Reaction Kinetics and Catalysis Letters (communicated, 1996).

16.   Structure- reactivity phenomena during the self reaction of 'N' and 'O' containing aromatics over large pore zeolites.
       Puyam S. Singh, Rajib Bandyopadhyay, S. G. Hegde and B. S. Rao.
       Journal of Chemical Society, Faraday Transactions, (communicated, 1996).

17.   Sorption properties of AEL type related materials.
       Puyam S. Singh, Rajib Bandyopadhyay, S. P. Mirajkar, B. S. Rao and V. P. Shiralkar.
       Journal of Colloid and Interface Science (communicated, 1996).

18.   Characterization of MeAPOs with AEL topology synthesized conventionally and in the presence of fluoride ions.
       Puyam S. Singh, Rajib Bandyopadhyay, Veda Ramaswamy, and B. S. Rao.
       Journal of Chemical Society, Faraday Transactions, (communicated, 1996).